Republic of Iraq
Ministry of Higher Education and Scientific Research
University of Misan/College of Engineering
Civil Engineering Department

FLEXURAL CAPACITY OF COMPOSITE BOX STEEL - ULTRA HIGH-PERFORMANCE CONCRETE BEAMS

A THESIS
SUBMITTED TO THE COLLEGE OF ENGINEERING OF
MISAN UNIVERSITY IN PARTIAL FULFILLMENT OF
THE REQUIREMENTS FOR THE DEGREE OF MASTER OF
SCIENCE IN CIVIL ENGINEERING
(STRUCTURES)

BY
MUSTAFA RAAD AZIZ
B.Sc. in Civil Engineering, 2016

Supervised by
Dr. Nasser Hakeem Tu'ma

March 2019   **Jomad/ second 1440**

بِسْمِ اللَّهِ الرَّحْمَنِ الرَّحِيمِ

ذَلِكَ فَضْلُ اللَّهِ يُؤْتِيهِ مَن يَشَاءُ وَاللَّهُ ذُو الْفَضْلِ الْعَظِيمِ ﴿ ٤ ﴾

صَدَقَ اللَّهُ الْعَلِيُّ الْعَظِيمُ

سُورَةُ الجمعة

Supervisors Certificate

We certify that this thesis entitled **"Flexural Capacity of Composite Box Steel - Ultra-High-Performance Concrete Beams''** was prepared by *"Mustafa Raad Aziz"* under our supervision at the Department of Civil Engineering in the University of Missan in partial fulfillment of the requirements for the degree of Master of Science in Structural Engineering.

Signature:

Name: *Dr. Nasser H. Tu'ma*

Date: / / 2019

Because of the above recommendations, I forward this thesis for debate by the
examining committee.

Signature:

Name *Asst. Prof. Dr. Abbas Oda Dawood*

(Head of Civil Engineering Department)

Date: /   / 2019

Certificate of the Examining Committee

We certify as an Examining Committee that we have read this thesis entitled **"Flexural Capacity Of Composite Box Steel - Ultra-High-Performance Concrete Beams"**, and examined the student *"Mustafa Raad Aziz"* in its content and what related to it, then found it meets the standard of thesis for the degree of Master of Science in Civil Engineering (Structural Engineering).

Signature:
Name: *Dr. Nasser H. Tu'ma*
       (Supervisor)
Date: /   / 2019

Signature: Signature:
Name: **Dr. Saad F. Resan**   Name: **Dr. Samir Mohammed**
    (Asst. Professor)   *(Lecturer)*
      (Member)   (Member)
Date: / / 2019   Date: /   / 2019

Signature:
Name: *Dr. Abbas A. Dheab*
      (Professor)
      (Chairman)
Date: / / 2019

Approved by the Head of the Civil Engineering Department

Signature:
Name *Asst. Prof. Dr. Abbas Odaa Dawood*
(Head of Civil Engineering Department)
Date: / / 2019

Approved by the Dean of the College of Engineering

Signature:
Name *Prof. Dr. Ahmed AL-Sharaa*
(Dean of College of Engineering)
Date: / / 2019

Acknowledgements

In the name of Allah, the most gracious, the most merciful

Abstract

Service paths are a significant part of any building. Therefore, the use of structural elements with different longitudinal openings is an effective solution to cover the need for these paths with other economic benefits. The economic benefits of constructions usually revolve around reducing the number of used materials and the dead-weight of the structural members. Therefore, the current research attempts to cover this aspect by reducing the amount of used concrete while maintaining and increasing the capacity of the section as much as possible by using the principle of the composite section in a new structural member. The present work included a study, trying to develop a new type of composite structural elements, a composite hollow beam containing a hollow steel section, which is fully encased in concrete by investigating its flexural behavior experimentally and numerically. This hollow steel section fully encased in concrete section to benefit from its steel properties as a structural function and hollow core as a service utility and economic reduction of the dead weight and used concrete materials, Therefore, the use of a costly concrete mixture such as ultra-high-performance concrete (UHPC) mixture in this type of elements has a somewhat useful purpose. UHPC is a quality mutation in the concrete technology because it exhibits superior properties such as compressive and tensile strength, durability and ductility, but so far it is relatively expensive.

The first part of the research was experimental investigation consisted of casting and testing fifteen simply supported UHPC composite and non-composite beams under two-point loads up to failure.

This study aims to investigate the ability to encase hollow steel sections in UHPC to increase the flexural stiffness and types of failure modes for UHPC beams. For this purpose, experimental, numerical, and theoretical parts were carried out to study Seven parameters which were best hollow core section material (concrete or cork or steel box), the size of encased steel box in UHPC section, the longitudinal reinforcement in these sections, shape of steel box in the middle and tension zone of section and location effect of steel hollow section.

The experimental results included determining the ultimate load and flexural moment capacities, and strains, load-deflection curves, stiffness, ductility, and crack patterns.

The second part is a numerical study using the finite element method was then employed in investigating the behavior of composite and non-composite UHPC beams. The numerical models were carried out by a software package (ANSYS 15).

The results of the finite element models included the deformed shape, ultimate load capacities, and load-deflection curves. The results were found to be in a convergent state with those obtained from the experimental tests.

Finally, the composite hollow beams had higher ultimate flexural carrying capacities than the non-composite hollow and solid beams at about 109%, while the encasing procedure of steel hollow section in UHPC enhanced the ultimate load and flexural moment capacity, stiffness, and toughness for UHPC beams.

From the results it is noticed that the flexural capacity decrease by 4.91%, when hollow core fabricated using cork material. But the flexural capacity and stiffness increased by 109% and 23.5% respectively when hollow core fabricated using steel hollow section.

The composite hollow beams with steel hollow section ratio 4.73% have a stiffness higher than those having steel section ratio of 3.27% and 2.17%.

The flexural capacity and stiffness of hollow composite beams increases when it is longitudinal reinforcement ratio increases.

Also, from the research it was found that the composite hollow beams which having encased steel section moment of inertia ratio 3.23% have stiffness higher than those having encased steel section ratios of 0.81% and 0.48%.

Also, was found that composite hollow beam which has shear connectors connecting the encased steel box with concrete by welded studs on 4 plates (flanges and webs) of the steel box, has the highest stiffness and higher by 3.9% than the beam which has studs welded only 2 plates (only flanges) of the steel box, and higher by 6.9% than the beam which has not any shear connectors connecting the steel box with concrete.

Contents

Title	Page No.

Section No.	Title	Page No.

List of figures

List of tables

LIST OF PLATES

Nomenclatures

Symbols	Description
a	Shear Span of the Beam, mm.
As	Area of Longitudinal Steel Bars, mm^2.
d	Effective Depth of the Beam, mm.
E_c	Modulus of Elasticity of Concrete, MPa.
f'_c	Specified Compressive Strength of Concrete Cylinder, MPa.
f_g	Ultimate Tensile stress of glass fiber reinforced polymer
f'_r	Flexural Tensile Strength of Concrete (Modulus of Rupture), MPa.
f_{sp}	Cylinder Splitting Tensile Strength of Concrete, MPa.
f_u	Ultimate Strength of Steel, MPa.
f_y	Specified Yield Stress of Steel Reinforcement, MPa.
P	Applied Load, N, kN.
Pcr	Cracking Load, N, kN.
Pu	Ultimate Load, N, kN.
ρ	Longitudinal Reinforcement Ratio.
Єy	Yield Tensile Strain of Steel.

[CHAPTER ONE]

INTRODUCTION

CHAPTER ONE

INTRODUCTION

1.1   General

In the structural engineering, the performance of the structural element depended upon its right function, so each material in the element must be in which the employee in the right place. So recently the trend began to use the composite elements, consists of more than one material in the construction buildings because there is no one material that gives us all the different structural properties. This is a logical reason for the use of two or more materials and connecting them together to obtain both properties of the materials together in one structural element. The use of the principle of composite sections in structural engineering provides us with access to the properties of two different materials simultaneously in one element. Where each material placed in the position that gives the maximum use of the material, with keeping in mind stiffness, strength, the economy of construction and the workability of the material. Previous studies have shown that the composite element gives higher structural capacity than the non-composite element. In the previous studies of the structural beam element, five types of composite sections were used as shown in Fig. (1.1).

1.2 Methods of connection in composite beams

In the composite beam, different materials are connected together to make them act as one unit material. And when these materials not connected together, will separate because of the horizontal shear force between them, leading to decrease the capacity of the composite beam. Methods of connections can be summarized by:

- Connection by bond

In this type, the method of bonding is based on the natural bonding available from the concrete surrounding the steel section from all sides and edges as shown in Fig. (1.2), but prefer to be the steel section surface deformed as with the deformed steel reinforcement in concrete.
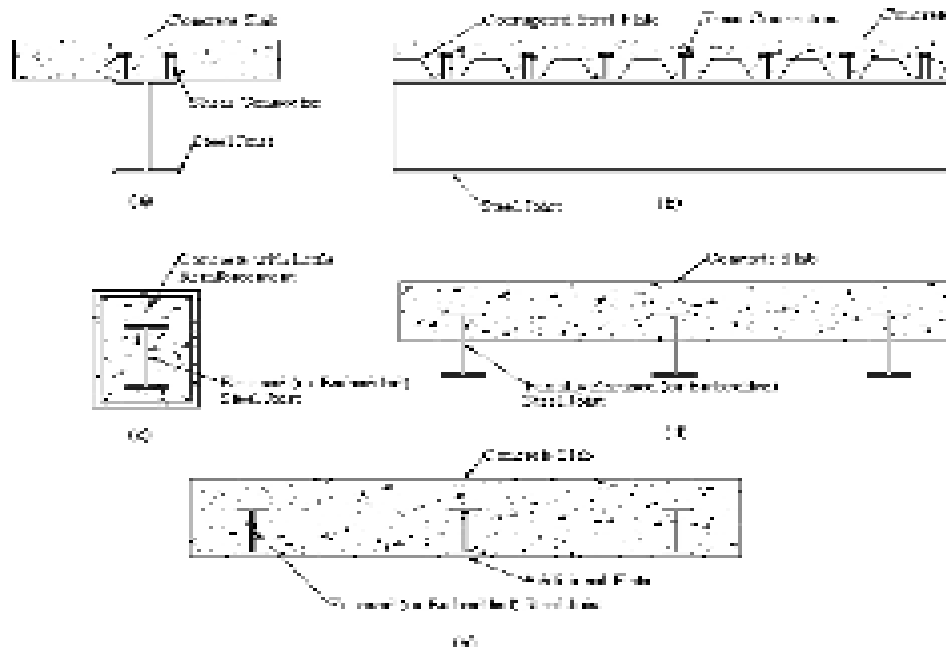
Fig. (1.1) Types of Composite Beams and Slabs [1].

a) Typical Composite Beam of Concrete Slab and Steel Joist. b) Composite Concrete Slab and Corrugated Steel Plate on Steel Joist. c) Composite Concrete Encased Steel Beam. d) Partially Encased Steel Beam. e) Slim Floor Construction.
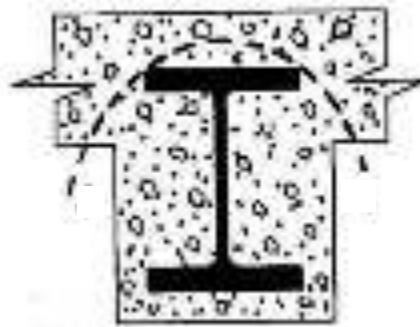
Fig. (1.2) Cross-section of composite encased beam Johanson1975 [2].

- Connection by shear connectors

There are many types of shear connectors and the determination method of the type is related to the shear forces distribution, function, and deformities [3]. It often categorized as rigid or flexible. But in case of resisting horizontal shear and vertical uplift forces in composite steel-concrete structures, the most commonly used type of shear connector is the head stud. As shown in Fig. (1.3).
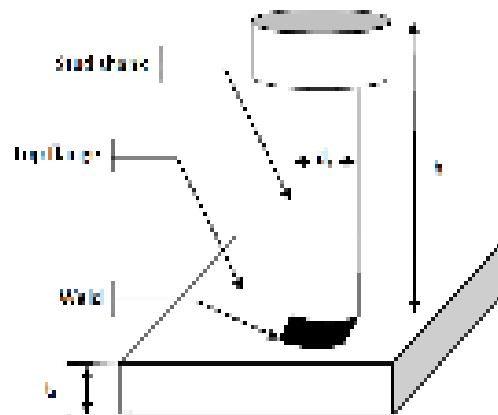
Fig. (1.3) Stud shear connector.

1.3 Evaluation new structural elements with hollow core

In the present research, a new type of composite section was suggested; this section is completely different from the composite sections studied in previous research. Recently, the developments in structural engineering are looking for a structural element that has the function of passing services in addition to its structural function in the building. In order to provide the complete comfort of the user by making the buildings equipped with all types of services. Also, the hollow core in the elements passing services through it with different types of services (plumbing pipes, electrical ducts and cooling/heating ducts). So in this research, a hollow steel section was chosen which expected to benefit from its steel properties as a structural composite function with concrete, economic and services function in reducing the element dead-weight and passing the services. One of the awaited positives of the

developing of this new type of structural element is give an increase in structural strength and reducing the dead weight with control the deflection.

1.4 Advantages of composite hollow sections

This new type of structural elements has several advantages:

- In addition to its structural function, it provides safe and isolated access to service pipelines and protects against environmental damages.
- Compared with the solid beam, this new element has a greater economic benefit in terms of reducing the quantities of concrete to the presence of hollow core and also reduce the dead weight of the beam element.

1.5 Disadvantages of composite hollow sections

The following disadvantages can be summarized as:

- On-site casting requires high precision and high-quality control unless the use of modern concrete free of coarse gravel for easy flow of the mixture in the composite mold.
- This type of structural element may costly as a result of the complex construction process but on the other hand, it is considered an economical to maintain the money related to service runs repairs.

1.6 Ultra high performance concrete (UHPC)

1.6.1 Evaluation of concrete technology

In recent years the process of concrete development has become an important role in civil engineering to produce several new types of concrete mixtures. Because the engineers are now using higher compressive strength limit in their designs, which led to the need for production of new concrete types that differ from ordinary concrete. Several experiments have been conducted to reduce the water content to a minimum and to add new plasticizers to increase the workability of the mixture without adding excess water. Other experiments have been performed to increase

compressive strength by substituting a percentage of the cement used with pozzolanic materials such as silica fume. In addition to the use of these additives materials, the methods of curing the concrete after casting have been changed by developing new methods of treatment, including heat treatment used in ultra-high-performance concrete mixture (UHPC) and pressure treatment by pre-setting the concrete mix.

- The Sherbrook Pedestrian Bridge in Canada was the first bridge in the world which was designed with UHPC as shown in Fig. (1.4).
- South Korea footbridge is another example of using this type of concrete in structural purposes as shown in Fig. (1.5).

Fig. (1.4) Sherbrook Pedestrian Bridge, in Canada.

Fig. (1.5) Seoul Pedestrian in South Korea.

1.7 Scope of the present study

The main objective of the current study is to identify the structural flexural behavior of these new structural elements (composite hollow beams) by applying two-point flexural loads, and recording all the readings resulting from loading in terms of deflections, maximum load capacity and etc. Current research covered the following variables for this new type of structural elements:

1- Effect of the presence of the longitudinal opening in the concrete beam sections and the material in which the longitudinal opening was made whether it was a compressed cork or a hollow steel box.

2- Effect of increasing the size of the hollow steel box encased in the concrete section.

3- Effect of changing the longitudinal reinforcement ratios in this new type of structural elements.

4- Effect of changing the shape of the hollow steel section.

5- Effect of changing the number and arrangement of the shear connectors (studs), that connect the concrete with the steel hollow section.

6- Effect of changing the location of the hollow steel box in the concrete section to find the best location longitudinal opening.

7- Effect of changing the steel hollow section shape within the tensile zone of the section.

1.8 Outline of thesis

The current research consists of six chapters:

Chapter one: explains a general introduction to the present research.

Chapter two: contains historical background and literature review, reviews a number of scientific studies and researches on current research topics published by accredited scholars and researchers.

Chapter three: covers the experimental works in all its aspects in terms of the characteristics of the materials used, the geometry details of the parameters studied for composite and non-composite beams, casting and the procedure of the testing.

Chapter four: includes the results of the experimental testing and provide all the readings recorded during the testing in terms of deflections, cracks, and etc., in addition to discuss the results of these tests.

Chapter five: contains a theoretical study to analyze this new type of structural elements by finite element principles using ANSYS 15.

Chapter six: includes the conclusions obtained from the current research and make several suggestions and recommendations for future studies to develop this new types of composite encased elements more broadly.

[CHAPTER TWO]

LITERATURE REVIEW

CHAPTER TWO

LITERATURE REVIEW

2.1 General

In order to obtain economic benefit and sufficient resistance of the structural members, new structural elements that evaluated by the researchers are the composite elements, consist of concrete and steel sections. The presence of concrete increases the stiffness of the steel, prevents buckling failure of the steel, protects it from weather conditions, and increases its failure capacity.

2.1.1 Shear connection between concrete and structural steel

In the composite beam, the interface between concrete and structural steel is subjected to a uniform load ranges between zero in the mid and it increases linearly until it reaches its highest value at the end. The distribution of the forces is directed towards the area of low stresses at the shear connectors [2]. When connectors reach to its elastic stage as shown in Fig. (2.1), it shows the type of flexible shear connectors as an example of these (bolts).

2.1.1.1 Types of shear connectors

I. **Stud shear connectors**

The most widely used form of shear connector is the headed stud. The head of the stud should be with minimum diameter =1.5d and a minimum depth of head = 0.4d.

(d: nominal shank diameter of the stud).

The material of the studs must be a mild steel type and must be tested and the results of the test should agree with minimum properties **BS 18** [4].

The welding of the steel should be as the requirements in **EN 1993** [6] and the welding of the headed studs and connectors agree with requirements in **EN 13918** [6].

II.   Other types of shear connectors

The other types of connectors may be used such as block, hoop, and channel connectors which are typically used where large shear transfers are required, as an alternative to closely spaced shear studs. The steel material used in the manufacture of any type of shear connectors must be identical to **BS 5950** [7] requirements.
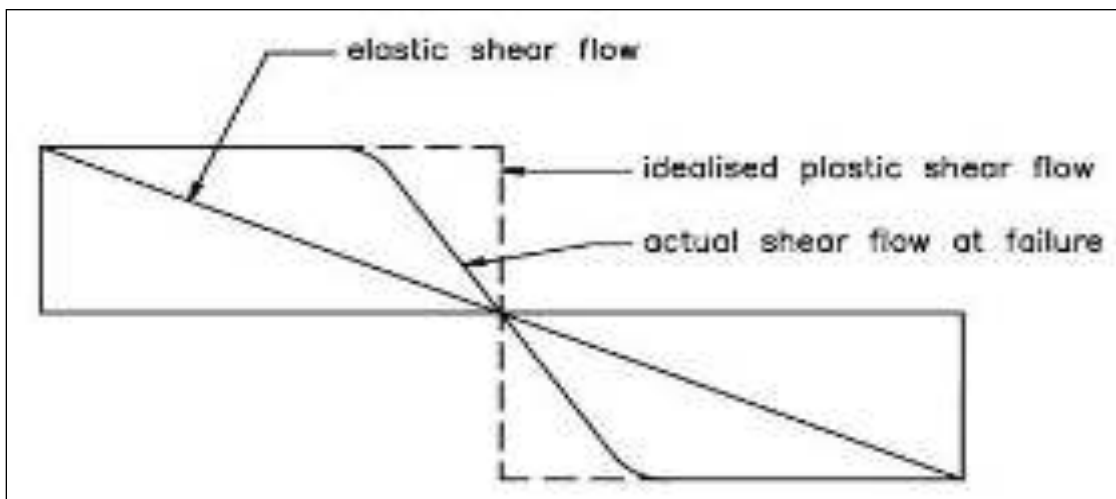
Fig. (2.1) Show the elastic shear flow of shear connectors [2].

2.1.1.2 Strength of the shear connectors

In order to calculate high shear strength of the shear connectors, there are some empirical equations in the international codes such as **Eurocode 4** [8], **AISC** [9], **AASHTO** [10], **Canadian** [11], **Chinese** [12] and **Korea Building** [13], All these codes show that the design resistance is a function of a cross section of the connector, the tensile strength of the steel and the compression resistance of the concrete.

2.1.1.3 Details and limits of the shear connectors

1- The minimum dimensions of stud head should be (h≥3d) and (300mm) as a projection above the bottom reinforcement in order to ensure there is a sufficient resistance exists to prevent separation of composite materials.

2- (**EN1994** [7], **BS 5950** [14]) limit the minimum spacing between the bolts, which have diameter d is (5d) in the longitudinal direction and (2.5d) for transverse spacing between the bolts, and the maximum longitudinal spacing between the bolts can be easily taken as lesser between (800 or 6*overall depth of concrete flange) because the transfer of the shear force by the connector in the design is considered continuous along the beam, as well as to prevent high uplift mentioned by **Johnson** [15].

To achieve the best performance of the shear connectors, the **Japan road association (JRA, 2002)** [16] code recommends that the maximum spacing between the bolts is not more than (800mm nor 3h).

AASHTO, 2005 [17] limits that the maximum spacing between the studs should be less than (800mm).

Eurocode 3 (CEN 2003) [5] the maximum spacing between the bolts should not exceed (4h nor 800mm), and also it gives an additional specification for section type based on thickness and the yield strength of the compressive flange to resist buckling.

Japan Road Association (JRA, 2002) [16] limits the longitudinal minimum spacing is the greater of (5*diameter of the shank) or (100mm) and transfer's minimum spacing is (d+30) mm.

AASHTO [10] limits (6d) as the least longitudinal spacing between the bolts and (4d) as the least transverse spacing between the bolts.

Eurocode 4 [6] limits (5d) as a longitudinal spacing between bolts, and limits transverse spacing as (4d) for rigid concrete and (2.5d) for other slabs.

2.1.1.4 Design of the shear connectors and its number

In 1960, the design of the composite buildings was based on the elastic theory to determine the bending capacity and the design of shear connectors, in this theory, the cross section of the concrete was converted to an equivalent steel section, and the number of bolts determined by the shear flow formula:

$$v = \frac{VQ}{I_c}$$
.....Eq. (2.1)

V = shear force applied

Q = first moment of the area of concrete about the neutral axis

I_c = transformed moment of inertia

In the design of the shear connectors, space must be provided between each shear connector. Space is calculated by dividing the shear strength of the shear connector by the shear flow in Eq. (2.1), because when the shear flow changes along the composite beam, the spacing between the shear connectors must also change.

In 1961, The theory of the plastic approach method was used to calculate the number of shear connectors even though the bending capacity was still based on elastic principles.

Slutter and Driscoll (1965) [18] found that the calculation of the shear connectors requirements by the elastic theory for ultimate bending capacity was very safe. The number of shear connectors is systematically divided along the beam in the interface between concrete and steel. The studs in the composite beam should be designed by total longitudinal shear at the interface determined by the lesser of:

$$V_h = A_s f_y$$
.....Eq. (2.2a)

$$V_h = 0.85 f_c' A_C$$
.....Eq. (2.2b)

A_s: area of the steel beam.

F_y: yield strength of steel beam.

F_C: compressive strength of concrete.

A_C: An effective area of concrete.

The plastic theory assumes that there is a slip between concrete and steel so the total shear force must be distributed equally between the shear connectors.

AISC [19] and **AASHTO** [20] depending upon the plastic theory in calculating the shear requirements of the composite beam, until 1985, the contradiction between elastic theory and plastic theory continued in estimated the bending capacity of the composite beam.

In 1969, **AISC** [21] found that when using Eq. (2.2), the number of shear studs increased when the size of the composite beam increase. Therefore, the standard has found a solution to this problem by proposing a term called (incomplete composite action) with effective section modulus ($S_{e_{ff}}$) which can be found by the formula :

$$S_{e_{ff}} = \frac{V'_h}{V_h}$$ .....Eq. (2.3)

V'_h: design shear force calculated for a given bending strength

In 1978 the term of (incomplete composite) changed to (partial composite), Until **1985**, the term of "partial composite section " continued to refer to the plastic stress distribution in the specification (**AISC**) until fixed in specification **AISC (2005)** [19].

2.1.2 The design philosophy of the composite beam

2.1.2.1 Moment resistance of the composite beam

The simplest form of the composite beam is a concrete connection to the steel section through the shear connectors. Determination of the ultimate capacity of the

composite beam has been mentioned in many international specifications, and all these specifications depended upon the principle of the plastic method approach in determining the ultimate capacity of the composite beam.

2.1.2.2 International code deals with composite beam

The design of the composite beam is mentioned in several international specifications and these specifications are **(AISC-LRFD)** [22], **AASHTO** [20], **British standards (BS 5950, part 3)** [23], **BS 5400** [24], **Eurocode 4-2004** [25], **Australian standards (AS 2327.1-2004)** [26], **Indian code (IS 11384-1985)** [27], **Japan society of civil engineers (JSCE 2009)** [28], and **Canadian Standards Association (S16-01, 2003)** [29]. While some of these codes have a closed –form solution for the bending strength calculation, in terms of stress blocks, and for individuals to refer to the individual regional standards to obtain the equations of bending strength and apply the proper load and reduction factors of capacity.

2.1.2.3 Calculation the capacity of the composite beam by the plastic theory

To calculate the moment capacity (Mp) of the composite beam sections using the plastic theory, consider the following assumptions:

1- There is a full bond between the reinforcement, the concrete, and the steel section.

2- The tensile strength of the concrete is neglected.

3- The construction material of the steel section reaches the yielding stage in tensile and compression at the same time.

4- Steel reinforcement in the concrete compression zone may be neglected.

5- The plan-section of the concrete and steel section remains plan after the load is applied.

6- The compression area of the concrete is stressed to a value (αf_C), and it is constant along the depth of the compression zone.

α: It is used to convert the complex stress block of the compression of the concrete into a rectangular block.

2.1.2.3.1 EUROCODE 4:

When the compressive force of the concrete in the flange the concrete area above the steel section is larger than the force of the steel section so the plastic neutral axis is located above the steel section within the concrete flange, in this case, the depth of the plastic neutral axis is calculated by the equilibrium between the compressive force of the concrete and the tensile forces below the neutral axis.

In the composite beam there are two very common cases as follows:

Case 1: full shear connector

Three cases may occur:

**1.1   *Neutral axis in concrete above steel section when* [25]*:* (see Fig. (2.2a))

$$0.85 \frac{(Fck)cy}{yc} beff\ hc \geq \frac{Aa\ fy}{ya} \qquad \text{.....Eq.(2.4a)}$$

The carry out of equilibrium forces to determine the plastic neutral axis

$$Ncf \frac{Aa\ fy}{ya} = beff\ x\ \frac{0.85(fck)cy}{yc} \qquad \text{.....Eq.(2.4b)}$$

This equation valid when x ≤ has

$$x = \frac{\frac{Aa\ fy}{ya}}{\frac{0.85(fck)cy}{yc}beff} \qquad \text{.....Eq.(2.4c)}$$

After finding the plastic neutral axis we found the neutral axis to get a plastic moment of forces to the neural axis:

$$Mp = \frac{Aa\ fy}{ya}\left(hg + ht - \frac{x}{2}\right) \qquad \text{.....Eq.(2.4d)}$$

**1.2   *Neutral axis in the top flange of the steel section when* [25]*:* (see Fig. (2.2b))

$Ncf < Na.pl$

$$beff \ hc \ \frac{0.85 \ (fck)cy}{\gamma c} \leq \frac{Aafy}{\gamma a} \qquad\qquad …..\text{Eq. (2.5a)}$$

The strength of steel in the compression may be assumed $= \frac{2 \ fy}{\gamma \alpha}$ to simplify the

calculation. So that, the force ($Na.pl$) and its line of action remain constant [25].

So, the plastic neutral axis will be in the top flange of steel section if:

$Na.pl – Ncf \leq 2 \ bf \ of \ fy/\gamma a$ …..Eq. (2.5b)

Equating tensile force with compressive

$Na.pl = Ncf + Nac$ …..Eq. (2.5c)

$$\frac{Aafy}{\gamma a} = \frac{0.85 \ (fck \ )cy}{\gamma c} \ beff \ hc + 2 \ (-ht \ )\frac{fy}{\gamma a} \qquad …..\text{Eq. (2.5d)}$$

The value of x is determined from Equation (2.5d). The plastic moment strength is

calculated from

$MP = Na. \ (hg+ht-hc/2 \ )-Nac(x-hc+ht)/2$ …..Eq.(2.5e)

1.3 Neutral axis lies in the web when [25]***:*** (see Fig. (2.2c))

If the neutral axis location (x) exceeds ($hc + tf$), this means, the neutral axis

position is within the web of the steel section. In structural design, this case is

not favored; otherwise, the web has to be tested for slenderness.

The same above procedure can be used to determined x:

$Na.pl = Ncf + Nacf + Naw$ …..Eq.(2-6a)

$$= Ncf + \frac{2 \ bf \ tf \ fy}{\gamma a} + 2 \ tw \ (x-ht-tf) \ fy/\gamma a \qquad …..\text{Eq.(2-6b)}$$

Plastic moment of resistance

$$MP = Na.pl \ (hg+ \ ht-hc \ / \ 2) - (\ ht+tf \ / \ 2-hc \ / \ 2) - Naw \ (\frac{x+ht+tf-hc}{2}) \quad .\text{Eq.(2-6c)}$$

The notations used here are as follows: -

Ncf: Compressive force in the concrete (N)

Na,pl: Yield force in the steel (N)

Nac: Compressive force in the top flange (N)

Naw: Compressive force in the web (N)

MP: Plastic moment resistance (N.mm2)

Aa = steel section area (mm2)

γa =partial safety factor for structural steel

γc = partial safety factor for concrete

beff =effective width of concrete slab (mm)

fy =yield strength of steel (MPa)

(fck)cy =characteristic (cylinder) compressive strength of concrete (MPa)

hc = concrete slab depth without profile deck (mm)

ht =total depth of concrete slab (mm)

hg = center of steel section depth from top flange of steel (mm)

tf: thickness of the flange (mm)

tw: web thickness (mm)

bf: flange width (mm)

Note: Cylinder strength of concrete *(fck)cy* is usually used as 0.8 times the cubic compressive strength.

Case 2: Partial shear connection

The partial shear connection used because of a problem in the distribution of the shear connectors or to reduce the cost in the shear connectors (economic benefit), so the force carried by the shear stud is taken from the total resistance, in the area where the moment is between zero and its maximum value.

(Fcf) refers to the concept of *(Ncf)* as used earlier. If *(nf)* and *(np)* are the shear connectors number required for full and partial shear connection respectively, then the degree of shear connection is defined as:

Degree of shear connection $= \dfrac{np}{nf} = \dfrac{Fc}{Fcf}$ …..Eq.(2.7a)

It may be assumed that all connectors have the same shear force.

The depth of compressive stress block in the slab is:

$$xc = \frac{Fc}{0.85\ b\frac{(ack)cy}{\gamma c}} \qquad\qquad .....Eq.(2.7b)$$

The neutral axis location may be in the flange or in the web of the steel section. In case the neutral axis is in the top flange of the steel section, the moment of capacity can be calculated using the stress block shown in Figure 2.4c. Here, the block of *Ncf* is replaced by *Fc*; therefore,

$$M_{Rd}= N_{a.pl}\ (hg+ ht- \frac{xc}{2}\ )- F\ \frac{xa+ ht- xc}{2} \qquad\qquad .....Eq.(2.7c)$$

   If the neutral axis is located on the web as shown in Fig. (2.2c), the moment capacity is obtained by taking moment about top surface [25]

$$MRd= Na.pl\ (h_g+ h_c) - \frac{Fcxc}{2} - N_{cf}\ (\ ht+ tf2) - N_{aw}\ \frac{xa+ ht- tf}{2} \qquad .....Eq.(2.7d)$$

Where;

$$Nacf=2bf\ tf\ \frac{fy}{\gamma a}$$

$$Naw= Na.pl- Fc- Nacf.$$
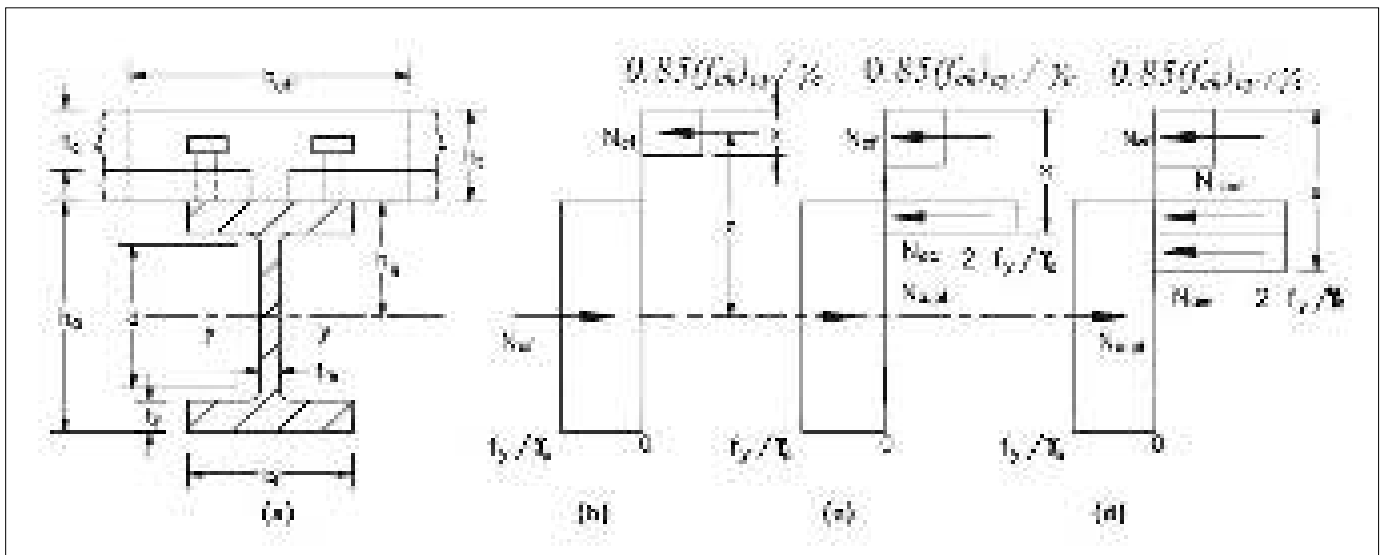
Fig. (2.2) Resistances to Sagging Bending of Composite Section (Full Interaction).
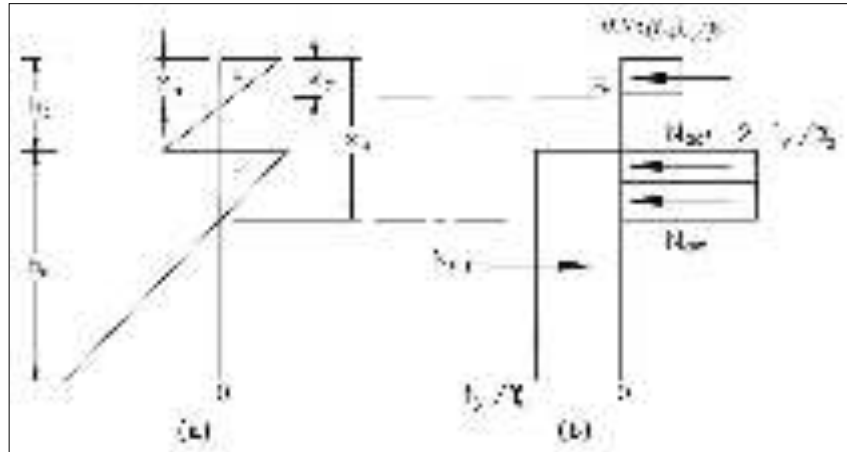
Fig. (2.3) Positive Bending of Composite Section (Partial Connection) [25].

2.2 Literature review of the composite beam

Neelima, (2016) [30] investigated the flexural and shear behavior of fully encased composite beams. The aforementioned study showed compared the uses of longitudinal steel rebars and encased the rolled steel section as major reinforcements. The resulting load-deflection curve (see Fig. 2.4) indicated that the use of the encased rolled steel section (type C) compared with the traditional reinforcing steel rebars (type N) as the main reinforcement was better. The reason is that the curves of the composite section illustrate a high increase in the ultimate strength and minimal deflection resulting from loads.

Shingade (2016) [31] examined the removal of shear reinforcement from the composite beams to study its flexural and shear behavior with and without shear reinforcement. The research variables were the beam with conventional steel reinforcement), the beam with rolled steel angle sections as reinforcement, and the beam with rolled steel channel sections as reinforcement. The experimental results showed that the crack width markedly increases if the shear reinforcement is unused compared with beams with shear reinforcement. Composite beams without shear reinforcement failed as a result of concrete crushing in a diagonal tension.
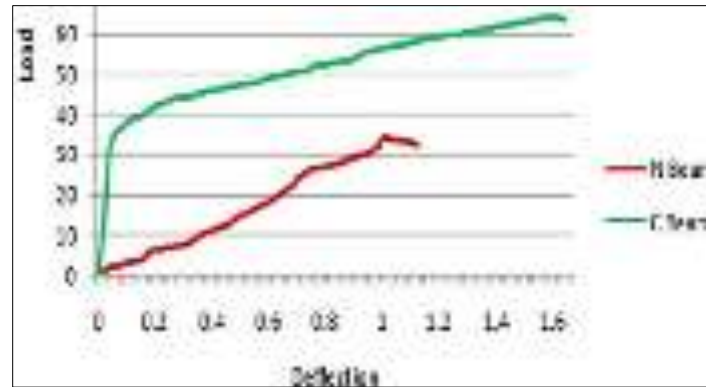
Fig. (2.4) load-deflection curves comparison by Neelima [30].

Kamal (2015) [32] studied the effects of the positions of the upper steel flange in fully encased beams on a composite beam's capacity (see Fig. 2.5). The variables were different ratios of steel section's width divided by the concrete section's width (v = bs / b) values of 0.33, 0.5, 0.67 and 0.86. Each group exhibits variable normalised height (g = hf / hs) values of 0, 0.25, 0.5 and 0.75. The study concluded that the ultimate capacity of the fully encased composite beams is particularly high. The increase in the steel section width showed an increase in the ultimate capacity. Moreover, the presence of the upper steel flange in the composite section delayed the initiation of concrete crushing. Accordingly, lowering the position of the steel section towards the tension zone will delay the initiation of concrete cracks. Lastly, the full encasing of a steel I-section in the concrete increases the capacity that is higher than that of the inverted steel T-section.
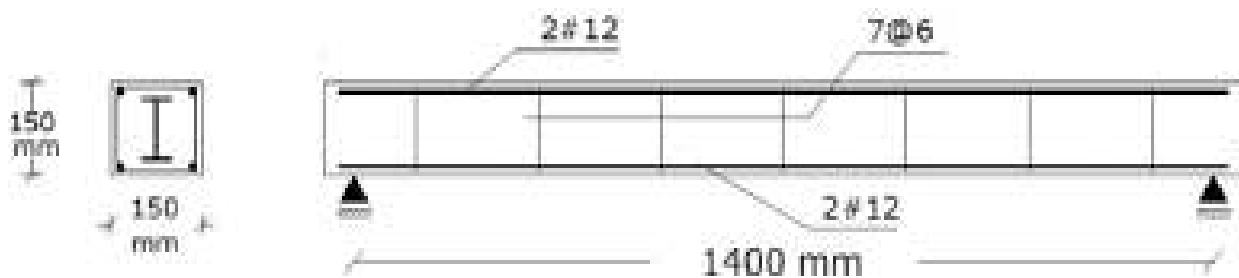
Fig. (2.5) Overall view of the model, by Kamal, 2015 [32].

Shallal (2018) [33] studied the flexural behavior of a composite beam consisting of tubular square sections filled with concrete. The depth-to-thickness ratios (D/t) of the tubular sections were 33.34 and 37.5. These composite beams were subjected to bending load, and the test results were compared with those of a tubular steel section without concrete. The comparison showed that filling a tubular section with concrete increases the maximum moment strength from 47.15% to 87.07%.

V. Kvocˇaˊka and L. Draba (2012) [34] Define their system of partially-encased composite beams as shown in Fig.2.6. Their system consists of encasing the web of steel-section into the reinforced concrete and connecting the concrete with the steel section by shear connectors. This means that the concrete and steel section in partially encased composite beams can be considered as a one-unite if connecting them with shear connectors, which leads to increased capacity and rigidity.
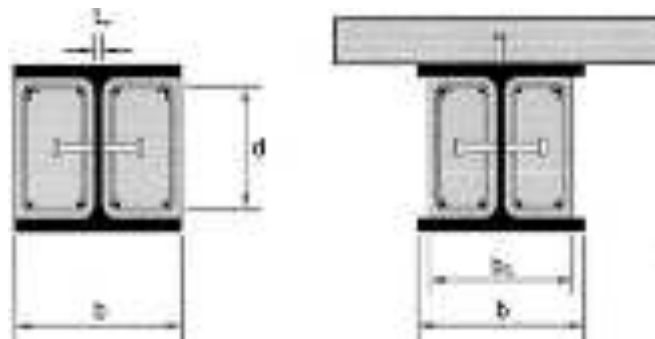
Fig. (2.6) Partially-encased beams cross sections by V. Kvocˇa aˊ ka 2012[34].

Hegger and Goralski (2006) [35] investigated increasing the load capacity for the composite beam, and the increasing bending stiffness. They examined composite concrete encased beam (partially encased) and subjected to a positive and negative moment. They found when the encased beam is fully encased, it will give greater the results in bending and in bearing capacity. During the test, observed the shear

forces between steel and concrete resulting from the forces of friction between them.

2.3 Ultra high-performance concrete (UHPC)

2.3.1 Historical background and development of UHPC

This new type of concrete performs the same tasks of the ordinary concrete mixture, but because of the changes in its composition, it shows better properties higher than the ordinary concrete. It is now one of the best new discoveries on the level of the portland cementitious materials as a main material in the concrete, in these days high strength concrete HPC doesn't still the strongest and durable of the concrete materials. Table (2.1) shows a comparison between UHPC and HPC:

Table (2.1) Comparison between UHPC and HPC.

Material Characteristic	UHPC Compared with HPC
compressive Strength	2-3 times greater
Flexural Strength	2-6 times greater
Elastic Modulus	1.5 times greater
Microporosity	10-50 times lower
Permeability	50 times lower
Water Absorption	7 times lower
Chlorine ION Diffusion	25 times lower
Total Porosity	4-6 times lower
Abrasive Wear	Abrasive Wear
Corrosion Velocity	8 times lower

In France and Canada between 1990 and 1995, concrete development operations were carried out, to develop a type of concrete mixture called (Poudres Réactives), but these days this type of mixture called (UHPC) as scientific names in the design calculations and the international codes such as the **Japanese code JSCE** [36]. To this day, the development research for this type of concrete continues in two different companies (Bouygues Construction) and (Eiffage Group (EIG))

with the help of some other material companies such as (Lafarge Corporation) and (Sika Corporation) as the two most famous construction materials companies, Which led to the development of two products of ultra-high performance concrete (UHPC), under the mediation of these two independent companies, the first company product named (ductal) and the other company product named (BSI) as commercial names, it belongs to the same type of concrete and the same characteristics as UHPC .

The first researchers produced this type of concrete (RPC), which is now called (UHPC) in the international codes, the researchers **(Richard and Cheyrezy)** **[37]**, in (Bouygues) company where they publish the first publication in 1994 developed UHPC200 which gives compressive strength up to 200 MPa, and In 1995, they publish second publication in which the concrete type UHPC800, which has a compressive strength up to 800 MPa, So there are two types of UHPC and each type has a different mixing method, different mixture ratios, different treatment methods, and different result properties. The characteristics and components of these two types are shown in Table (2.2).

Table (2.2) Comparison between UHPC200 and UHPC800.

Composition	UHPC200				UHPC800	
	Non-Fibered		Fibered		Silica Fume	Steel aggregate
Portland Cement	1	1	1	1	1	1
Silica Fume	0.25	0.23	0.25	0.23	0.23	0.23
Sand 150-600 m	1.1	1.1	1.1	1.1	0.5	-
Superplasticizer	0.016	0.019	0.016	0.019	0.019	0.019
Steel fiber 12mm	-	-	0.175	0.175	-	-
Steel fiber L=3mm	-	-	-	-	0.63	0.63
Steel agg. 800 mm	-	-	-	-	-	1.49
Water	0.15	0.17	0.17	0.19	0.19	0.19
Compacting pressure	-	-	-	-	50MPa	50MPa
Heat curing temp.	20	90	20	90	250-400	250-400

2.3.2 Previous studies on UHPC

Parbha [38] investigated the optimal ratio of the steel fibers in the UHPC mixture by using different ratios for several types of steel fibers. The result optimal ratio was 3% for (6 mm) steel fiber length and 2% for (13 mm) length and diameter of 0.16 mm, Specifications of these types of Steel Fiber used were 2000 MPa tensile strength and (38-81) aspect ratio. The optimum ratio of steel fibers in UHPC should be range between (2-3)% of the size of the mold. Other studies showed that the use of Steel fiber with the aspect ratio (45-72) will increase the flexural capacity of UHPC.

The bonding between the steel fiber depends on several factors :

1- matrix spalling and Matrix fracture.
2- De bonding between Fiber and matrix.
3- Friction after the debonding stage.
4- Fracture of the fiber itself.
5- Fiber yielding (plastic bending).

Silvia et al. [39] Investigate the effect of the type of steel fibers used in UHPC mixture and used four types of steel fiber; brass plated steel (13/0.18), deformed steel (30/0.45), deformed steel (30/0.62) and deformed galvanized steel fibers (30/0.62). The proportions of the mixture used composed of 904 kg cement, 226 kg silica fume, 944 kg sand of 0.1 mm particle size, 12.3 kg of carboxylate acrylic superplasticizer, 181 kg of steel fibers, and water-cement ratio (w/c ratio) was 0.24. The results showed that the use of the brass plated fibers in this mixture gives higher compressive and tensile strength than the other types of steel fibers. *Gowriplan* [40] proved that the steel fiber has an effective role in the tensile strength of UHPC, by bridging the crack and prevent it from continuing to

increase, depending on the amount and orientation of the steel fiber. It was found that the decrease in the tensile strength due to pull out some of the steel fibers. Also, it was found that UHPC tensile strength equal to 8MPa when its compressive strength is between (150-220) MPa.

Si-Larbi [41] studied the flexural behavior of UHPC beam with steel fiber, and the aim of the study was to obtain the highest ductility member and the design was based on the European code, It examined the effect of He studied the effect of the existence of shear reinforcement with the longitudinal reinforcement. The result showed that the use of shear reinforcement with Longitudinal reinforcement increases the load by 50% and the use of the UHPC reduced the dimensions of the section from (190*315)mm to (150*250)mm, Therefore, the dead load will decrease by 40%, and compressive strength increase from 40mpa to 140MPa.

2.3.3 Previous studies in the design of UHPC sections

JSCE Code [36] showed the simplification of the stress-strain curve of the UHPC section subjected to a compressive or flexural force, by simplifying the curve by dividing the compressive strength (f'c) on design safety factor (γc=1.3). The standard also sets the value of the modulus of elasticity UHPC as (50000 Mpa).

FHA [42] "Federal Highway Administration, Publication No. FHWA-HRT-06-103", derived an exponential equation depends on the method of curing systems of UHPC to find the stress-strain curve under a compressive load. The equation containing two factors (a,b) to simplify the actual compressive stress-strain.

$$fc = \varepsilon_c (1-\alpha) \qquad\qquad …..Eq.(2.8)$$

Where: $\quad \alpha = a\, e^{\frac{\varepsilon c\, E}{fc\, b}} - a \qquad\qquad …..Eq.(2.9)$

Curing Regime	A	B
Steam	0.001	0.243
Untreated	0.0114	0.440
Tempered Steam	0.0041	0.341
Delayed Steam	0.0044	0.358
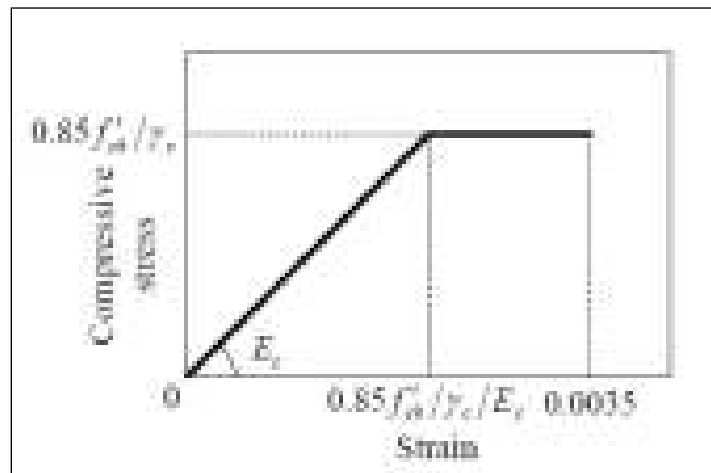
Figure (2.7) Stress-strain relationship -JSCE [36].

2.3.4 Nominal bending moment capacity (Flexural behavior) of UHPC sections

All the design codes of concrete recommend that the flexural design should be (under-reinforced) in order to obtain a ductile failure in the longitudinal reinforcing steel before a compressive failure occurs in the concrete, because the ductile failure in the steel gives a (warning) to evacuate the building but in case of (over-reinforced) the failure will be suddenly and no warning is given.

Most of international codes does not mention the nominal capacity of the (UHPC) sections, but some codes and some researchers proposed equations to estimate the capacity of the section. The difference between these equations is in the simplification of the stress block of compression and tension, some equations

simplify the actual stress block to (a rectangle) stress block and some of them simplify the actual stress block to (a triangle and a square) stress block.
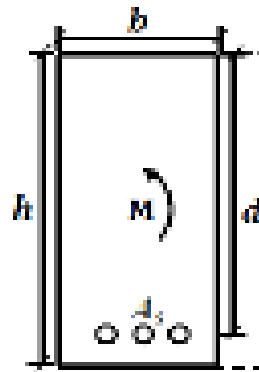
Fig. (2.8) Cross-section of the beam subjected to a pure moment.

1) *Hekmet* [43] simplify actual stress block to rectangular stress block:
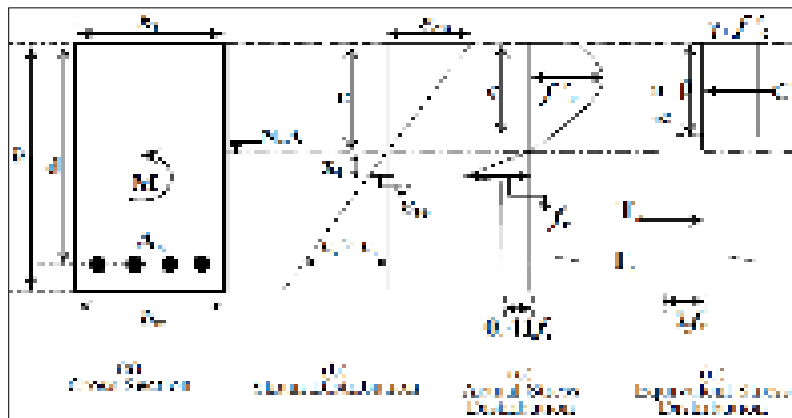
Fig. (2.9) Stress-strain distribution by Hekmet [43]

2) *Samir* [44] simplify actual stress block to rectangular stress block:
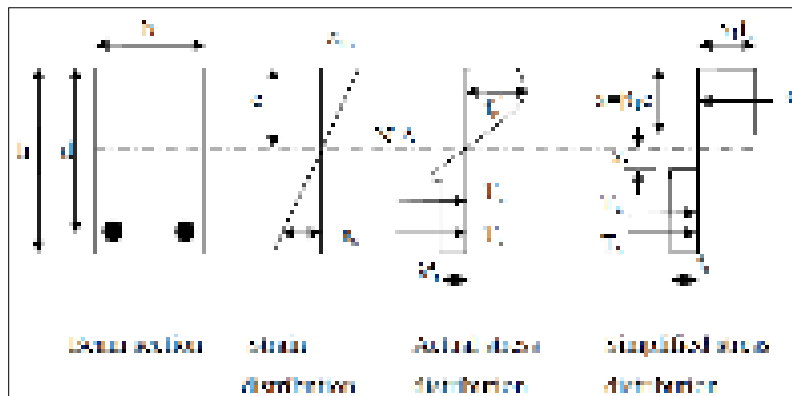
Fig. (2.10) Stress-strain distribution by Samir [44]

After computing the total compressive forces and total tensile forces from the simplified stress blocks, and according to equilibrium between the compressive forces and tensile forces to find the depth of compressive block and the neutral axis, then determining the nominal moment by summation moments around the neutral axis caused by all compressive and tensile forces.

2.4 Literature review of the longitudinal opening (Hollow core beams)

In general, the presence of openings in the concrete beam is an important subject, take the attention of the researchers in the last three years. Because in the past no information is available in books, research journal or the proceedings of conferences on the strength and flexural behavior of RC beams having a longitudinal hole.

Murugesan (2016) [45] investigate the influence of the longitudinal circular hole on the flexural strength of reinforced concrete beams, by testing thirteen beams with dimensions (1.700, 150, 250) mm. All tested hollow RC beams had one hole with (25, 40 or 50) mm diameter longitudinally. The longitudinal holes fabricated using a frictionless PVC pipe and fixed reinforcements cage in the molds before casting. The parameters the research shown in Fig. (2.11). The results showed that the first crack load depended on the distance from the center of the hole to the horizontal centroidal axis of the cross-section. The holes with the higher diameter reduced the moment of inertia higher than others and the resulting reduction in the cracking moment strength.

In 2013, Ghadhban [46] studied the behavior of five non-prismatic RC beams with different hollow shapes and materials. All beams have dimensions of (150x260x1170) mm with the hollow core of (50x50) mm square steel or (50mm)

diameter of circular PVC. The beams are tested in simply supported ends and subjected to two points load. The results demonstrate that the presence of a hollow core in the beam section has led to the decreasing in stiffness and to an increase in deflections and strains. The square steel pipe has led to an increase in load capacity and to the decreased in deflections compared with circular PVC pipe.
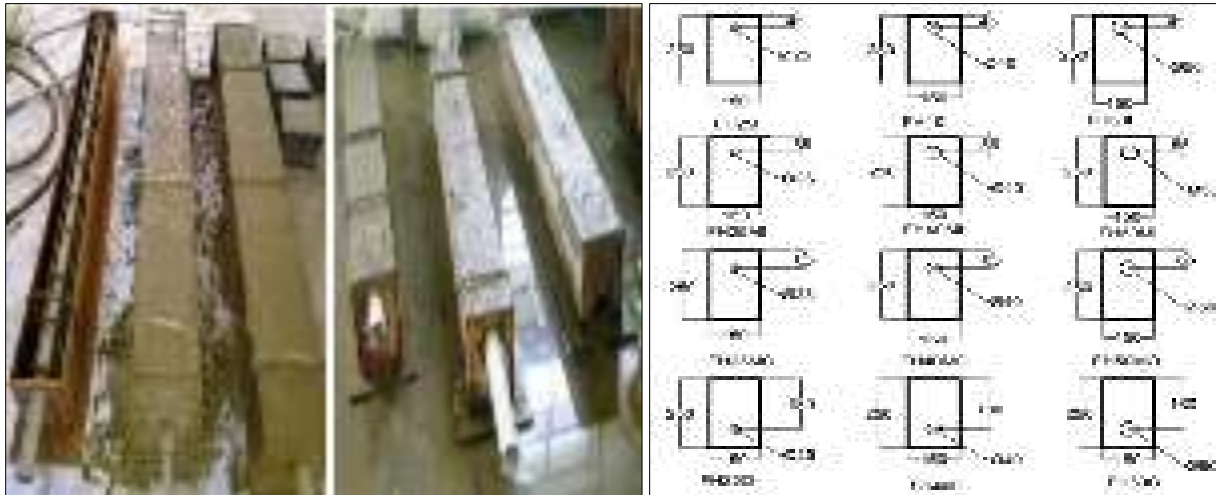
Fig (2.11) The parameters of the casted beams by Murugesan [45].

2.5 Concluding remarks

During the literature review, can conclude the following remarks:

- The composite section used in this study has not yet been studied. Previous researches has focused on the composite section consisting of a steel I-section attached to a concrete slab.

- The effect of using ultra-high performance concrete in this type of composite sections was not studied yet.

- Most of the previous research used cork or plastic pipes in the construction of the longitudinal openings and did not investigate the possibility of using the steel hollow section in constructions of these longitudinal openings.

[CHAPTER THREE]

EXPERIMENTAL WORK

CHAPTER THREE
EXPERIMENTAL WORK
3.1 General

This chapter contains an experimental program of the flexural capacity of composite hollow concrete beams with longitudinal holes in different proportions and different variables to evaluate the effects of these new structural element section and find its structural behavior. These longitudinal holes were made using different materials, such as a hollow steel section in order to increase the flexural capacity of the beams while at the same time using this longitudinal opening section to passing the service runs and to reduce the self-weight of beams. Another material used to make the longitudinal opening mold the (Polystyrene cork blocks). One of the objectives of this experimental work was to obtain the UHPC mixture so, several concrete mixtures were used at different proportions to obtain a target compressive strength of 150 MPa. The maximum obtained compressive strength was 143 MPa which classified as Ultra-High-Performance Concrete. The experimental program containing fifteen composite and non-composite beams. All beams cast and tested under two-point static loads, to see the effect of the hollow steel section in the concrete beam section, in terms of changing the dimensions of the steel box, locations of the hollow steel box, the shape of the steel box and shear connectors. In this experimental part, two types of strain gauges were used for concrete and for steel box to measure strains along the depth of the composite hollow beams. This chapter also includes the specifications of the used materials, the details of the specimens, the molds, the casting tools, and the testing.

3.2 The work schedule

Materials used

| Cement | Fine Sand | Silica *Fume* | Water | SP |

Trial mixes

Select Best Percentages

Mixture with different Silica fume by weight of cement   **Reference Mixture**

| 15 % | 20 % | 25 % | 30 % |

Tests at 28 days

Compressive strength

Split tensile strength

Modulus of rupture

Casting the beams

Curing the beams by heat treatment

Testing the beams after 28 days
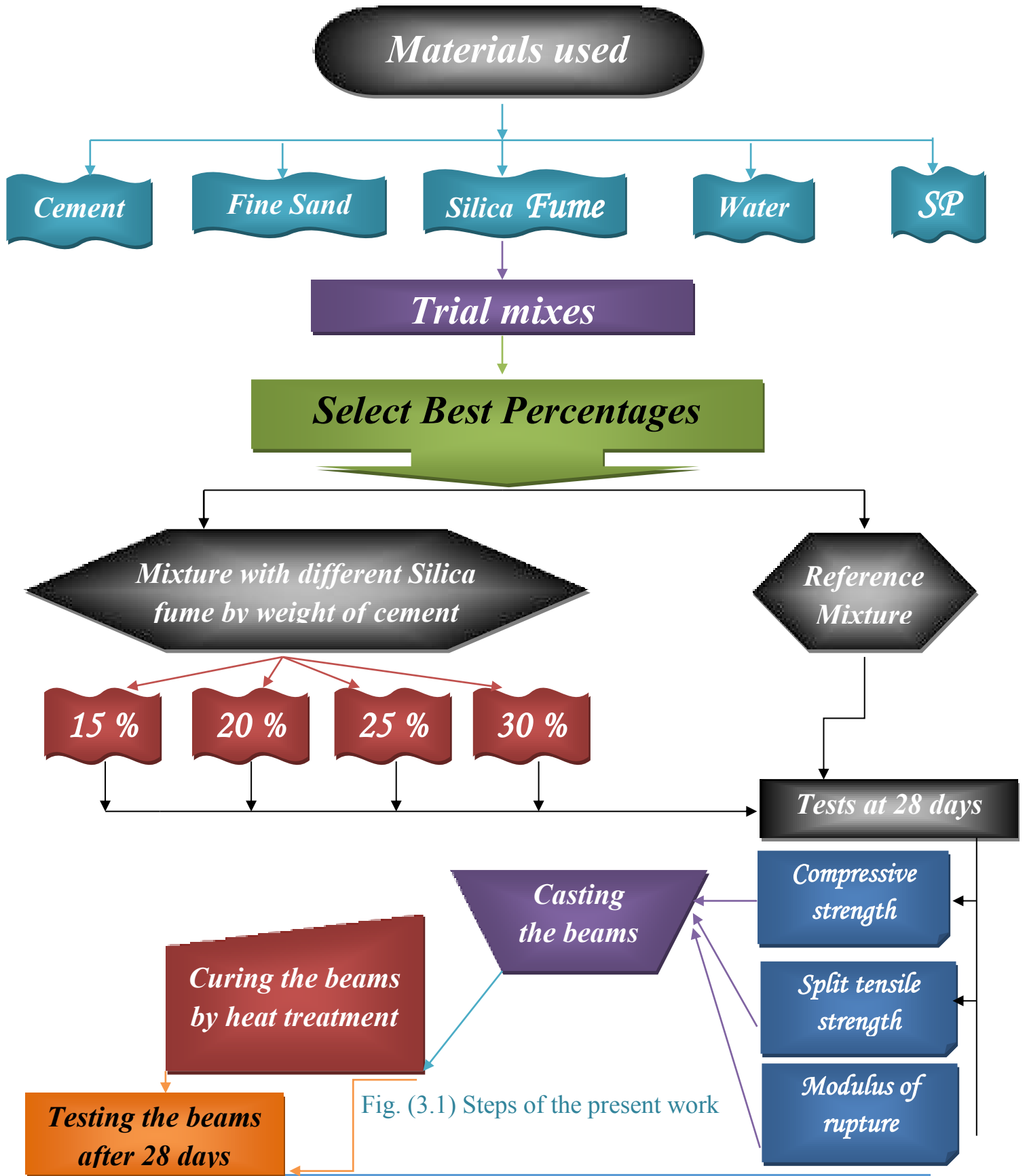
Fig. (3.1) Steps of the present work

3.3 Ultra high-performance mix design

Up to date, no international standard or code is dealing with the Ultra-High-Performance Concrete mixture in terms of the design of the mixture or terms of the design of the structural elements of this mix. There are several previous studies and researches produced this mix and obtained the results based on the laboratory conditions because the ultra-high-performance concrete mix requires special laboratory conditions in terms of casting and curing.

3.4 Compressive strength of UHPC of the current study

In this research, the scope is the reaching to the target compressive strength of 150 MPa, and this target was done based on the past experiences, viz, trial mixes. Several experiments have been worked involving four concrete mixtures of different proportions, in which the compressive strength of concrete noticed to increase due to increasing the proportion of silica fume. So, the ratio of silica fume as additional ratio was used, not as replacement ratio as in the previous researches. As well as reducing the proportion of water as low as possible while maintaining the workability of concrete by increasing the mixing time as long as possible.

3.5 Mixing proportion of the trial mixes in the present work

After carry out the trial mixes, it was found that the trail mix number (1), which contains the highest ratio of the fine materials (cement + silica fume) and less w/c ratio gives the highest characteristics as shown in Table (3.1). So, a trail mix number (1) has been took as a reference mix proportions for structural member (beams) in present research after increase the silica fume ratio from (20%→ 25%) as an (additional) ratio of cement and increase the time of thermal curing from (3→10) days. However, the ratio of silica fume usually takes as

(replacement) ratio from the cement content by (15 to 25) % in the previous researches [51].

Table (3.1) Trial mixes

Trail number	Trial 1	Trial 2	Trial 3	Trial 4
Cement (kg/m³)	1000	1000	825	770
Sand (kg/m³)	1000	1000	1100	1100
Silica Fume (kg/m³)	20 %	15 %	25 %	30 %
W/C	0.2	0.2	0.18	0.188
HRWR	3 %	3 %	5 %	5 %
Steel fiber	2 %	2 %	2 %	2 %
f_c' (MPa)	105.3	91.1	72.9	72.8

Table (3.2) The result of trial mixes of 28 days

Trail number	fc'
Trial 1	105.3Mpa
Trial 2	91.1Mpa
Trial 3	72.9Mpa
Trial 4	72.8Mpa

So, the final mixing proportions of the trail mix (5) are shown in Fig. (3.2):

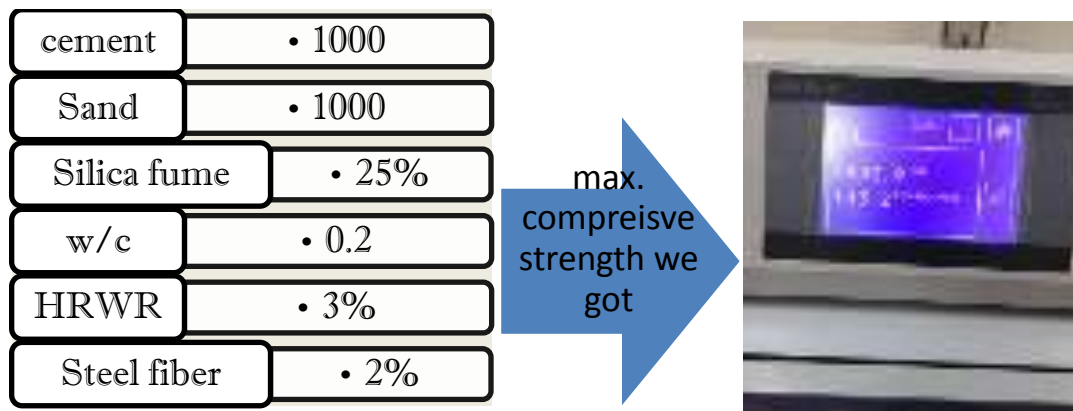| cement	• 1000
Sand	• 1000
Silica fume	• 25%
w/c	• 0.2
HRWR	• 3%
Steel fiber	• 2%

max. compreisve strength we got →

Fig. (3.2) The max. compressive strength we get (trial five).

3.6 Materials properties used for UHPC

The properties of the materials used in this research are listed below, and the process of casting these materials was carried out at the University of Missan-Laboratory of Engineering College.

3.6.1 Cement

Ordinary Portland cement type II, his trade name is Cresta, was used in the present work, which is commonly available in the local markets. It conformed to Iraqi specifications (IQ.S No. 5/1984) [47]. The chemical and physical properties of the used cement are shown in Tables (3.3) & (3.4).

Table (3.3) Chemical Composition of Cement

Oxide composition	Abbreviation	Content (percent) By weight	Limit of Iraqi specification No.5/1984
Lime	CaO	63.96	---
Silica	SiO_2	21.32	---
Alumina	AL_2O_3	4.58	---
Iron Oxide	Fe_2O_3	3.25	---
Sulphate	SO_3	2.48	< 2.8%
Magnesia	MgO	2.75	≤5%
Loss on Ignition	L.O.I	3.46	≤4%
Insoluble residue	I.R	1.07	≤1.5%
Lime saturation factor	L.S.F	0.97	0.66-1.02
Main compounds (Bogue's equations)			
Tricalcium Silicate	C_3S	50.69	---
Di Calcium Silicate	C_2S	18.28	---
Tri Calcium Aluminate	C_3A	8.14	---
Tetra Calcium	C_4AF	9.89	---

Table (3.4) Physical Properties of the Cement

Physical properties	Test Result	Limits of Iraqi Specification NO.5/1984	(7) ASTM C150
Fineness Using Blain Air Permeability Apparatus (m²/kg)	384	≥230	≥280
Setting time Using Victa's Method Initial (hrs: min.) Final (hrs: min.)	2:00 3:45	≥ 0:45 min ≤ 10 hrs	
Soundness Using Autoclave Method	0.22	< 0.8	
The compressive strength of mortar 3Days, MPa 7Days, MPa 28 Days, MPa	20.8 27.4 34.7	≥15 ≥23	≥12 ≥10

3.6.2 Silica Fume

Natural pozzolanic materials have become a significant source in the production of essential materials that enter in the composition of ultra-high performance concrete mixtures, including micro-silica and fly ash. Micro silica is one of the necessary materials in this mixture of UHPC, which is commercially called as silica fume or micro-silica. It is available in local markets with 20 kg sacks. Micro-silica granules are less than 0.1 microns. It is a chemical composition contains (Sio_2). The chemical composition of this type of silica used in present work conformed to ASTM C 1240-04 [52] Standard as shown in the Table (3.5).

Table (3.5) Chemical Composition of Silica Fume

Compound composition	Chemical Composition	Oxide Content (%)	Limit of Specification Requirment
Lime	CaO	0.5	---
Iron Oxide	Fe_2O_3	1.4	---
Alumina	AL_2O_3	0.5	---
Silica	SiO_2	92.1	85(min)
Magnesia	MgO	0.3	---
Sulphate	SO_3	0.1	---
Potassium oxide	K_2O	0.7	---
Sodium oxide	Na_2O	0.3	---
Loss on ignition	L.O.I	2.8	6 (max)

*this technical description provided by the manufacture

3.6.3 Fine aggregate (sand)

The sand used in the ultra-high performance concrete mixture must be free from impurities and mud. Therefore, in the present work, which is stored in 20 kg sags. Its granular gradient conforms to B.S. specification (No.882/1992) [50], the maximum size of its granule is 600µm.

3.6.4 Water

In this work, RO water (Reverse Osmosis, is a water purification technology) was used during the casting and curing process.

3.6.5 High Range Water Reducing Admixture

One of the disadvantages of Ultra-High-Performance Concrete mixture is reducing the water content to reach a too low percentage (W/C =0.2%), in which it is difficult to mix this type of mixture, so it is necessary to add a suitable plasticizer, with highly efficient in compensation for the low water-cement ratio. In the present work a superplasticizer type PC, 260 was used. This type of

plasticizer conforms ASTM C494-99 type A&G [51] standard. It is specially developed for the UHPC mixture in addition to its other uses for other concrete types such as Self-Compacted Concrete SCC or Ordinary concrete casting in a hot atmosphere. This plasticizer is free of chlorides, based on the polycarboxylic-ether-polymer with a long chain especially was designed to enable a water content concrete to perform as more effectively, which directly affects in increasing the workability of the concrete and give it sufficient flow during mixing. The technical specification for this type of plasticizer is described in Table (3.6).

Table (3.6) Technical Description of Flocrete PC 260 *

Chemical Base	*Modified polycarboxylates based polymer*
Appearance/colors	*Light yellow liquid*
Freezing point	*-7 ^{o}C approximately*
Specific gravity @ 25 ^{o}C	*1.1±0.02*
Air entrainment	*Typically less than 2 % additional air is entrained above control mix at usual dosages*
Dosage	*0.5 to 4.0 liter per 100 kg of binder*
Storage condition/Shelf Life	*12 months if stored at temperatures between 2 ^{o}C and 50 ^{o}C*

*this technical description provided by the manufacture.

3.6.6 Steel fiber

The type of steel Fiber used in present work was straight steel fiber with length and diameter (13 mm) and (0.173 mm) respectively. It is imported from China, and its manufacturer is Bekaert corporation. Table (3.7) illustrates the characteristics of this type of steel fiber and Plate (3.1) shows a sample of it.

Table (3.7) Characteristic of the Steel Fibers*

Type of steel fiber	Density (kg/m³)	Length of fiber (mm)	The diameter of Fiber (mm)	Tensile strength (MPa)	Modulus of Elasticity (GPA)
Straight	7800	13	0.175	2600	210

*this characteristic provided by the manufacture.

Plate (3.1) Steel fibers used in the present study.

3.7 Geometry of the tested beams

In the present experimental program, all of the fifteen simply supported beams were in the overall dimensions 1500mm, 150mm, 220mm in length, width and depth respectively as shown in Fig. (3.3), the overhanging length was 50 mm while the shear span was 466 mm. All of the beams specimens were tested under two point loads. The distance between loads was 466 mm. In order to stay away from the requirements of the deep beam principle, the specimen dimensions were

strictly meet ACI318M-19 [52] requirements to overcome the two requirements of the deep beam, because the deep beam gets if one of the following cases occur:

- **If Ln/h ≤ 4 (deep beam) → to avoid that should ≥ 4 (shallow beam)**

- **If a/h ≤ 2 (deep beam) → to avoid that should ≥ 2 (shallow beam)**

In the present research, the clear span (*Ln*) is taken 1400 mm, and overall depth (h) is 220 mm so that the aspect ratio (*Ln*/h) will be 6.36 so, the beam specimen is far from falling in the deep beams' principle.
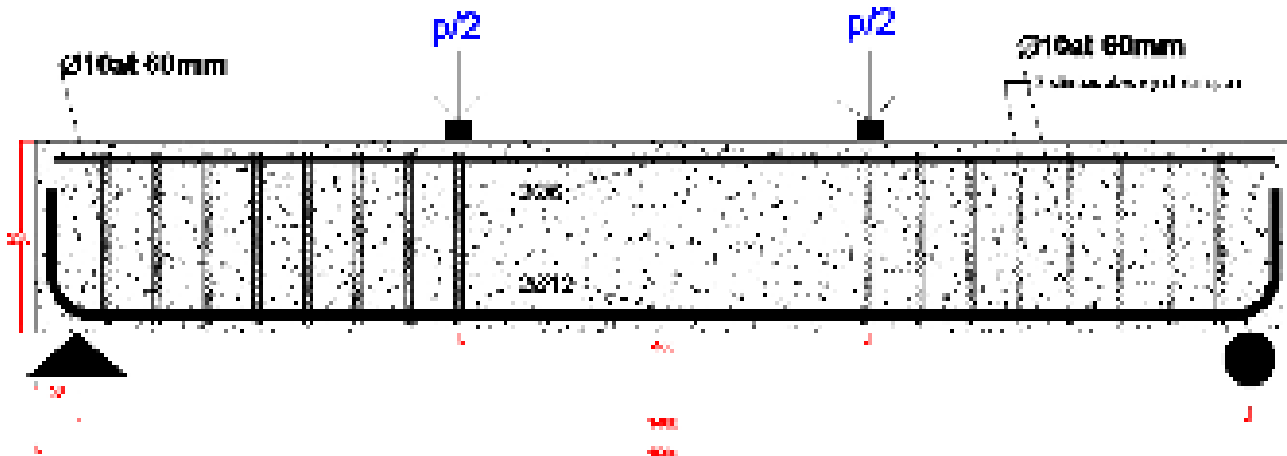

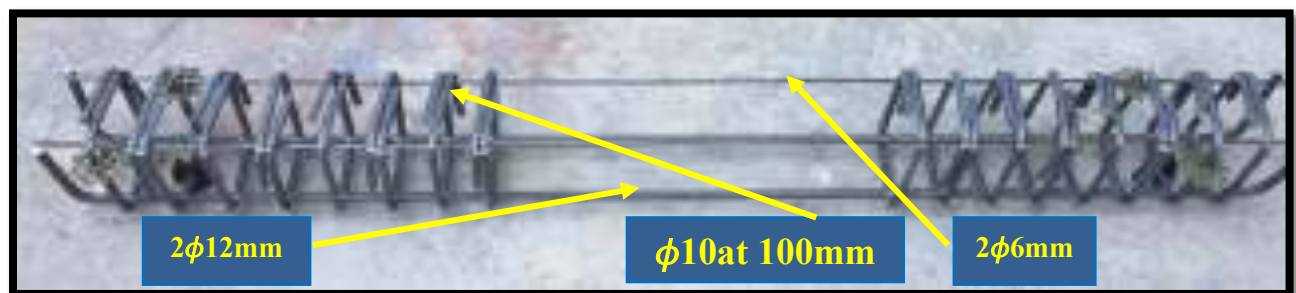Fig. (3.3) Flexural test and geometry (for control beam).

Plate (3.2) Reinforcement details.

The design calculations for the reference composite hollow beam is attached in Appendix A. Its flexural design based on JSCE specification (Japan Society of Civil Engineers) [28] in simplifying the compression zone of ultra-high-

performance concrete (UHPC), and based on the principles of EUROCODE 4 [25] standard in the flexural design of composite sections as mentioned in the previous chapter. The design of the shear was also calculated to avoid falling into the shear failure, and its calculation is attached in Appendix A, it was based on the Japanese (JSCE) [28], British (BS) [14] specifications and researcher (Bunni) [66] for the design of shear capacity of ultra-high performance concrete. Because the present study focused on the flexural behavior, so all the specimens were designed with enough steel stirrups reinforcement (ϕ10 at 60mm) to avoid the shear failure at the shear span, while the pure moment span was not reinforced with steel stirrups. All the control beams were designed by 2ϕ12 (ρ= 0.008) in the bottom of the section. The tension rebars were hooked with (90-degree) and with hook length (144mm). For all beams used 2ϕ6mm steel bars to hold the stirrups in their zone. All the composite beams involved in this research were connected fully bond between the concrete and the hollow steel section by using Enough number of shear connectors (studs). The number of shear connectors is designed to be fully bound by the international standard (Eurocode 4) [25]. Forty-four (44 studs) used in each composite beam, 11 studs for each plate of the four plates of the steel box (flanges and webs). The spacing between these shear connectors was 140mm and conforms to (AISC-LRFD) [54].

3.8 Specimens variables

The main parameters studied in this research are the type of material to make the longitudinal opening (cork and steel hollow section), size, location shape of the hollow steel section. The specimens were divided into seven groups in order to make comparisons between these specimens in terms of the type of failure,

maximum load failure, deflections, cracks and strain levels. Table (3.8) shows a summary for groups of the specimen variables.
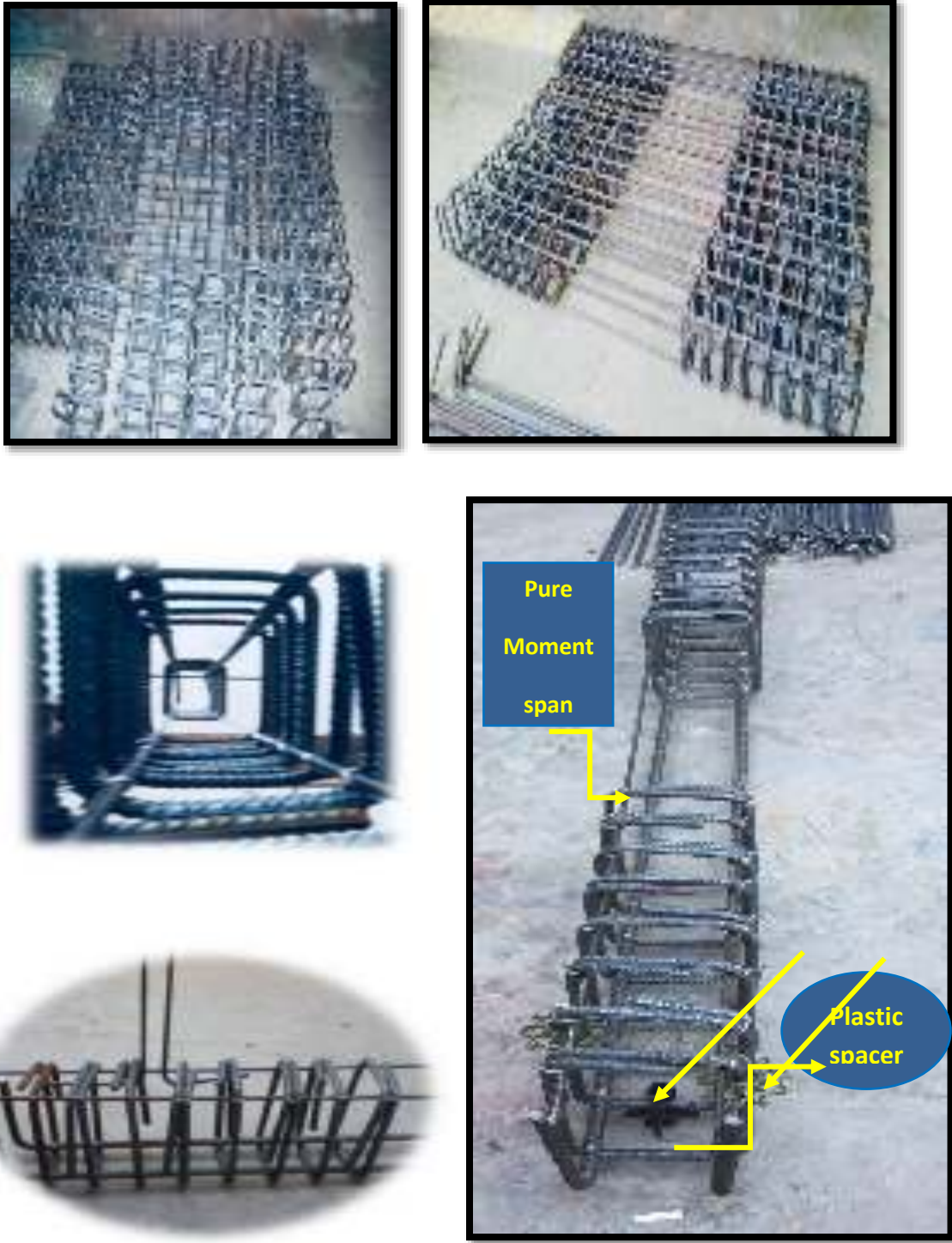

Plate (3.3) General Form of Reinforcement Cages.

The first group consisted of a square longitudinal hole that was once fabricated by compressed cork and then by an embedded steel hollow section, in order to make a comparison between the solid beam (B1), non-composite hollow beam (B2) and composite hollow beam (B3).

The second group investigates the effect of increasing the dimensions of the hollow steel section, evaluating the effect of the area of embedded steel hollow section, and the effect of increasing thickness of concrete flanges. The comparison was made between composite hollow beams encased with hollow steel sections have the following cross-area [(60*60) mm², (80*80) mm² and (100*100) mm²].

The third group includes changing the ratio of longitudinal steel reinforcement to find out its effect on the flexural capacity in these composite hollow beams. So, the comparison was made between the composite hollow beams with the following ratios of steel rebars [$2\phi10$ ($\rho= 0.005$), $2\phi12$ ($\rho= 0.008$), and $2\phi16$ ($\rho= 0.01$)].

The fourth group involves in changing the shape of the hollow steel section to study the effect of the changing the moment of inertia of the embedded steel section on the flexural capacity, where the comparison between composite beams containing (square steel box, circular steel box, and rectangular steel box).

The fifth group includes changing in the arrangement and number of the shear connectors of these elements, where the comparison was made between a composite hollow beam encased with steel hollow section connected to the concrete through the shear connectors along its length from all its plates (flanges and webs). The other composite hollow beam encased with the steel box connected with concrete by connectors in the above and below flanges only, and

another composite beam contains a steel box with any shear connectors. Studs of diameter size 8 mm and 50 mm in overall height with a head diameter 14 mm and height of head 5 mm were used in the above and below flanges of the steel box.

This comparison in the fifth group is to find out the possibility of reducing the number of the shear connectors in the webs of steel box and study the composite action of steel box and UHPC, to prevent the separation between the steel section and the concrete due to the presence of two opposing stresses in the direction.

The sixth group studies the effect of changing the steel hollow section's location, where the comparison is made between the composite hollow beams encased with steel hollow section in the middle of the section, so part of the hollow steel section will be in the compression-zone and part of it in the tensile zone. The other composite hollow beams encased with hollow steel sections in the bottom zone of the UHPC section so that the entire steel box will be in the tension zone of the UHPC beam.

The seventh group includes the effect of pushing the steel box downward to the tensile zone of the UHPC section, to investigate the effect of steel hollow section's shape in the tension zone, and to find the effect of change of the moment of inertia of the steel Box within the tensile zone.

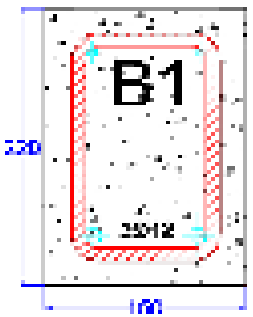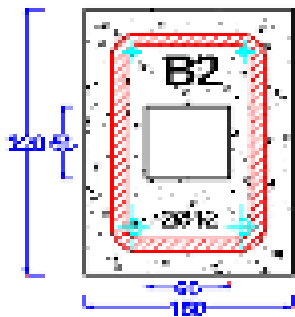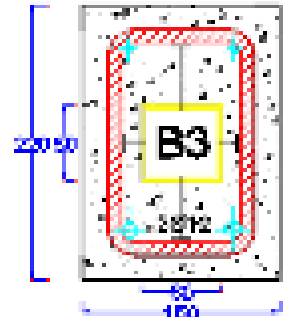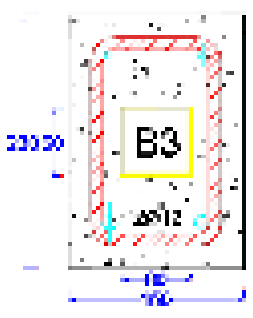Table (3.8) Groups of the beam tested with details
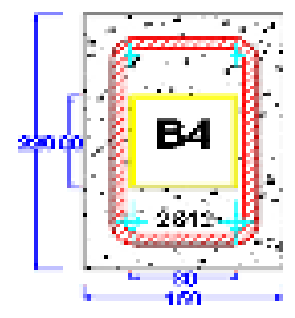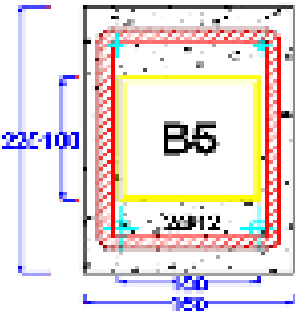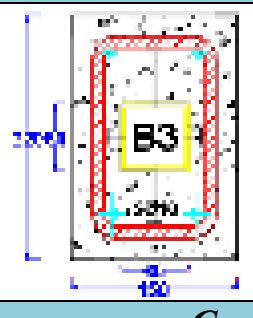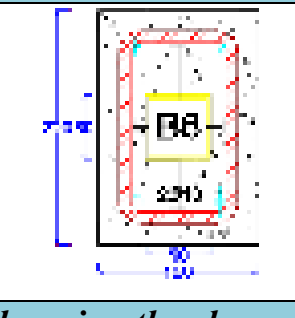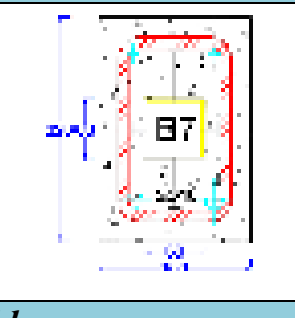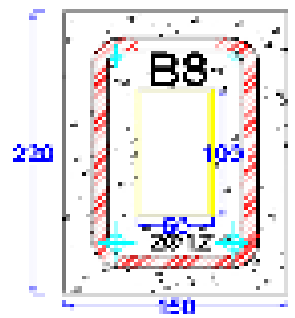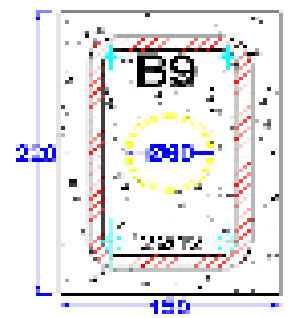
Group No.(1): Comparison between the solid and hollow beam and composite hollow beam		
Group No.(2): Changing the size of the steel box		
Group No.(3): Changing longitudinal reinforcement		
Group No.(4): Changing the shape of the steel box		

Table (3.7) Continued.

Group No.(5): Changing the arrangement of shear connectors
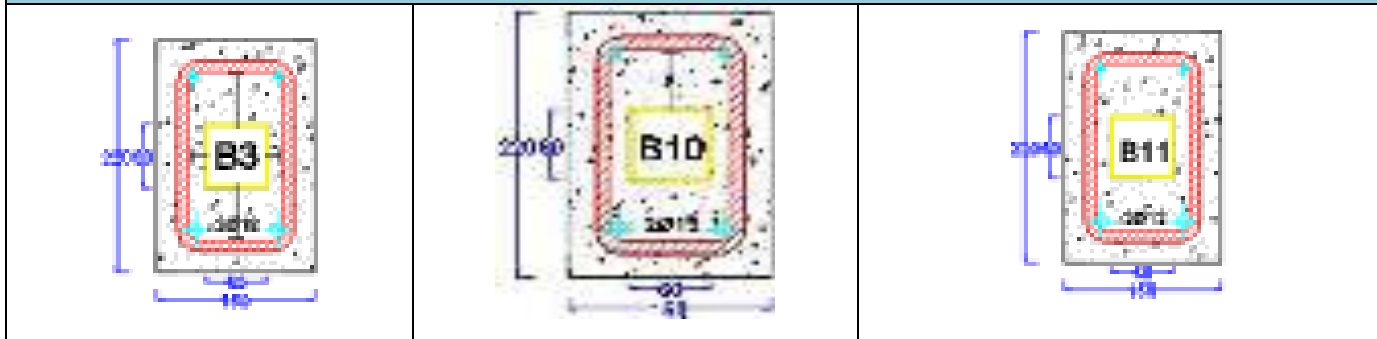
Group No.(6): Changing the locations of steel box
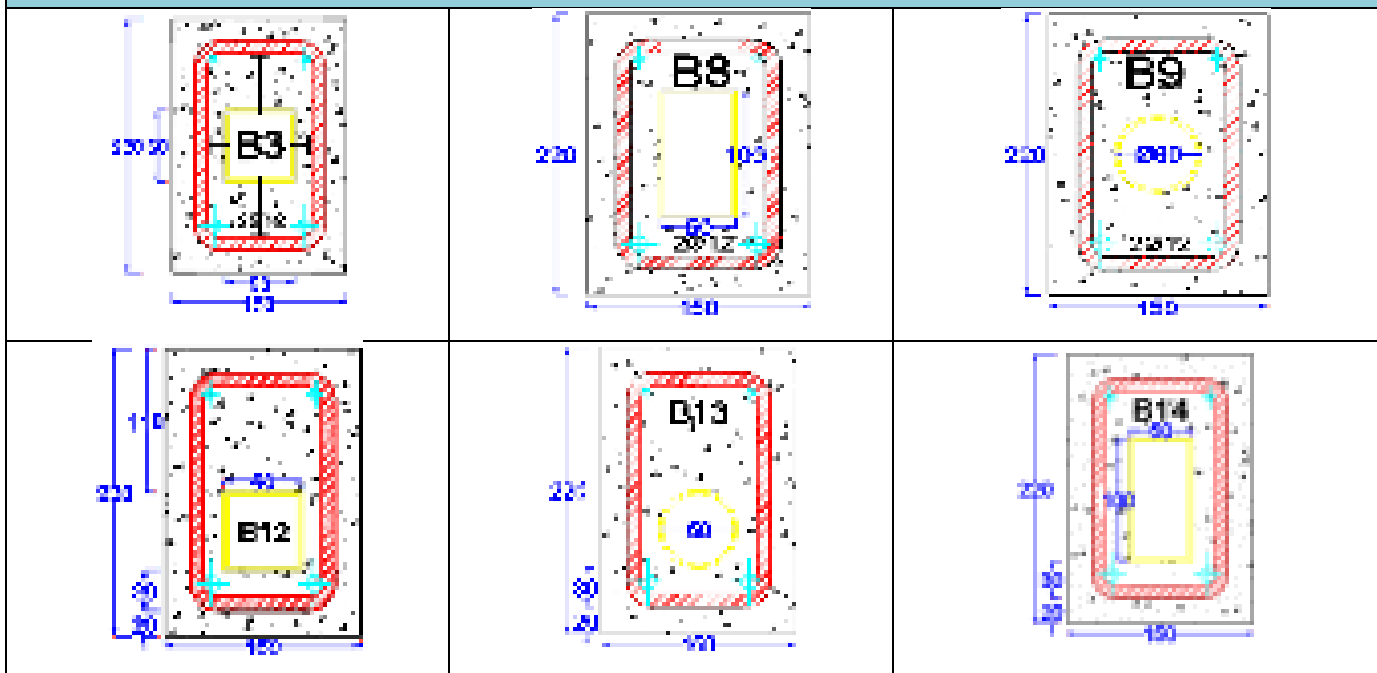
Group No.(7): Put the steel box in the bottom part (tension zone)
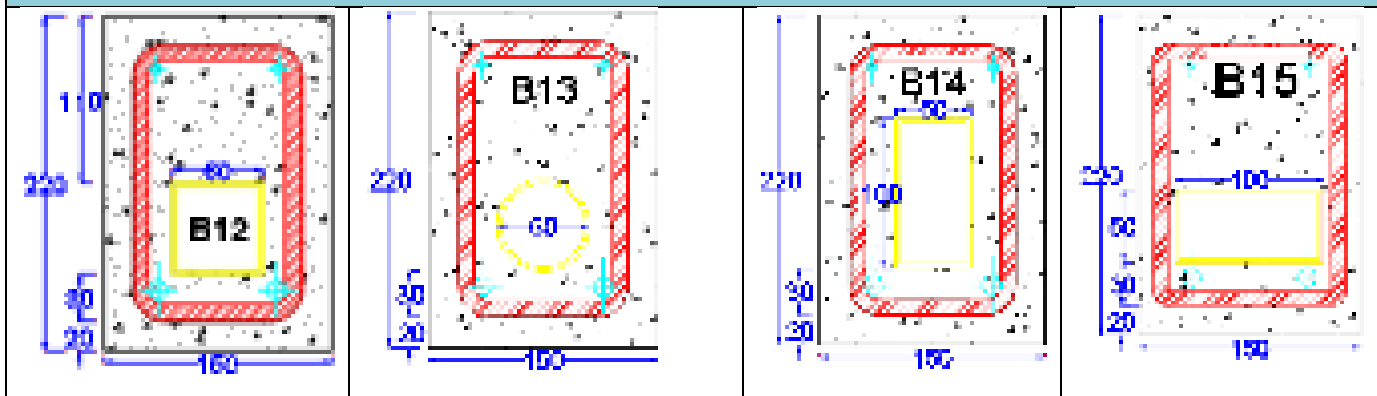
3.9 Steel material used in the present work

In the present work composite hollow beams contain many steel materials such as (hollow steel section, shear connectors, and the steel reinforcement). In this section, the properties of the steel materials will be included.

3.9.1 Steel hollow sections

Several steel hollow sections were used in the present research in different shapes and dimensions. All the steel sections have the same thickness (2.8mm). All steel sections were purchased from local markets, which are imported from Turkey. All the steel section sold in local markets with a length of 6000 mm, it is cut into a length of 1700 mm by Electrical cutter as shown in the plate (3.4). The shapes and dimensions from the used steel sections are summarized in Table (3.9).

Table (3.9) Steel hollow section used in the present study

| Steel section shape	square hollow section	rectangular hollow section	circular hollow section
Cross-section area	(60*60, 80*80 and 100*100)mm²	(50*100) mm²	ϕ 60mm
Thickness	2.8 mm	2.8mm	2.8mm

All the hollow steel sections were tested according to the American specification for steel materials testing ASTM A370-10 [55], where the section was cut to be in the form of bone as shown in Fig. (3.4).
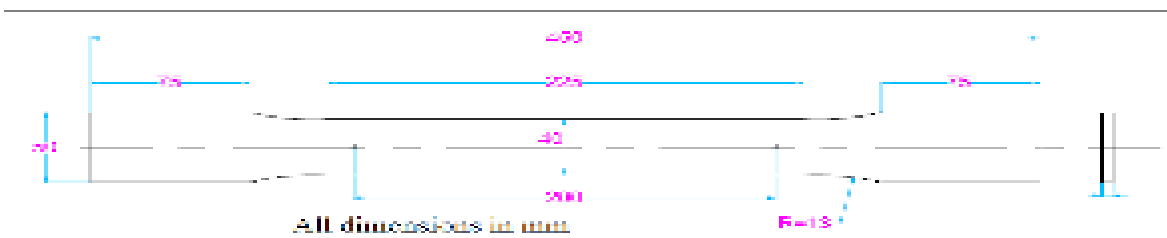
Fig. (3.4) Dimensions of Standard Specimens According to ASTM [55].

Table (3.10) Tensile properties of the steel sections (average of three samples)

Dimensions of steel hollow box	Average of Yield Tensile Strength (MPa)	Average of Ultimate Tensile Strength (MPa)
60*60	320	375
80*80	317	380
100*100	316.97	395.39
60	327	446

Plate (3.4) Different steel sections used in this research.

3.9.2 Shear connectors

Shear connectors were used between the steel box and the concrete to provide a full bonding interaction and to prevent the separation between them by resisting the different shear stresses between them during the loading. The type of shear connectors used in the present research is headed studs (bolts). Studs of diameter

size 8 mm and 50 mm in overall height with a head diameter 14 mm and height of head 5 mm were used in the above and below flanges of the steel box. In the webs of the steel box, the studs had the same dimensions except the overall height was 30 mm. In composite section there are two criteria for estimating the required number of shear connectors depended on the type of bonding, a lower number provide (partial bond), and upper number provide (full bond). The upper number of the shear connector was used in the present work in order to obtain the full interaction bonding, and designed according to (EUROCODE 4) as shown in (Appendix A). Welding the shear connectors 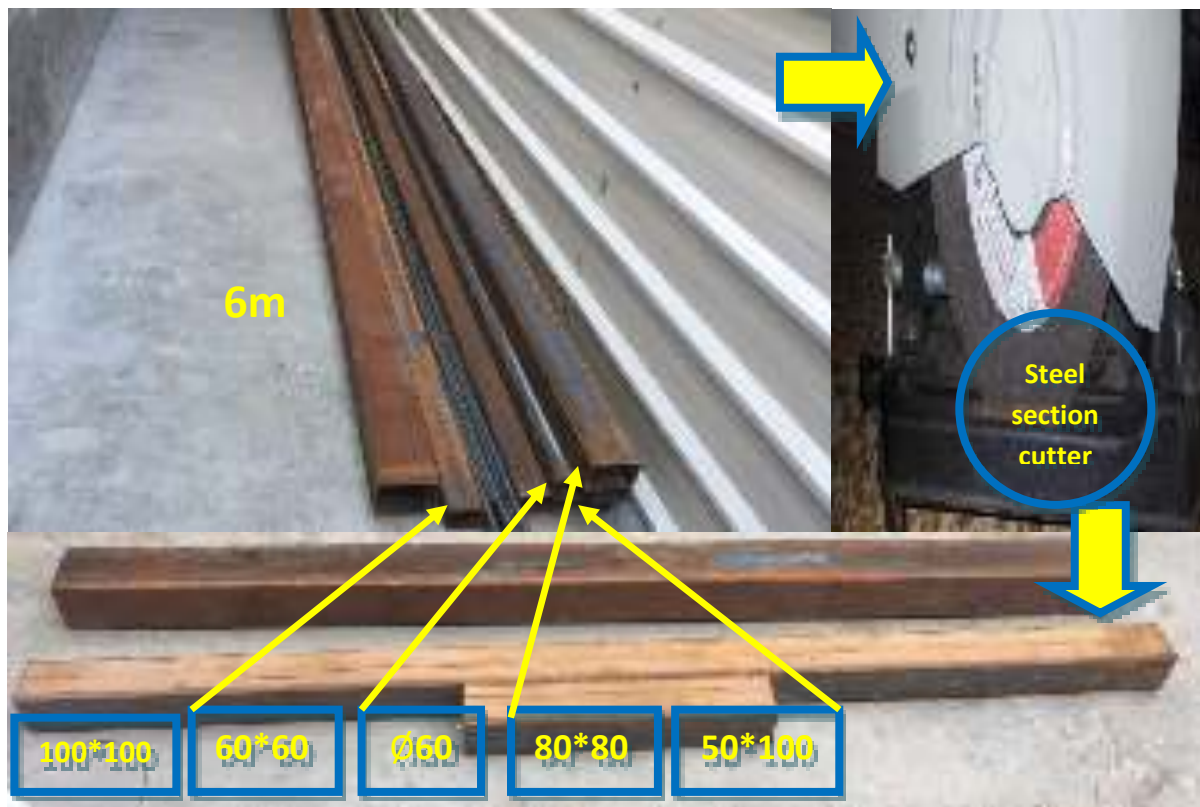on the above and below flanges, and on the web is done using by using Electrical arch welding as shown in the plate (3.5). Mechanical properties of the shear connectors used are shown in Table (3.11).

Table (3.11) Tensile properties of the used headed stud shear connectors

Shank Diameter of Shear Connector's (mm)	*Average of Yield Tensile Stress (MPa)*	*Average of Ultimate Tensile Strength (MPa)*	*Average of the Tensile Modulus of Elasticity (MPa)*
10	*315*	*450*	*207500*

3.9.3 Steel reinforcement

In this research, four sizes of steel reinforcement were used (φ6, φ10, 12φ & φ16)mm, as longitudinal or horizontal steel reinforcement (stirrups). All the steel rebar were Ukrainian and can be identified through the brand stamped on the blinds as shown in the plate (3.6).
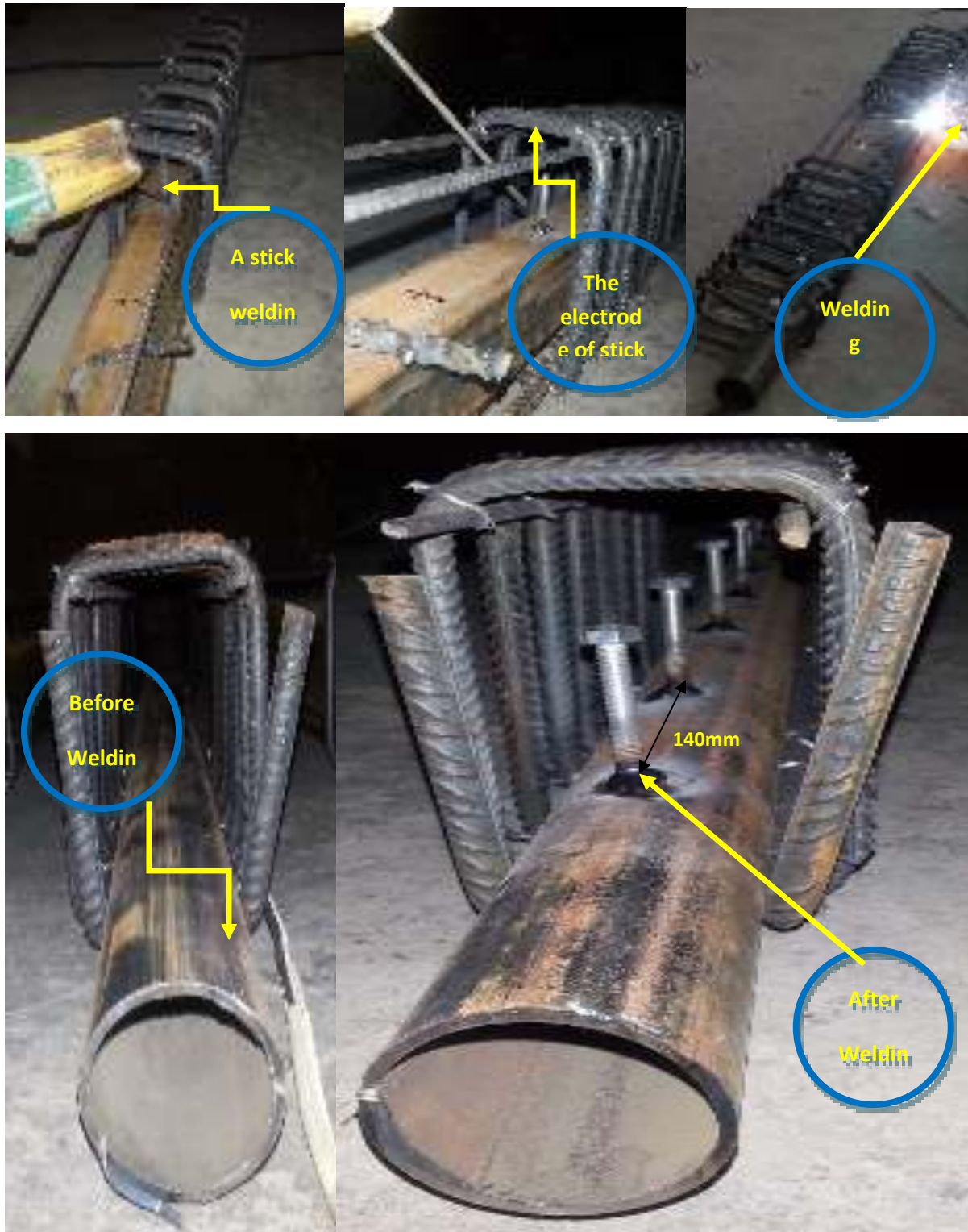
Plate (3.5) The welding of shear connectors.
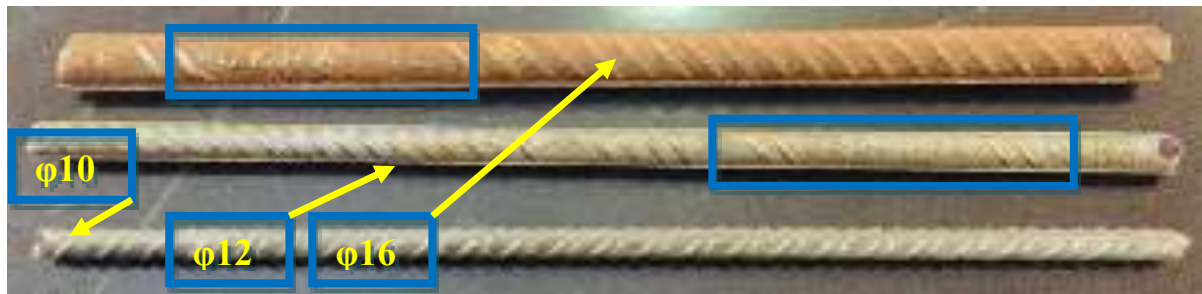
Plate (3.6) Sizes of rebars used in the research.

The British B.S. specification (B.S.4449/1997) [56] was used to determine the tensile strength of the reinforcing steel used in the research. Three samples were taken from each diameter of reinforcing steel bars. The tests were carried out in the Department of Production and Metal Engineering at the University of Technology using the testing machine SANS 1000 kN. The results of the tests are shown in Table (3.12).

Table (3.12) Properties of Steel Reinforcement

Bar diameter (mm)	Bar area (mm2)	Yield strength fy (MPa)	Tensile strength fu (MPa)	Yield strain
6	28.26	533	631	0.00267
10	78.5	515	624	0.00258
12	113.04	493	583	0.00247
16	201.06	500	610	0.00223

3.10 Specimens preparation

3.10.1 Mold preparation

Fifteen ply-wood type molds were prepared, and the plywood was selected with the highest thickness available in the market. The mold parts were tightly linked in a way that made it easier to separate the parts after the casting process

without any effect on the concrete beam, and the single wooden mold consists of five parts:

1-Base mold dimensions 1500×150×18 mm

2- Sidewalls with dimensions of 1500×220×18 mm

3 - Small side pieces of dimensions 220×150×18 mm and have an opening with the same dimensions of the steel box of each composite beam for installation of the steel box.

In the present work, the beams having a longitudinal opening (hollow core). Either made those openings by encased steel hollow section or the compressed cork which must be extended from both sides of the beam. Therefore, a length of 10 cm of the steel box or compressed was left from each side in order to fix them and to ensure the stability the steel box or compressed cork and prevent the movement during the casting process. Due to the concrete mixture used this work without coarse aggregate, which leads to the smooth exit of the mold from the small openings or the edges of the wooden mold and the edges of the steel box, a silicon pistol has been used to put silicon on these edges and prevent the mix from exiting from it. In order to maintain the geometrical dimensions of the concrete beam after casting, two wooden pieces were placed on the top of the mold to fix the mold tightly. After completing the mold, plastic spacers were placed on the base of the mold and on the two side walls of the mold to provide a concrete cover for the reinforcing steel cage. In order to make concrete specimens having one level, several wooden pieces were connected to the bottom of the mold to lift the mold from the ground. Also, after manual bubbled leveling instruments leveled that molds. The fifteenth molds are shown in the plate (3.7).
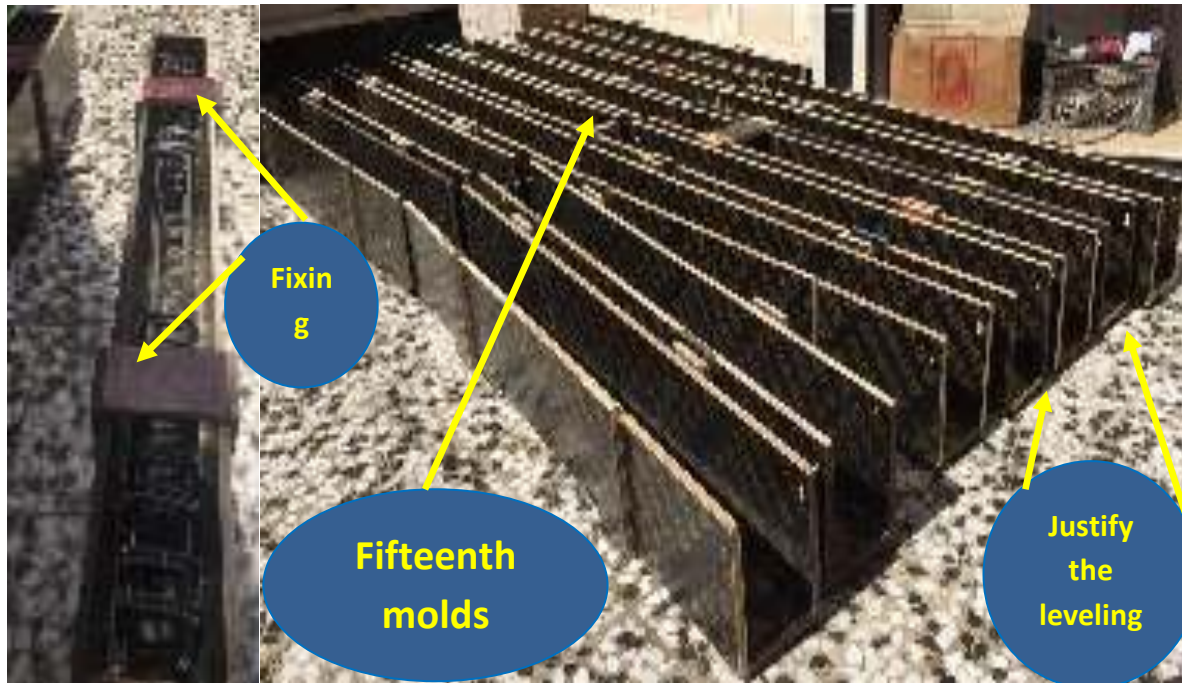
Plate (3.7) The fifteenth molds used in this research.

3.10.2 LONGITUDINAL OPENING FABRICATION PROCESS

In this study, two types of materials were used for fabricating the longitudinal opening (hollow core) in the cross-section of the UHPC beams. These materials are listed below:

1- By Polystyrene compressed cork blocks:

For obtaining a longitudinal hole (hollow core) in a non-composite hollow beam (B2). Core mold was made of styropor (compressed Polystyrene cork blocks), the cork material was packed with adhesive tape to increase its resistance to breakage during the casting process. It was passing through the steel gage. To obtain a hollow opening section by about (60mm*60mm) in the longitudinal direction. The cork was connected to the steel cage using a tiny steel sticky **(∅6)**mm, and silicone glue is used to connect it with the plywood mold. Plate (3.8) shows the process details of using cork in fabricating the hollow core.

2- By Steel box section:

Steel sections were used with different dimensions and shapes (square, rectangular and circular). It was passed through the steel cage and the wooden mold from two sides (for fixing purposes). Plate (3.9) shows the process of installation of the hollow steel box within the mold.

3.11 Mixing procedure for the specimens

Mixing is the most challenging part in the UHPC mix casting because of its low w/c ratio. So, the method of mixing is an essential issue in this mix because the UHPC mix needs high-speed mixing. The past researchers usually using a horizontal mixer with a vertical shaft and rapid mixing. However, in the present work two manual mixers with (120-500r/min) which give a rapid rate of mixing to obtain the UHPC. The Ultra-High-Performance Concrete mixing process involves several steps. Ultra High-Performance Concrete shall be free of coarse gravel. Therefore, the UHPC has a similar characteristic of self-compacted concrete which is outside the scope of our study, so the workability test (slump test) did not measured.

3.12 Pouring of the specimens

Before starting the casting process into beam molds, the molds of structural beams were placed on the ground and leveled by small wooden pieces in the bottom of plywood mold for (leveling purpose) and then level the molds by manual bubbled leveling instrument. The water used in the casting process was RO water (Reverse Osmosis, is water of purification technology). Due to the presence of the steel box and the compressed cork in the molds, the process of compaction by the gasoline vibration machine is not possible, so the compaction stick was used instead of it. After the pouring of concrete, the surface of

specimens is leveled by a steel trowel. A wet rib lab was used to cover the specimens after pouring the concrete into the molds as shown in the plate (3.11).

3.13 Curing process of UHPC

"Heat treating is performed after the concrete has set, by simply heating at ambient pressure. Heat-treating at 90°C substantially accelerates the pozzolanic reaction, while modifying the microstructure of the hydrates which have formed. However, these hydrates remain amorphous". This curing process was adopted by past researchers such as Mahdi [57] and Jungwirth [67]. Plate (3.12) shows the water tank that was locally manufactured for heat treatment. It was equipped with two thermometers to heat the water to a temperature of 90 ° C. It was supplied with thermal insulation consisting of two layers of thermal sponge designed for this purpose as shown in the plate (3.13).

3.14 Testing for mechanical properties of UHPC

To determine the main mechanical properties of Ultra-High-Performance Concrete UHPC mix, three tests are performed to determine three mechanical properties (compressive strength, splitting tensile strength and modulus of rupture). These tests were carried out according to the specifications of the American Society for Materials Testing (ASTM). Fig. (3.5) shows a simple outline for these tests. All these tests were done at the University of Misan - Faculty of Engineering Laboratory.

Fabricating hollow core by cork

Cork material into the steel

Fixing stick

silicon glue

Hollow core beam ready for casting

Plate (3.8) Preparing the opening mold for the hollow beam(B2).

1.Cultivate hollow steel box through the steel cage

2.fix the steel box within the plywood mold

3.fifteenth composite beam ready to cast

Plate (3.9) Installation steel box and fixed it.

Plate (3.10) Mixing's steps of UHPC.

Plate (3.11) Pouring specimens.

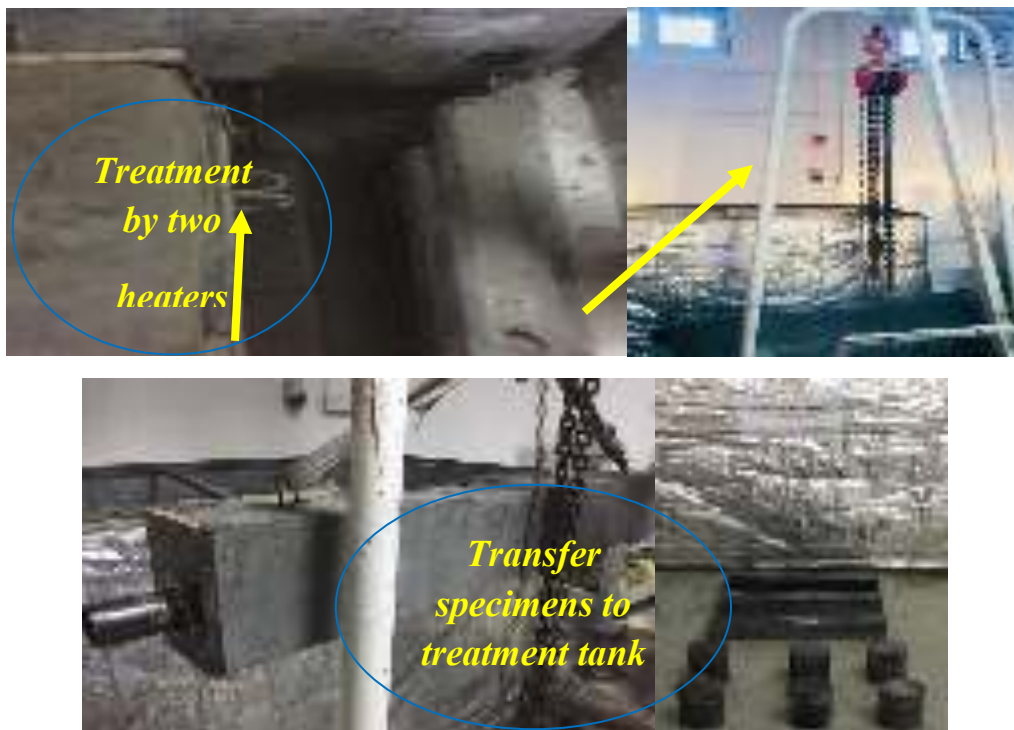Plate (3.12) Preparation of the treatment tank.

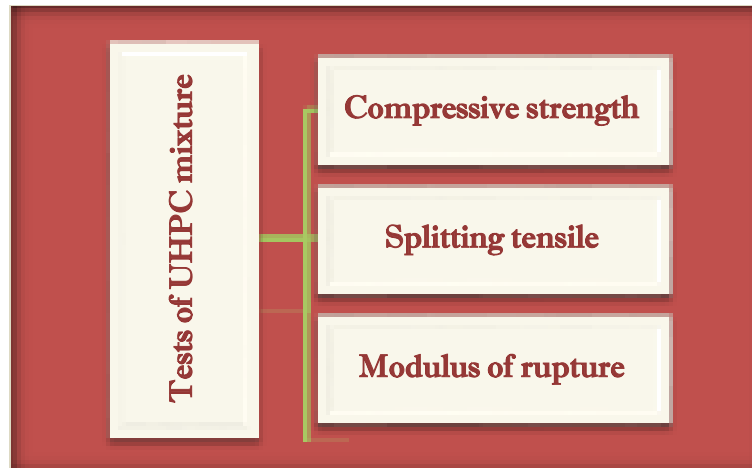Plate (3.13) Heat treatment tank for specimens.

Fig. (3.5) Tests of UHPC mixture.

3.14.1 Compressive strength

To test the compressive strength of UHPC according to ASTMC39-86 [59] Standard, three cylinders were used with a diameter of 100 mm and a length of 200 mm. The tests were carried out in the laboratory of the Faculty of Engineering, University of Misan, by using a universal ELE Compression Machine model with a capacity of 2000 kN to test the cylinders by axial loading. In accordance with ACI 318M-19 [60] Standard to find compressive strength, the mean of three cylinders readings was taken at the age of 28 days. Graybeal [68] studied the effect of shape and size of specimens of UHPFRC with strength from 80-200 MPa. The shape effect had no more than 8 percentage difference, in a general, and the ratio between cubes strength to cylinder strength of 100 mm in length and diameter, respectively, are equal to one. Table (3.13) shows the result of compressive strength of cylinders specimens.

3.14.2 Splitting Tensile Strength (fsp)

To test the tensile strength of the concrete, there are several methods of testing, but the most common and easiest method at the moment is the Brazilian method

which is the indirect tensile strength test conforming to ASTM C 496-04 [61] specification, and this method was used in the present work, by testing three cylinders with a diameter of 100 mm and length of 200 mm placed horizontally in the universal ELE Machine with a capacity of 2000 kN to apply the load vertically along the length of the cylinders. The results of the tests are shown in Table (3.14).

Table (3.13) Result of compressive strength for cylinders

Specimen number	*fc' (MPa)*
Specimen 1	*138.2*
Specimen 2	*133.5*
Specimen 3	*120.5*

Table (3.14) Result of split tensile for cylinders

Specimen number	*fsp (MPa)*
Specimen 1	*11.9*
Specimen 2	*11.8*
Specimen 3	*10.6*

3.14.3 Modulus of Rupture (fr)

To test the flexural strength of concrete according to the ASTM C78-84 [64] standard. The test was performed by using three points of loading. Three prisms having dimensions (100*100*500) mm are cast for this test. The results of tests are calculated by the mathematical formula below. The results obtained in the present work shown in Table (3.15).

$$fr = \frac{3pl}{2bd^2} \qquad\qquad ....Eq. (3.1)$$

where:

f r= the Modulus of rupture (MPa).

P = the Ultimate failure load (N).

l = the Span length between the supports, (center to center) (mm).

b = prism cross section width (mm).

d= prism cross section depth (mm).

Table (3.15) The flexural test results

Prisms Test		Specimens' values		
	Test load (kg)	*2996.5*	*2562.0*	*2295.5*
Rupture test	*Test Load (N)*	*29385.6*	*25124.6*	*22511.1*
	Stress (MPa)	*19.83*	*16.95*	*15.19*
	Average Stress	*16.32*		

3.15 Measuring devices

The tools used in the present work to measure (deflections, strains, crack width, load, crack projection, crack patterns) during the testing of each beam specimen are listed below:

- **Universal testing machine with capacity of 200 ton:**
  To apply the load on the beam specimen.
- **Instruments for measurement of strain (measurement strain tool):**
  To find the local strain and save the readings in different stages of loading.

- **Measuring instruments of deflection (dial gauge) :**

  To measure deflection during loading at specified points.

3.15.1 Deflections measurement devices

During the testing of each beam, the resulting deflections were recorded at each loading stage, by using a dial gauge placed in the middle span of the beam to read the deflections in the pure moment zone.

3.15.2 Strain measurement on steel box and concrete

There are several ways to measure the strains mechanically and electrically, but the fastest and best way is the strain gauges. As a result of their superior measurement properties. All the strain gauges used in this study were placed in the pure moment zone at the middle span of the beam specimen. In the present work, two types of strain gauges were used:

- **Strain gauges for the concrete surface:**

  These strain-gauges were placed on a side surface of the beam specimen in the mid-span. Two concrete strain gauges used for the beam specimen. One placed in the upper edge on the extreme compression zone of concrete to find the compressive strains of concrete during the loading process. The other placed in the bottom edge in the tension zone of concrete to find the tensile strains of the UHPC during the loading process.

- **Strain gauges for the steel hollow box flanges:**

  Two steel strain gauge were used in the composite hollow beam specimen. These strain gauges were placed on the above and below flanges of the hollow steel section. To investigate the compressive and tensile strains of the hollow steel section at each loading stage. Plate (3.14) shows the hollow steel sections and the strain gauges placed on it.
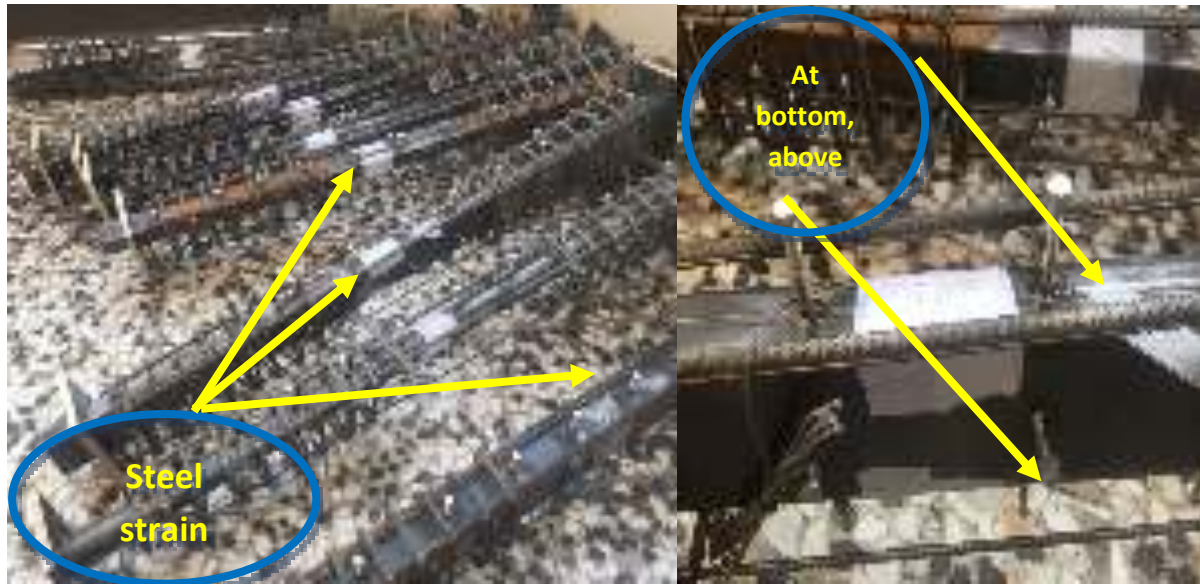
Plate (3.14) The steel strain gauges and their locations.

3.15.2.1 Types of strain gauges

In the current research, a strain gauge was imported from Japan (Tokyo Sokki Kenkyujo Co., Ltd.) company. The brand of these strain gauge was **TML** strain gauges, which represents the abbreviation of the name of the company producing the strain gauges (**T**okyo **M**easuring instruments **L**ab) [58]. These strain gauges are characterized by their accuracy, stability, and ease of use. In this research two types of strain gauges were used:

- **For concrete :** to measure the strains on concrete **PFL-30-11-3L** strain gauges were used, (PF) refers to the gauge series (polyester foil gauge) and (L) refers to pattern configuration (single), (30) Indicate to the length of the strain gauge is 30mm, The length of the strain gauge depends on the location of the stress that we want to measure its strain so that if we know the location of the stress can be used less length strain gauge, but if we do not know the location of stress we should use a longer length. (11) is compensation material ppm/C°. (3L) Indicates the length of the existing

wire with the strain gauge is 3 meters. Based on the experience of previous researchers, the strain gauge that is imported with its wire gives more accurate results than those which do not have a wire with it.

- **For hollow steel section:** to measure the strains on flanges of hollow steel box FLA-5-11-3L strain gauges were used. (FLA) refers to that the strain gauge used for general steel materials. (5) Refers to the length of the strain gauge is 5mm, (3L) refers to the length of the existing wire with the strain gauge is 3 meters. Plate (3.15) shows the strain gauges used in the present research.

3.15.2.2 The process of installation the strain gauges

The process of bonding the strain gauges shown in the plate (3.16) is summarized as the following steps:

1- **Surface preparation:**

   After complete the process of determining where the position of strain gauge should be installed. The surface of the material must be cleaned from all rust, grease, paint, etc. A slightly more extensive area of the strain gauge bonding area should be smoothed by using abrasive paper 80 to 120 for concrete, and #120 to 180 for steel.

2- **Little cleaning:**

   The strain gauge bonding area was cleaned using a cleaner solution.

3- **Bonding the strain gauge:**

   After completing the preparation of the strain gauge bonding area, the strain scale is determined by a pencil. Special adhesive (CN adhesive series), was imported from Japan. A sufficient amount of adhesive is placed on the base of the strain gauge and usually using one drop of CN adhesive was applied. The adhesive one drop is then distributed on the

strain gauge base by using the adhesive nozzle. Then place the sheet of strain gauge above the strain gauge and press by thumb with constant pressure for a period ranging from (60-120) seconds depending on the temperature of the room and the humidity of the air.

3.15.2.3 Strain tool measurement

In the present work, the Data Logger device was used for reading the strains measured by strain gauges bound in the beam specimens.

3.16 Test setup and instrumentation

The beam specimens were tested under two-point load to study the flexural behavior at the pure moment zone. The applying of loads was done using a hydraulic jack as shown in Plate (3.17), and the hydraulic jack was previously calibrated to provide the required load. Dial gauge was used to measure the central deflection. It was installed at the center of the beam specimens. A strain gauge (TML) was used to read the strains on concrete and steel hollow section during the loading. The strain gauges used for reading the steel strains were installed on the top and bottom flanges of hollow steel section, while the strain gauge used for reading concrete strains were installed on the side of the concrete beam at its compressive and tensile fibers. All strain gauges were connected to a digital data logger to display the result strains during the loading. Testing of the beams was conducted in the laboratory of the Faculty of Engineering - University of Basrah.
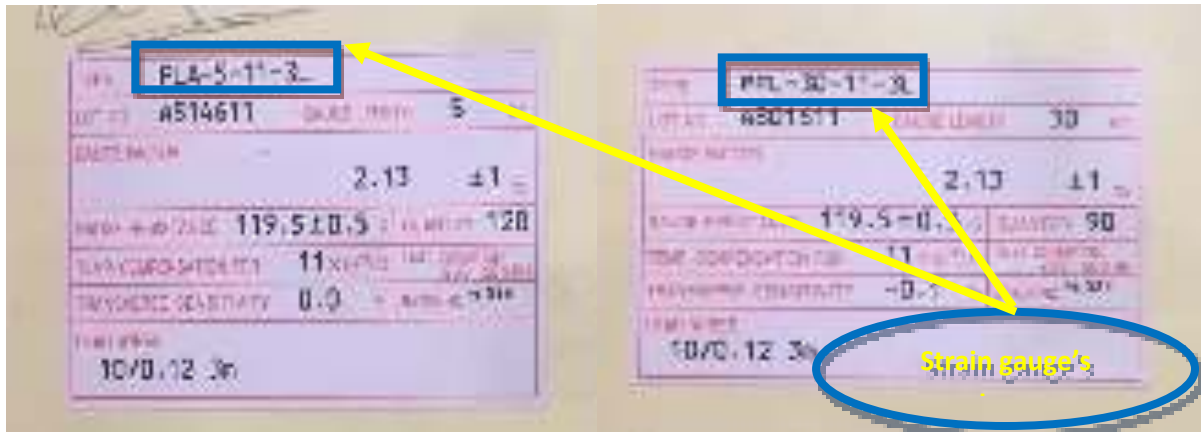
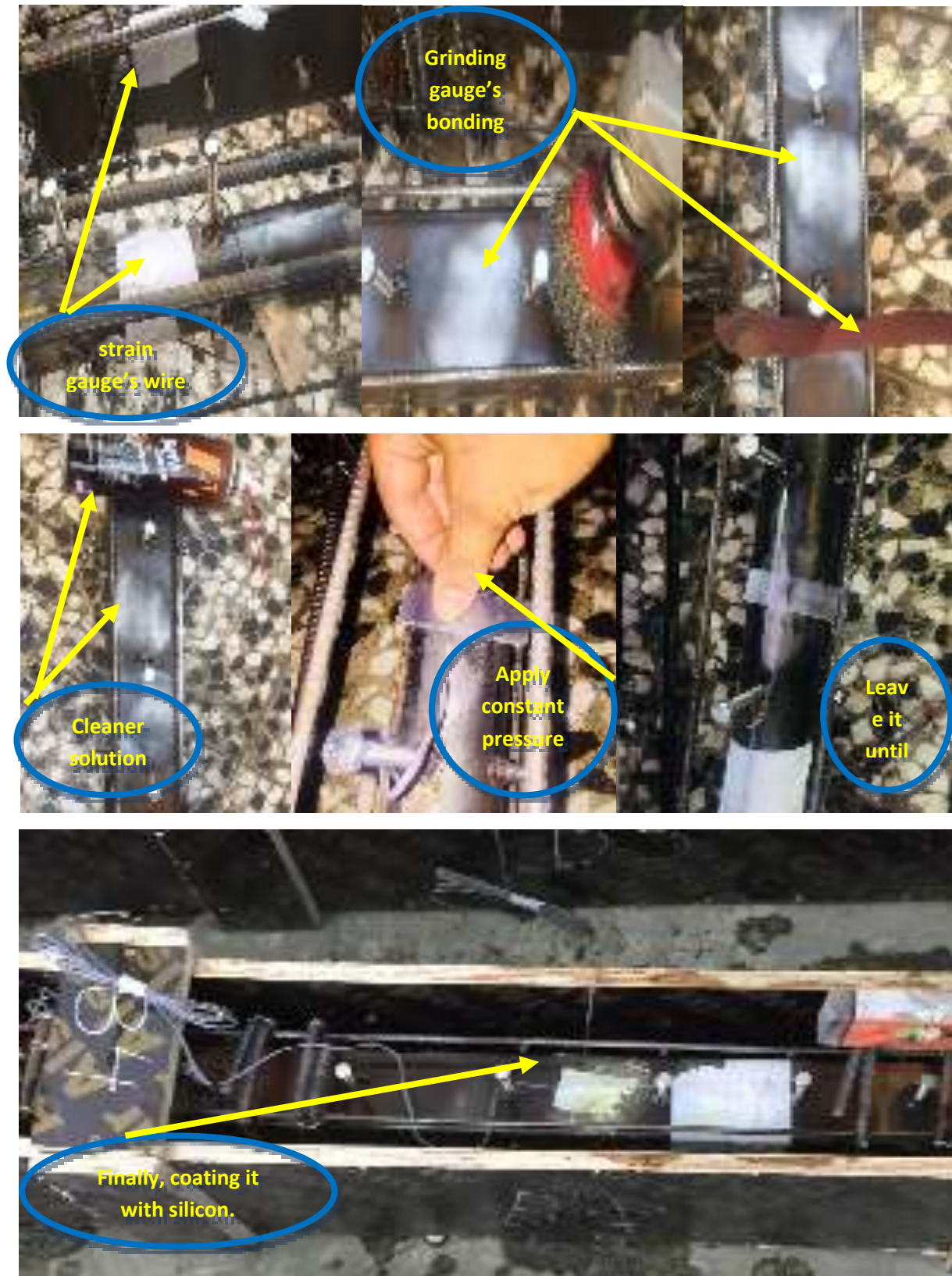Plate (3.15) The strain gauge types used in this research.
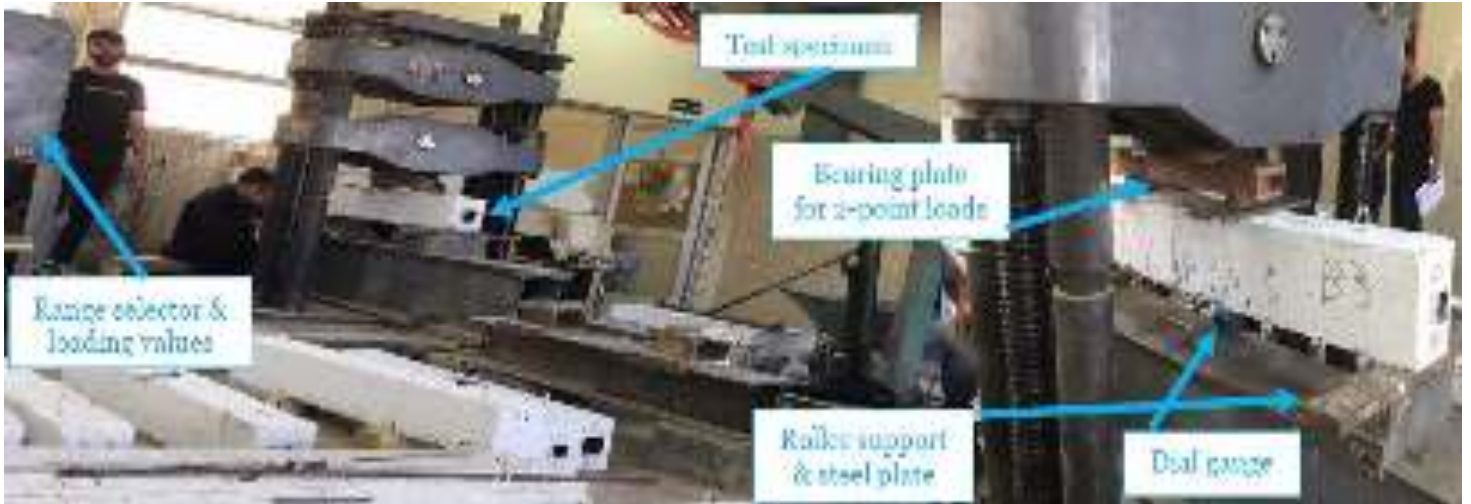
Plate (3.16) Strain gauge installation steps.

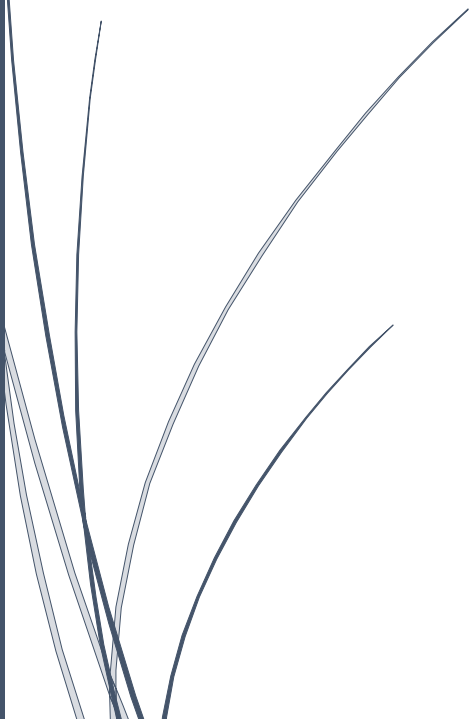Plate (3.17) Test Setup of the Experimental Study.

[CHAPTER FOUR]

EXPERIMENTAL RESULTS

AND DISCUSSION

CHAPTER FOUR

EXPERIMENTAL RESULTS AND DISCUSSION

4.1 General

As mentioned in the previous chapters, the main purpose of this work is to investigate the structural behavior of fifteenth beams. Then comparisons for structural behavior by investigating the effect of those variables were made. All the tested beams presented in this chapter have the same dimensions, properties, reinforcement cages and the same concrete type (UHPC) illustrated before. This chapter shows all the results recorded after the flexural test of the fifteenth beams tested under two-point loads. Results were collected and discussed. All the load carrying capacity and deflections in the elastic stage and non-elastic stage were assembled. Load-deflection behavior for each tested beams was presented with its corresponding sketched photo of the beam during the test. For the tested beams, sketching has been done on the beam to recorded ultimate loads, first cracks and crack patterns in which applied load occurs. The stiffness and ductility are also presented and discussed in this chapter. Toughness also presented for each tested beam. All the strain readings recorded by strain gauges were analyzed.

The flexural failure mode with the applied loads was analyzed. Discussions and the results of the effect for all the variables presented in the previous chapter were recorded in this chapter by changing the location of the hollow steel box, changing its shape, changing the ratios of longitudinal reinforcement, etc.

4.2 General structural behavior of beams during the testing

The recorded test results are shown in Table (4.1). The table consists of fifteenth specimens of simply supported beams subjected to a flexural test using two point

loads. The first group included a comparison of the type of longitudinal opening material. The second group contained varying of the size of the hollow steel box. The third group studied the change of longitudinal reinforcement ratio. The fourth group included a study of the effect of the steel hollow box's shape. The fifth group included a study of the effect of changing the arrangement of shear connectors. The sixth group includes a study of the effect of steel hollow box location. The seventh group includes a study of the effect of changing the shape of the hollow steel box which is located in the tensile zone of the section. All beams have the same geometric and mechanical properties. No special reinforcement has been used around the longitudinal openings (hollow core) because of the use of steel hollow box instead of it.

During the testing, each beam showed a different behavior when reaching the ultimate load, but in the initial phase of loading, all the beams showed an elastic behavior and the deflections were very small. During this phase of loading, it was observed that the cross section was fully effective in resisting the loads and the resulting strains were very small. By increasing the loads, both dial gauge and load-cell stopped slightly, which indicates internal micro crack occur. The first crack was observed in the lower part of the beams in the pure moment zone (constant moment region) between the two-point loads or nearby. After increasing the loads, non-linear behavior began which is an indicator that tested beams reach its plastic phase. The bending cracks in all beams started to increase and took a vertical direction towards the two loading points. Since cracks have a steady growth process with increased loading. However, the extension of cracking was interrupted by the presence of tensile stresses provided from the presence of steel fibers in UHPC mixture and steel reinforcement. Other flexural cracks appeared almost in the mid-span of the beams and increased. At the end of loading, the existing cracks began to grow and extended

rapidly to the compressive zone of the concrete. The cracks were uneven in speed as some cracks were faster from others in reaching the compressive flange. Concrete crushing near the loading points was minimal due to the properties of Ultra-High-Performance Concrete (UHPC) and its high compressive strength. Table (4.1) shows the details of the results recorded during the testing.

4.3 General failure modes in the composite hollow beams

In general, the flexural failure mode expected to be in these new elements is divided into two types; one is the flexural failure with splitting failure between the hollow steel box and the concrete. This type of failure can be identified if a horizontal crack appears near the upper flange of the hollow steel box (compression steel flange) when a crack along the beam appears on the outer concrete surface as shown in Fig. (4.1.1), giving evidence of separation occur between the concrete and the hollow steel box. The steps process in this type of failure (flexural failure & splitting failure) can be explained and clarified in the load-deflection relationship as shown in Fig. (4.1.1). The other type of failure is the flexural failure without splitting between concrete and hollow steel box, in this type of failure concrete and hollow steel box resists the loads as one unit until the end of the test. Fig. (4.1.2) show the steps process of resisting loads in this second type of failure (flexural failure).

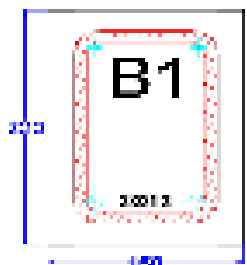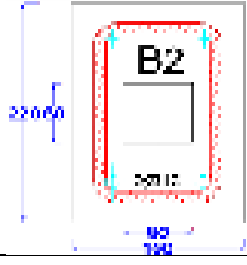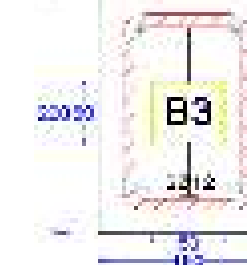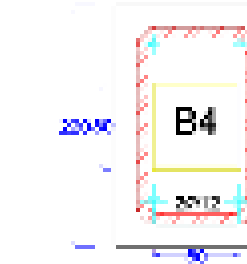Table (4.1) Tests Results of Tested Beams.
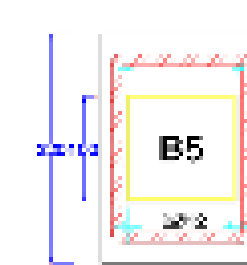
Beam Designation	Load Characteristics (kN)		Max. Deflection (mm)	Pcr/Pu %	Failure mode	Cross section
	First crack	Ultimate				
B1	70	110	9.34	0.63	Flexural	
B2	80	105	9.6	0.76	Flexural	
B3	60	230	15.81	3.83	Flexural	
B4	70	240	16	3.42	Flexural	
B5	80	290	19	3.62	Flexural	

Table (4.1) Continued.

B6	80	200	14.76	2.5	Flexural	
B7	70	290	17.65	4.14	Flexural	
B8	100	239	13	2.39	Flexural	
B9	100	200	15.38	2	Flexural	
B10	80	220	15.71	2.75	Flexural	

Table (4.1) Continued.

B11	80	200	14.7	2.5	Flexural	
B12	90	240	12	2.66	Flexural	
B13	60	240	13.6	4	Flexural	
B14	60	245	11.34	4	Flexural	
B15	50	250	11.36	5	Flexural	
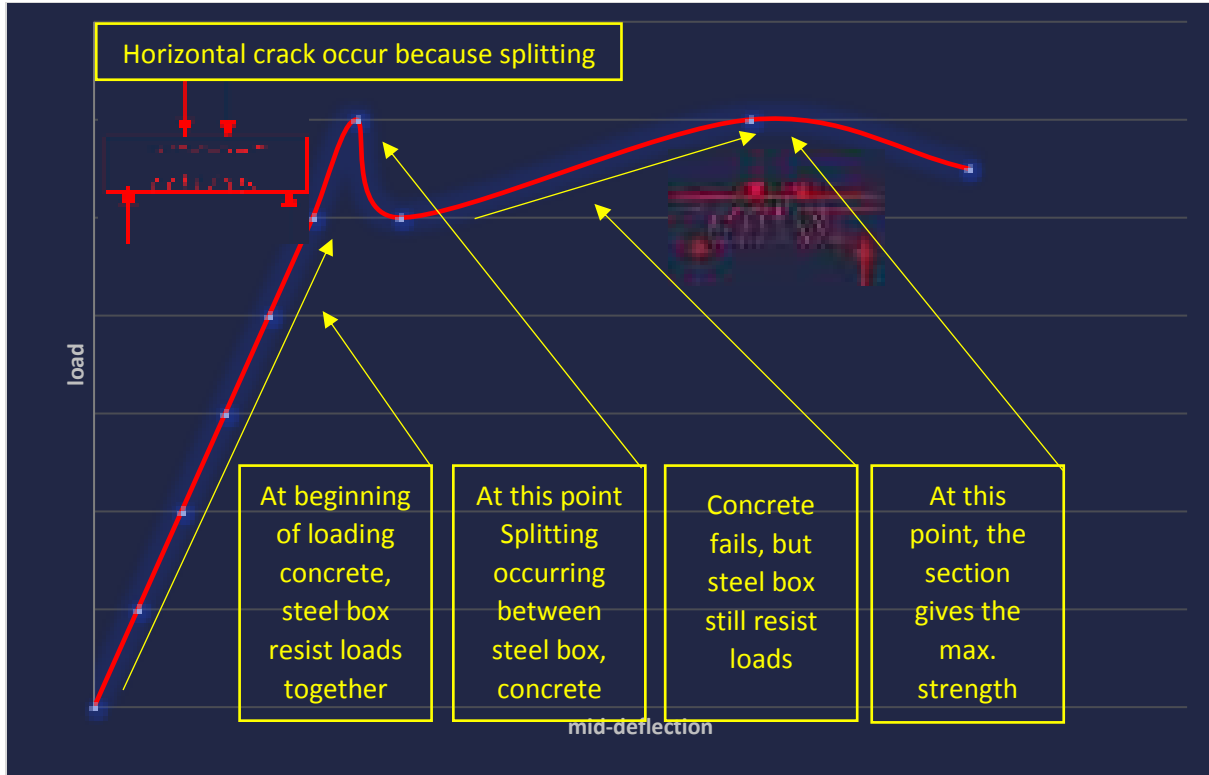
Fig. (4.1.1) Splitting failure in the composite hollow beam [1]
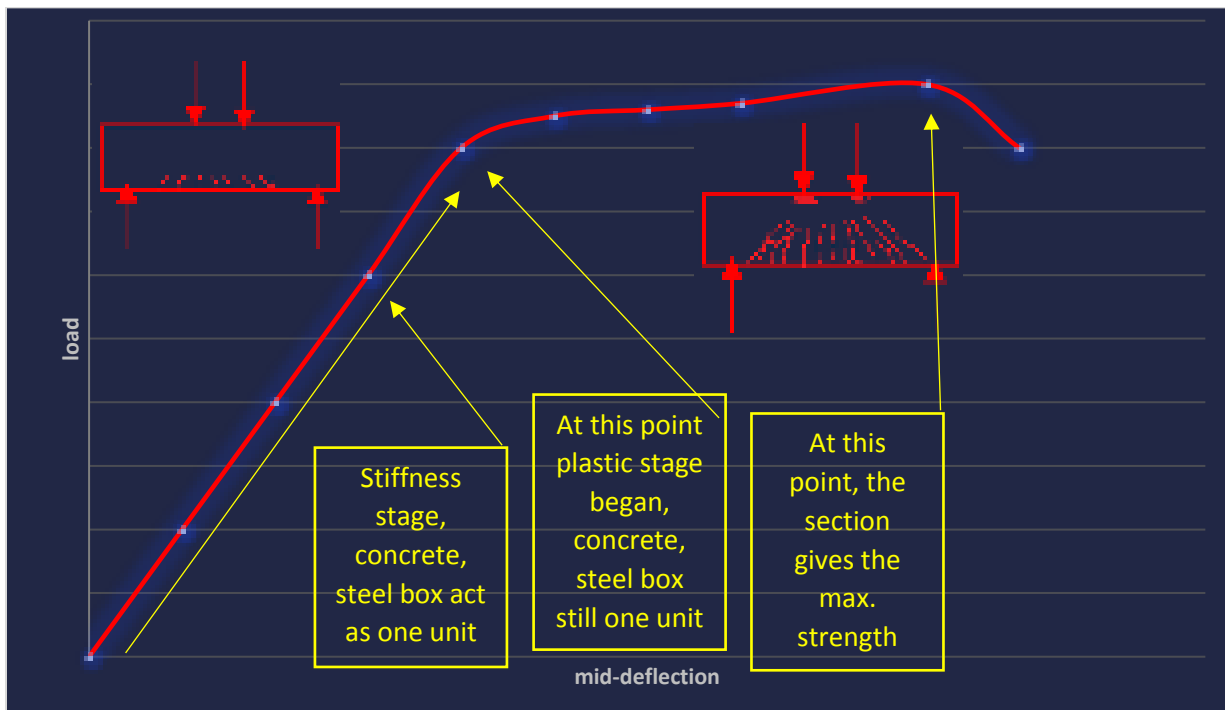
Fig. (4.1.2) Flexural failure in the composite hollow beam [1]

4.4 Load-Deflections behavior and crack patterns for tested beams

After the curing process of beams was finished, the beams were painted with white color and transferred to the testing machine, and the load was applied in the center of the beam specimens by increasing the pressure of hydraulic jack. Strains and deflections were recorded during the test. The general experimental behavior of the composite hollow beams noticed during the test that can be summarized as follows; when increased the applied load the first crack occurs in the tension zone and give us an indication that the concrete loss its tensile strength. Furthermore, the applied loads increased until a sudden increase in the dial gauge reading occur that give us an indication that the steel section has been yielded. The increasing in applied loads led to crush the concrete at compression fiber. Finally, with increasing the loads further the upper flange of the steel-hollow section has been buckled.

The main final cracks were in the pure moment zone for all tested beams, including the control beam (solid beam) and showed an indication that all the tested beam fails in flexural failure without splitting failure between concrete and hollow steel box.

The data for (control beam in group No.1) solid beam specimen (B1) are shown in the fig. (4.2.1), the first crack was observed at a load of 70kN in the tensile tension zone of the specimen as shown in Fig. (4.2.1), which indicate that the concrete start to lose its tensile strength after the first crack occurs. When the load increases and the central-deflection recorded by the dial gauge were also increased linearly until reaching load P_y = 80 kN, it was observed that the deflection was increasing non-linearly, giving the impression that the section reaches its plastic phase. As the load increases, the final failure of the concrete is achieved at an ultimate load P_u = 110 kN as sketched in Fig. (4.2.1). the results of load-deflection for (B1) are shown in Fig. (4.2.1).

The data and load-deflection values for different stages for the non-composite hollow beam (B2) are shown in Fig. (4.2.2). From the figure, it is noted that (B2) cracking at a load of 80 kN, and reach the plastic phase immediately after the first crack at $Py = 80$ kN. With increasing the load, the concrete crushing at $Pu = 105$ kN.

The data for (control beam for the composite beams) composite hollow beam (B3) is shown in Fig. (4.2.3). It is indicated that the first crack was recorded at a load of 60 kN in the tensile zone as sketched, and concrete lost its tensile strength after the first crack occurs. The loading continued, and the deflection was observed to increase linearly until a load of $Py = 180$ kN then become increasing non-linearly, which indicates that the steel section has been yielded. With the increase of loads until reaching a maximum load of $Pu = 230$ kN, it was observed that the concrete was crushed entirely, giving the impression that the compression flange of the steel section had buckled. The result of load-deflection for (B3) shown in Fig. (4.2.3).

The results of load-deflections behavior and crack patterns for different stages for all the tested beams are shown in the Figs. (4.2.4 to 4.2.15).
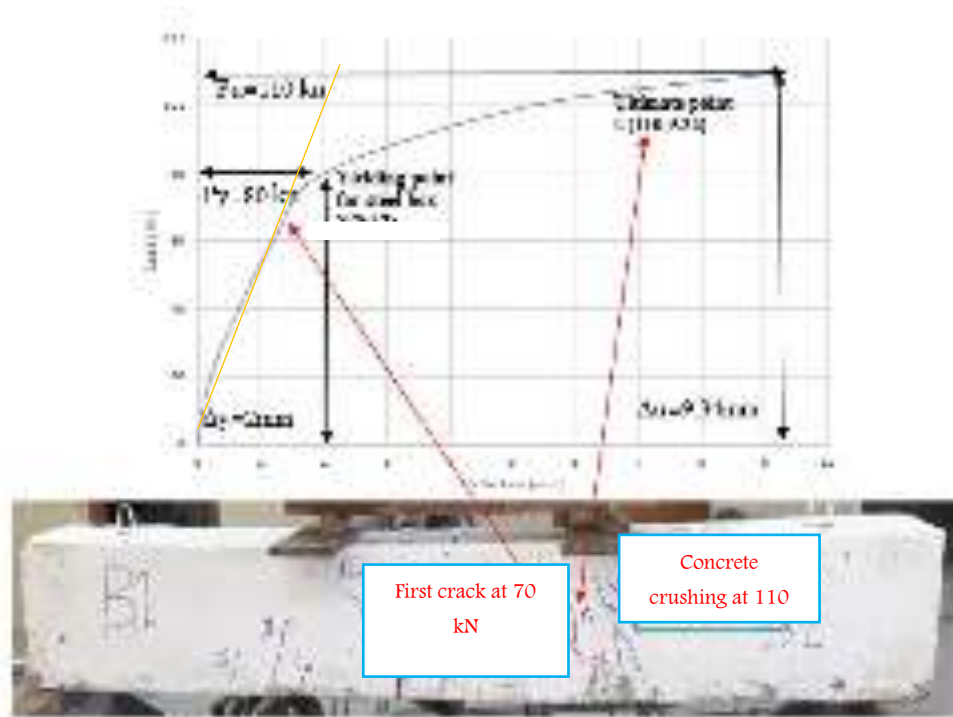
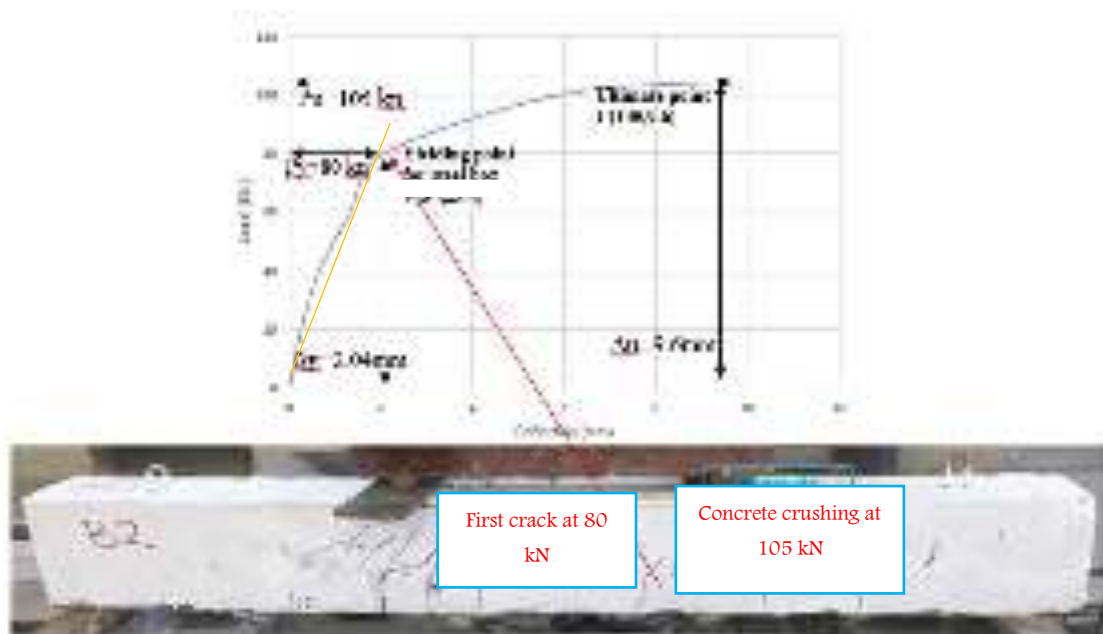Fig. (4.2.1) Load-deflection behavior and crack patterns of the solid beam (control) B1.

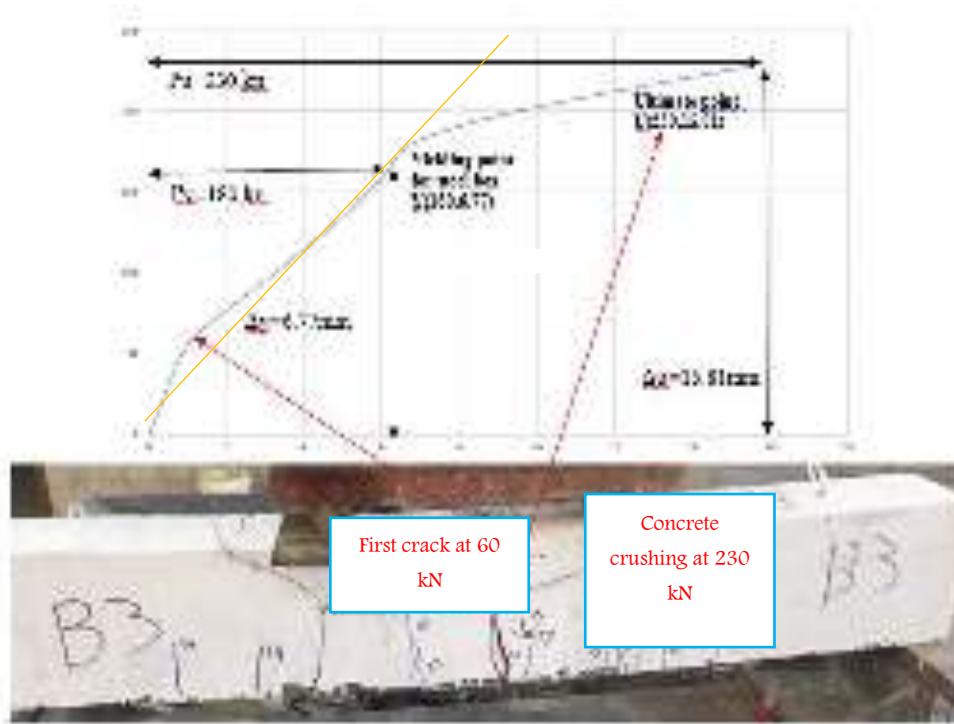Fig. (4.2.2) Load-deflection behavior and crack patterns of non-composite hollow beam B2.

Fig. (4.2.3) Load-deflection behavior and crack patterns of the composite hollow beam (control) B3.
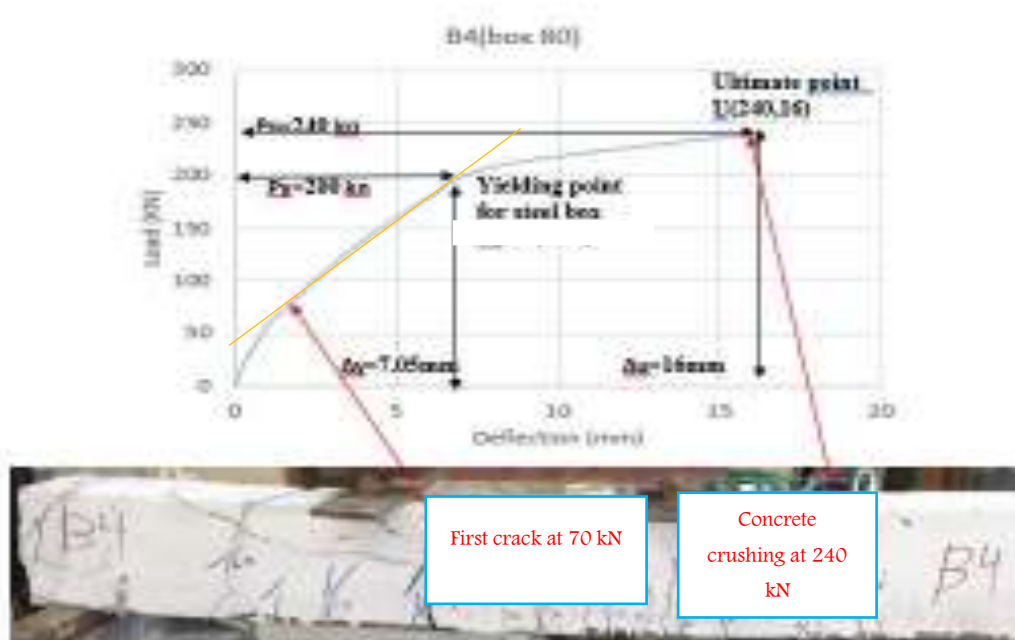

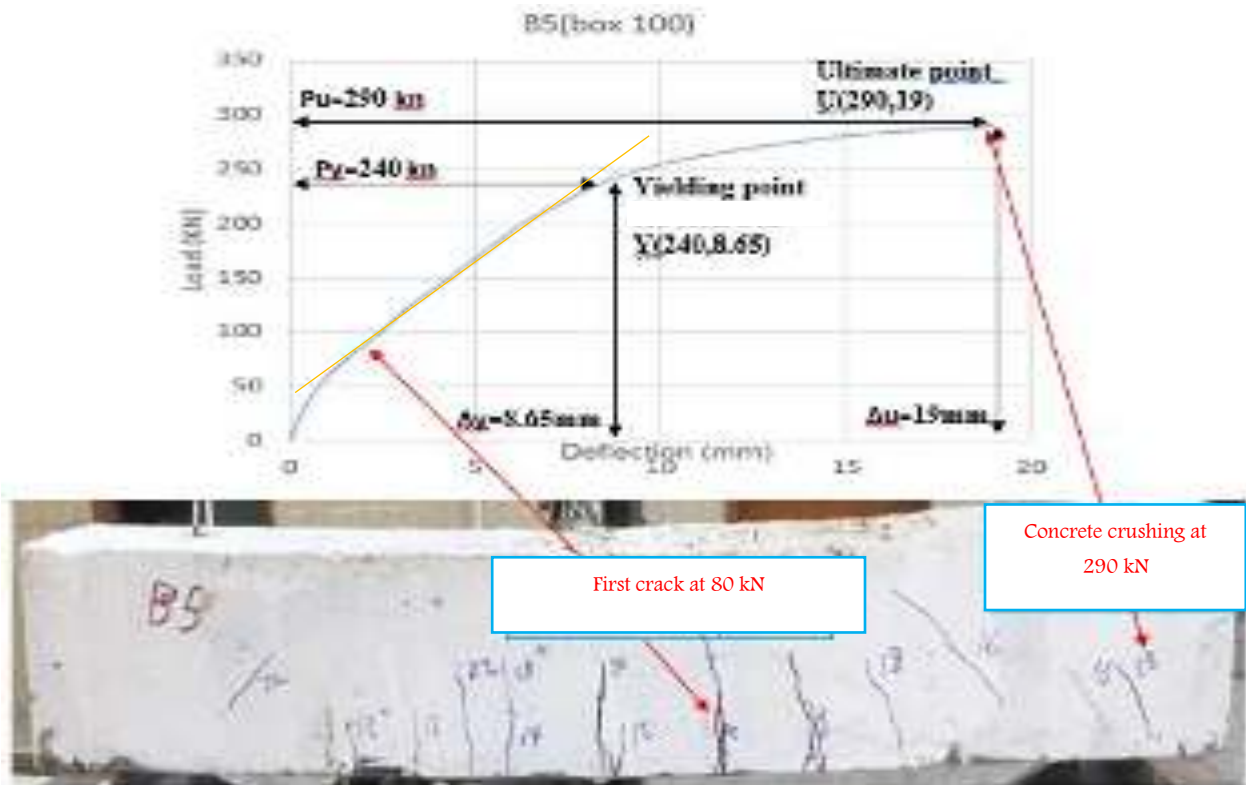Fig. (4.2.4) Load-deflection behavior and crack patterns of composite beam B4.

Fig. (4.2.5) Load-deflection behavior and crack patterns of composite beam B5.
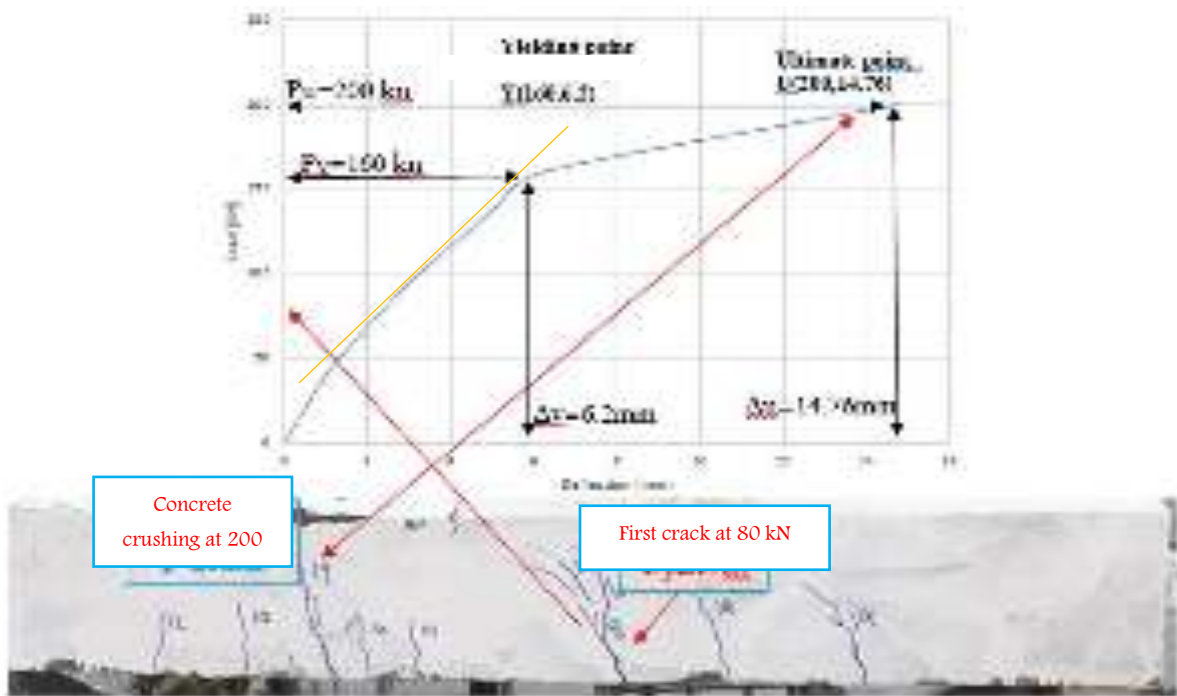

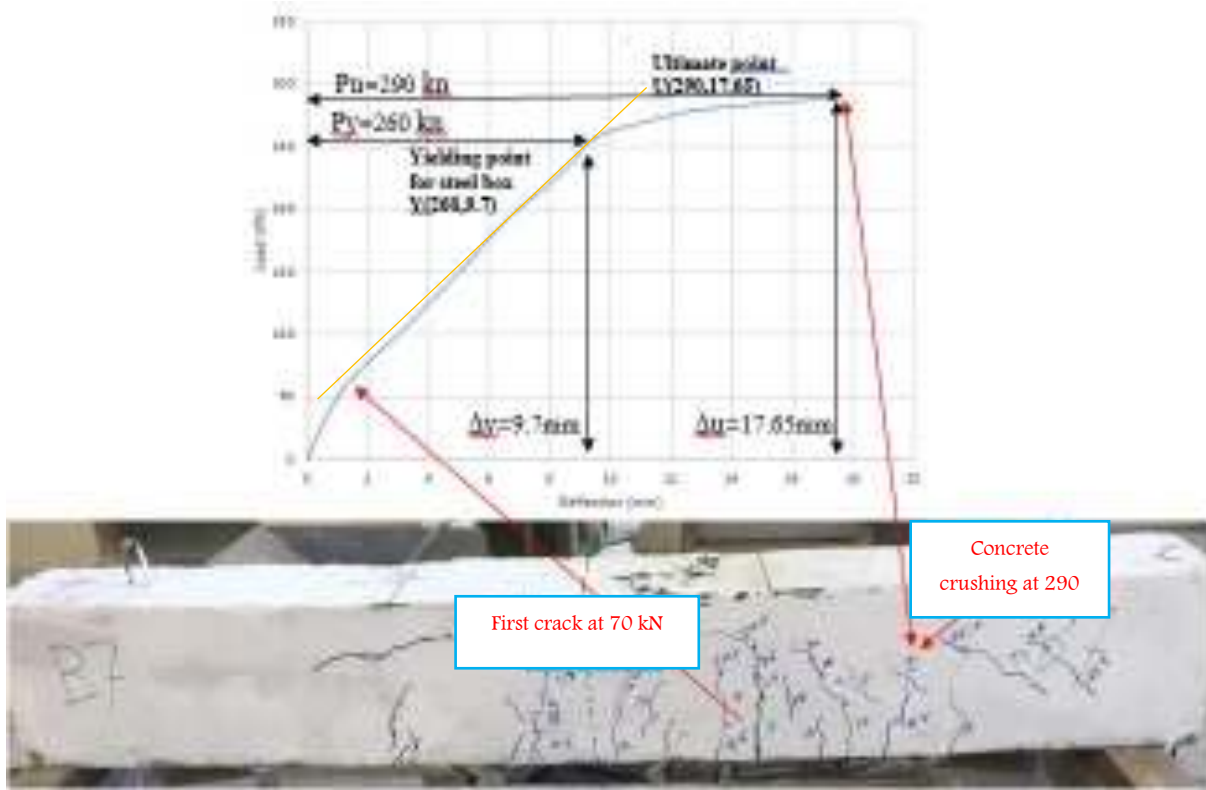Fig. (4.2.6) Load-deflection behavior and crack patterns of composite beam B6.

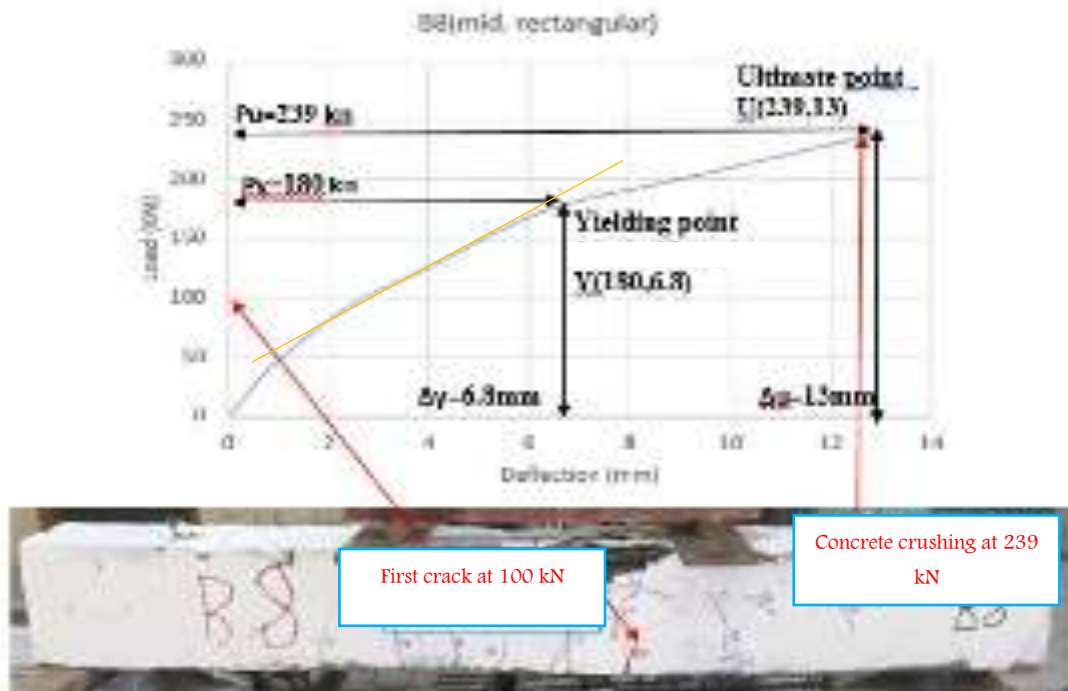Fig. (4.2.7) Load-deflection behavior and crack patterns of composite beam B7.

Fig. (4.2.8) Load-deflection behavior and crack patterns of composite beam B8.
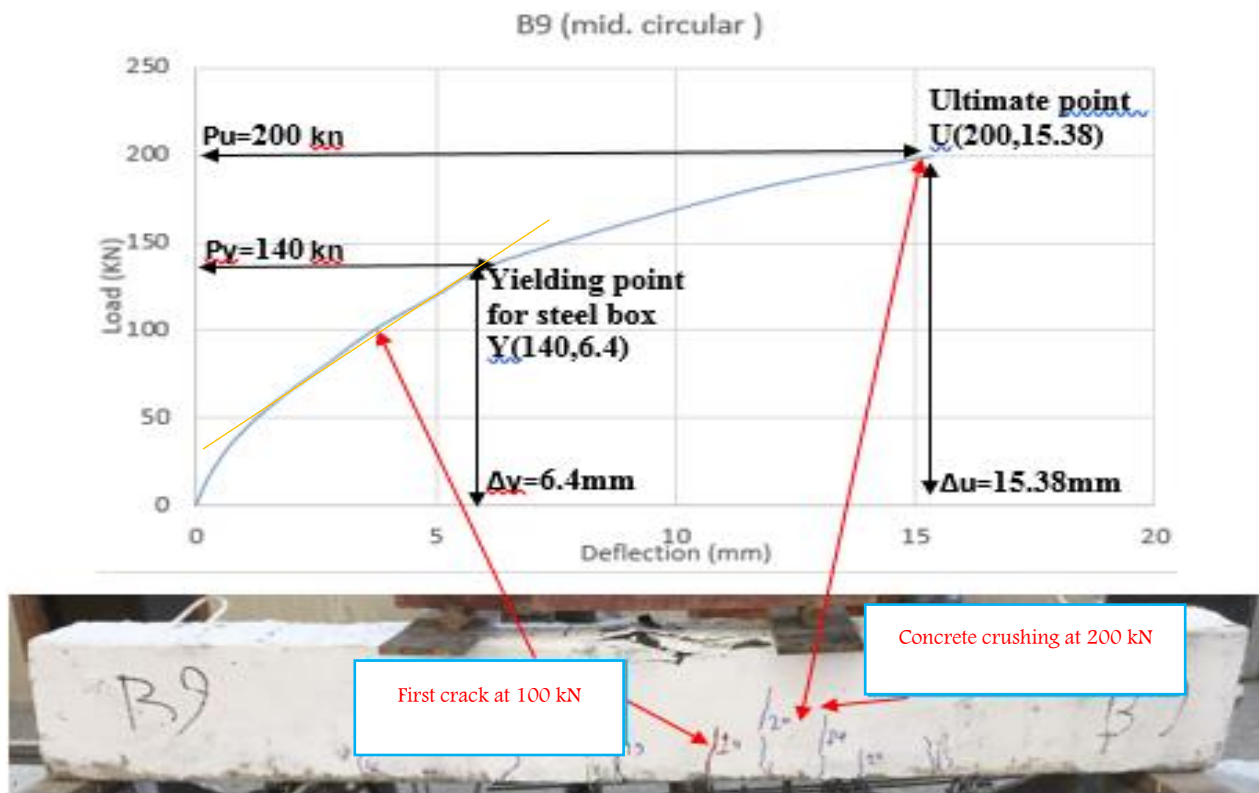
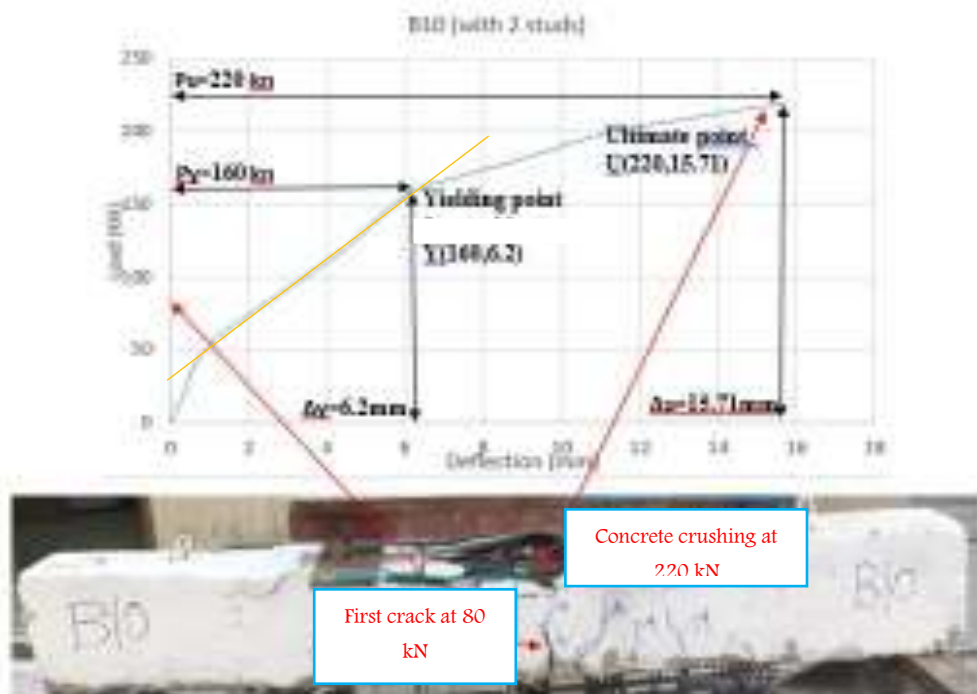Fig. (4.2.9) Load-deflection behavior and crack patterns of composite beam B9.

Fig. (4.2.10) Load-deflection and crack patterns of composite hollow beam B10.
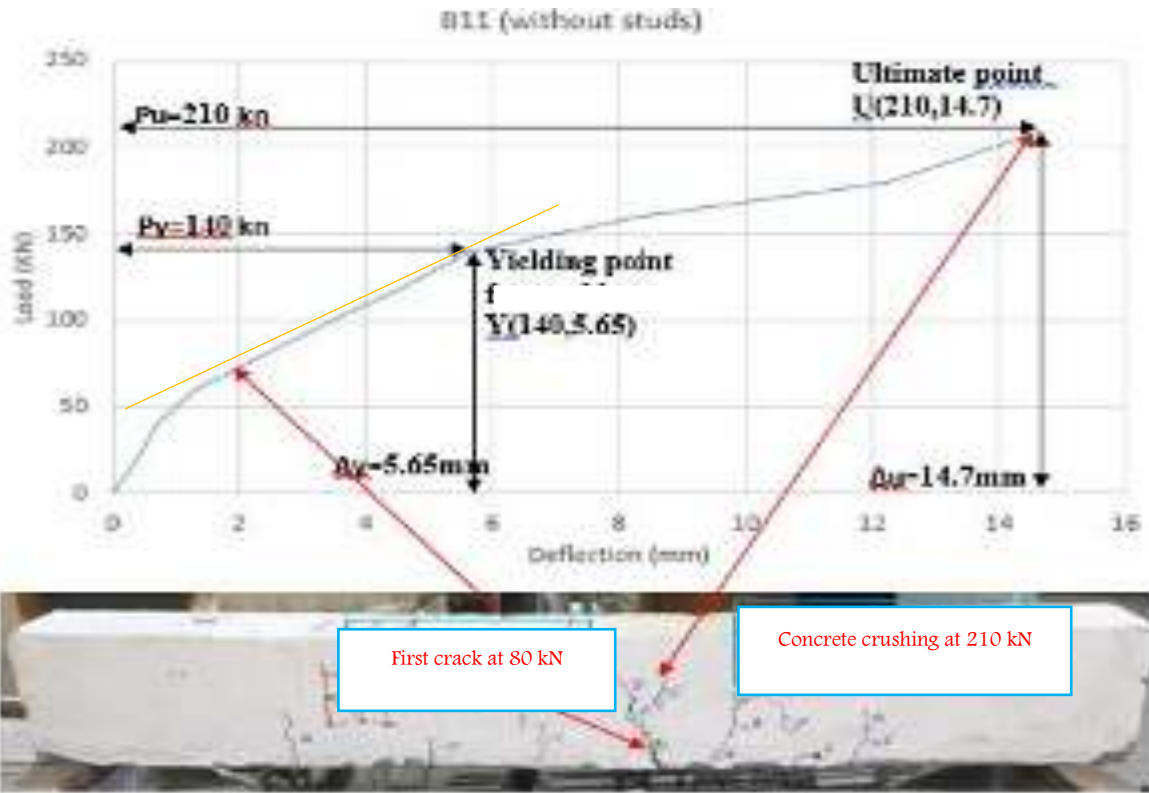
Fig. (4.2.11) Load-deflection and crack patterns of composite hollow beam B11.
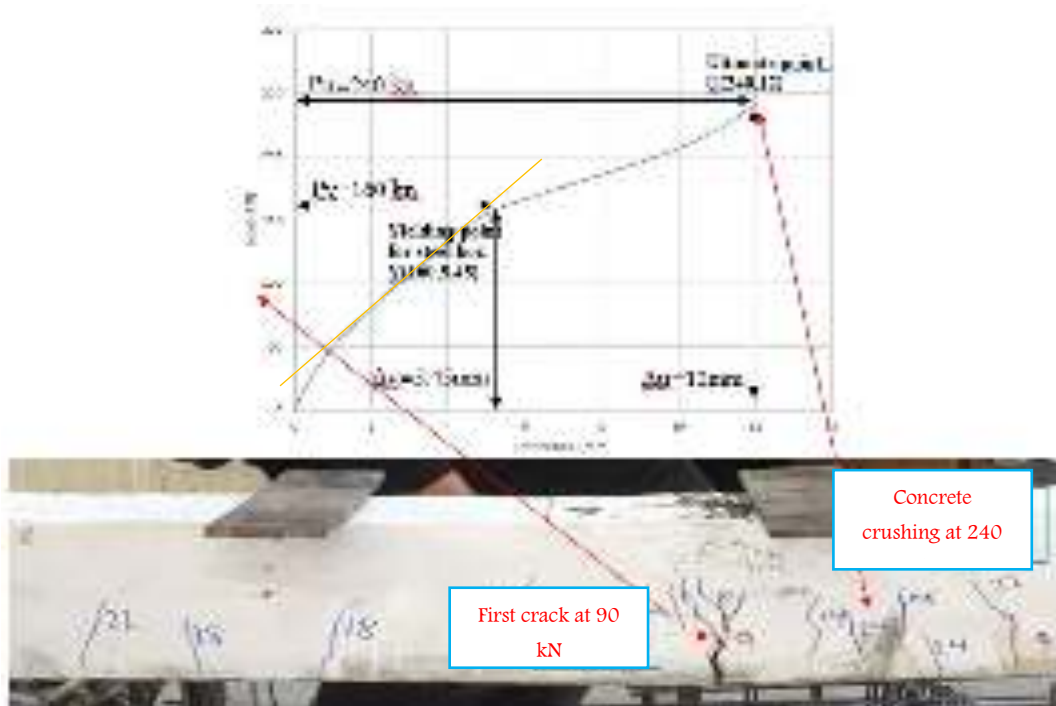

Fig. (4.2.12) Load-deflection and crack patterns of composite hollow beam B12.
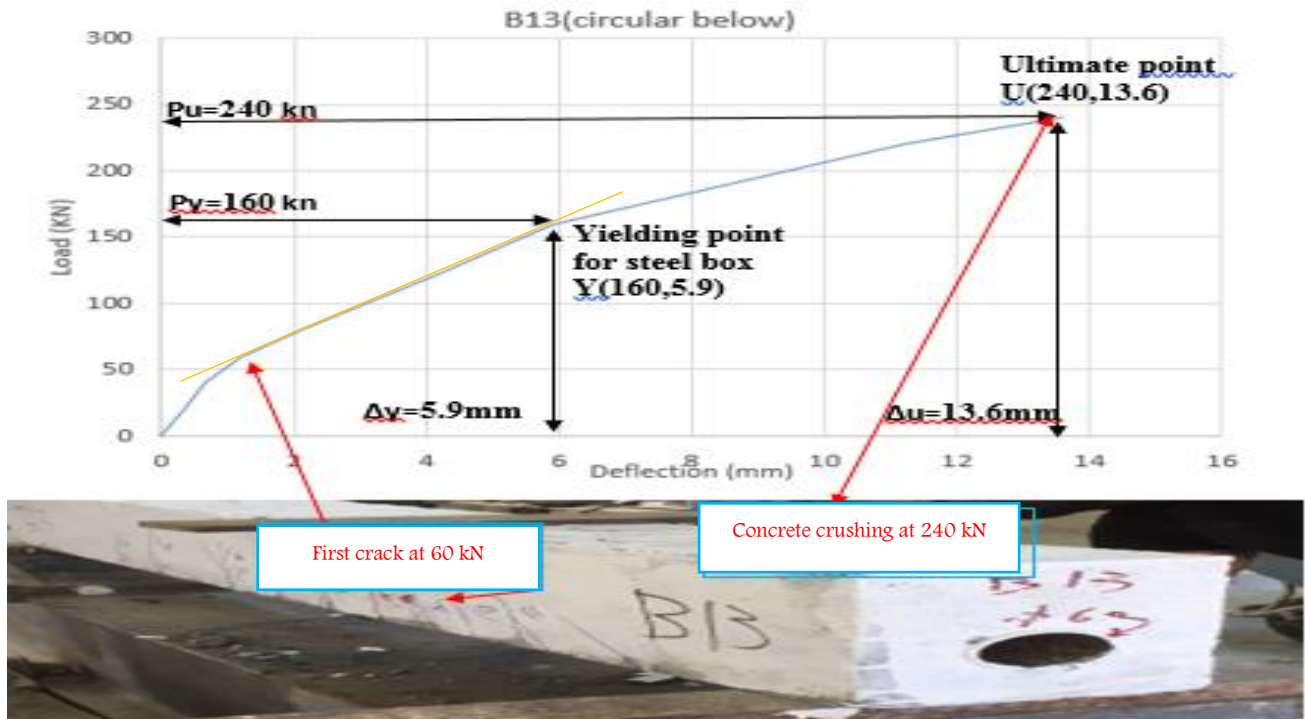
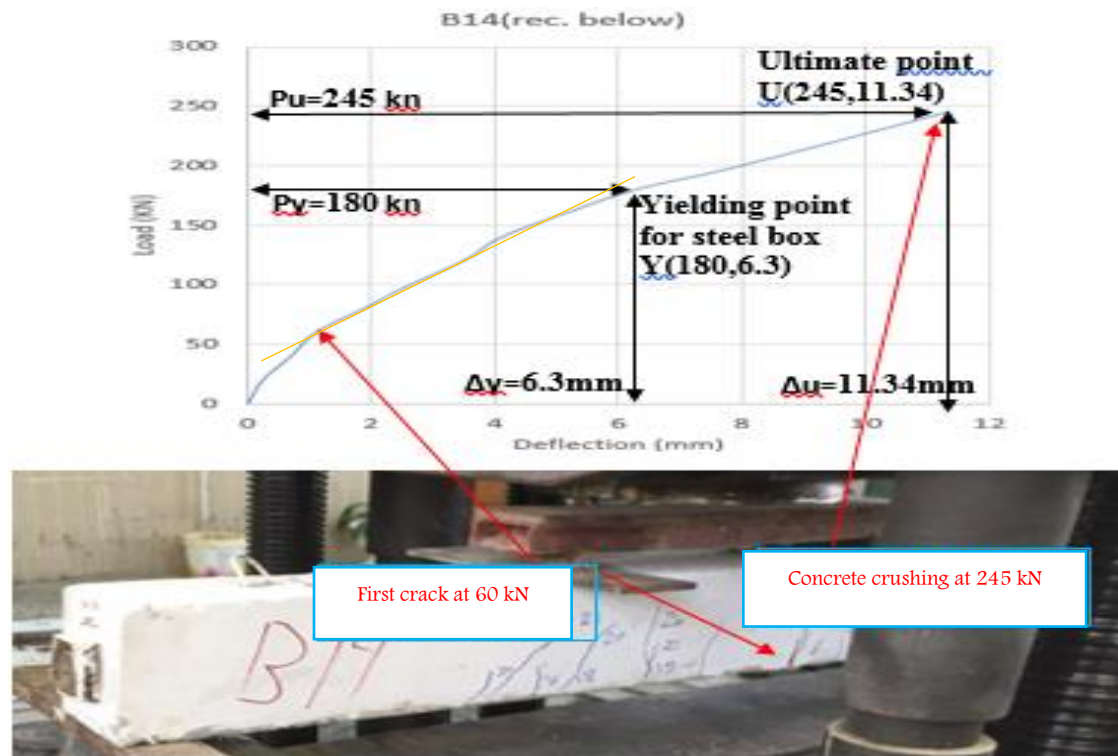Fig. (4.2.13) Load-deflection and crack patterns of composite hollow beam B13.

Fig. (4.2.14) Load-deflection and crack patterns of composite hollow beam B14.
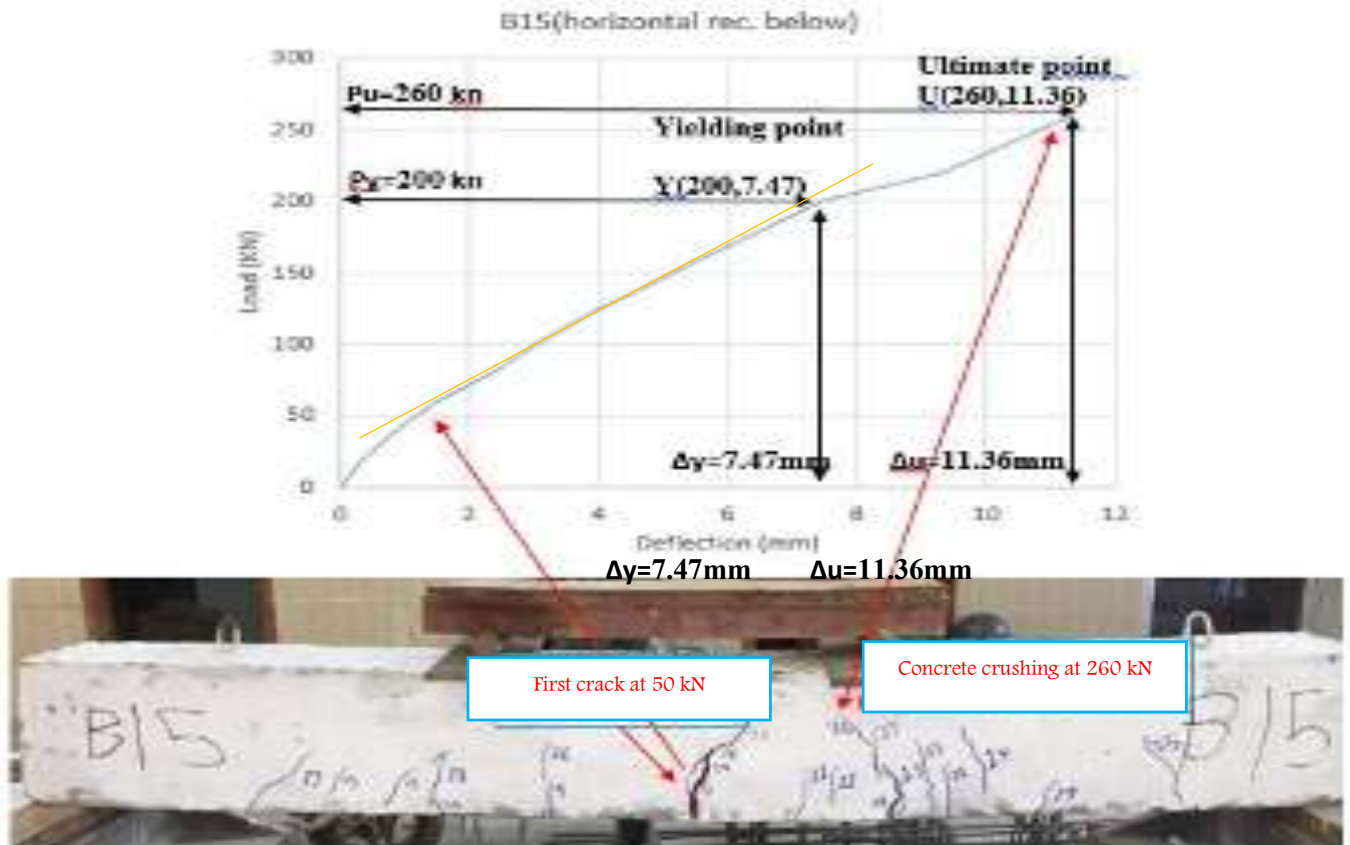
Fig. (4.2.15) Load-deflection behavior and crack patterns of composite hollow beam B15.

4.5 Flexural moment capacity and flexural loads

The ultimate load capacities of the tested beams are given in Table (4.2). Fig. (4.3) Shows the moment capacity comparisons for all tested beams. It is noticed that the flexural capacity of the composite hollow beams was in general higher than that of the corresponding solid and non-hollow beams. It is clear that the increase in capacity is due to encased steel hollow sections in the concrete sections.

For **GR.No.1**, in compared with the solid beam (B1) as control beam, it is noticed that the ultimate load and moment capacity decrease by 4.76% and 4.91%, respectively, when hollow core fabricated using cork material in a non-composite hollow beam (B2). However, the load and moment capacity increase by 109%

compared with the solid beam (B1) when steel hollow box embedded in a composite hollow beam (B3).

For **GR.No.2**, in comparison with composite hollow beam (B3), which its steel hollow section area is (60x60) mm², it noticed that the load and moment capacity increase by 4.3% when increase the area of steel hollow section from (60x60 to 80x80) mm², while increased by 26% when increase area of steel hollow section from (60x60 to 100x100) mm².

For **GR.No.3**, in comparison with composite hollow beam (B3), which has $2\phi12$ (ρ= 0.008) longitudinal reinforcement, it is noticed that the load and moment capacity decreases by 15% when decreasing the longitudinal reinforcement amount to $2\phi10$ (ρ= 0.005) in (B6) and increased by 26% when longitudinal reinforcement amount increased to $2\phi16$ (ρ= 0.01) in (B7).

For **GR.No.4** in comparison with the composite hollow beam (B3), which has square steel hollow section, it is noticed that the load and moment capacity increased by 3.9% when the shape of steel hollow section changed from (square (60*60)mm² in (B3) to rectangular (50*100)mm² in (B8)), the explanation for this increase may be due to the increase in moment of inertia of the section when the shape of the hollow steel section is changed from square to rectangle. It is also noticed that the load and moment capacities were decreasing by (15%) when the shape of hollow steel section changed from (square (60*60) mm² in (B3) to circular of (ϕ60) mm in (B9)).

For **GR.No.5**, it was found that the load and the moment capacity decreased by 4.4% when decreased number and arrangement of shear connectors from (44 studs in (B3) to 22 studs in (B10) as shown in Table (4.2), and decreased by 9% compared with (B3) when no shear connectors were used in (B11).

For **GR.No.6** in comparison with the steel section located in middle of concrete section, it noted that the load and moment capacity increased by (4.3% for square, 2.5% for rectangular and 20% for circular) steel hollow sections, when changing steel hollow sections location and pushing down to the tensile zone of the concrete section. This increase in flexural capacity happens due to the pushing of the steel box towards the bottom led to an increase in the tensile forces of the section.

For **GR.No.7**, in comparison with the composite hollow beam (B12), which contains square steel hollow box in the tension zone, it is noticed that the load and the moment capacity increased by (2%) when changing the shape of the steel hollow box within tension zone from (square to vertical rectangular) and this increase happens due to the increasing in the moment of inertia of the section, while increased by (4%) when changed shape of steel box within tension zone from (square to horizontal rectangular) and this increase due to the increase in the amount of steel material in the tensile zone, while there is no significant difference when changing the shape of box from (square to circular) within the tension zone of the section.

4.6 Loads- Deflections at yield and ultimate loads

The load carrying capacity and deflections of tested beams at yield and ultimate points are given in Fig. (4.4).

For **GR.No.1** shown in Fig. (4.4.1) It is clear that the values of yielding and ultimate loads were reduced when a longitudinal opening was fabricated using cork, in the non-composite hollow beam (B2), but these values increased when hollow steel section was used to fabricate the hollow core in the composite hollow beam (B3). It is also noticed that the deflections of the composite hollow beam (B3) at yield and ultimate points were higher than the non-composite beams (B1) and (B2), because the composite hollow beam (B3) show higher resistance to deflections and reached

yield and ultimate points late and with higher yield and ultimate loads. This increase in the deflections resistance of the composite hollow beam (B3) may be due to the increase of the moment of inertia and the effect of the steel box in increasing the compressive and tensile forces of the section during loading.

For **GR.No.2** shown in Fig. (4.4.2) Indicating that values of yielding and ultimate loads were increasing when increasing steel hollow section area from [(60*60)mm² in (B3)] to [(100*100)mm² in (B5)]. This increase in loading capacity was causing increasing in the values of deflections at yield and ultimate points.

For **GR.No.3** shown in Fig. (4.4.3) also indicate values of load and deflections at yield and ultimate points increased significantly when the percentage of longitudinal reinforcement amount increased, from [2ϕ10 in (B6)] to [2ϕ12 in (B3)] to [2ϕ16 in (B7)].

For **GR.No.4** in Fig. (4.4.4) it is clearly observed that the hollow composite beam (B8) which encased with rectangular steel hollow section having geometric properties [A=(5000)mm² and I=416,6666 mm⁴] show the higher load and ultimate loads than the composite hollow beam (B3) with geometric properties of square steel section [A=(3600)mm² and I=108,0000 mm⁴], and than the composite hollow beam (B9) with geometric properties of circular steel section [A=(2827.4)mm² and I=63,6172 mm⁴].

For **GR.No.5** shown in Fig. (4.4.5), it recorded that the composite hollow beam (B3) which has steel box had shear connectors on (4 plates of the box) shows greater loads capacity; therefore, the deflections also greater at both yield and ultimate points. It noticed that composite hollow beams (B11) which have no shear connectors that connect plates of the box with surrounding concrete show smaller values of yield and ultimate load and deflections than (B3) and (B10). So It indicated that composite

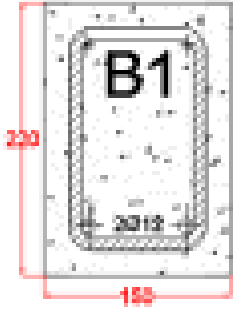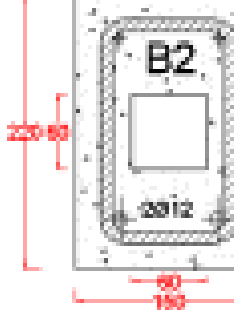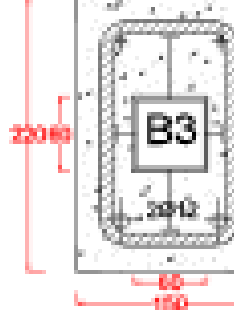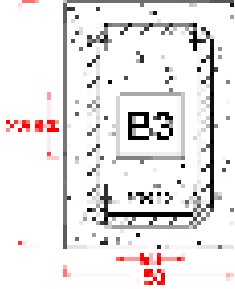Table (4.2).   Ultimate load and Moment capacity of the tested beams.
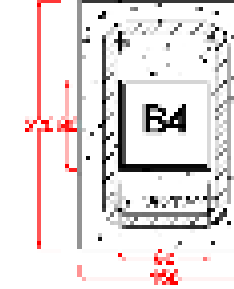
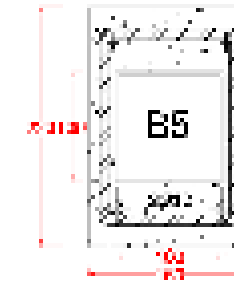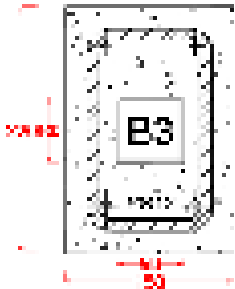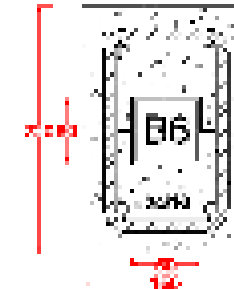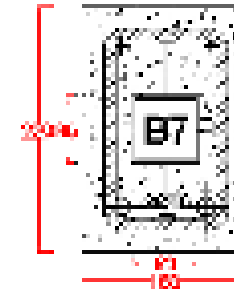| Name of group	Group No. (1): Comparison between the solid and hollow beam and composite hollow beam		
Cross-section	B1	B2	B3
Load capacity	110 kN	105 kN	230 kN
Moment capacity	25.6 Kn.m	24.4 Kn.m	53.6 Kn.m
Name of group	Group No. (2): Changing thickness of the concrete flange		
Cross-section	B3	B4	B5
Load capacity	230 kN	240 kN	290 kN
Moment capacity	53.6 kN.m	55.9 kN.m	67.6 kN.m
Name of group	Group No. (3): Changing longitudinal reinforcement		
Cross-section	B3	B6	B7
Load capacity	230 kN	200 kN	290 kN
Moment capacity	53.6 kN.m	46.6 Kn.m	67.6 Kn.m

Table (4.2). Continued.
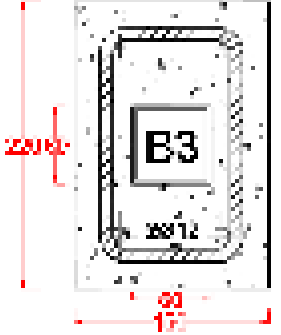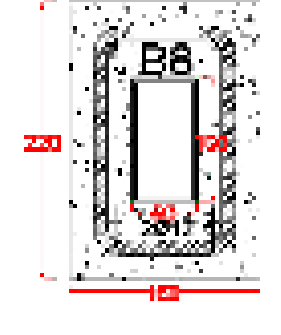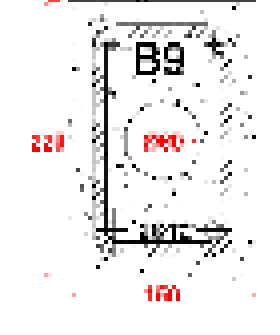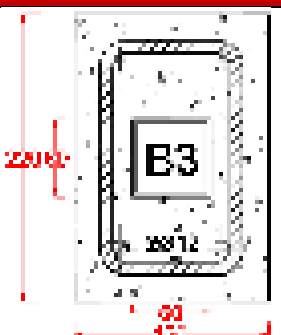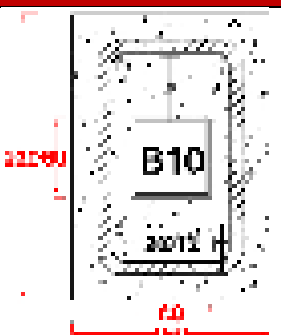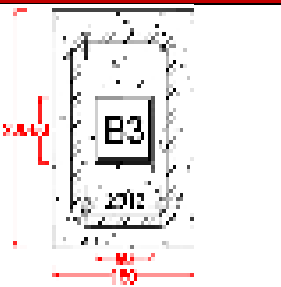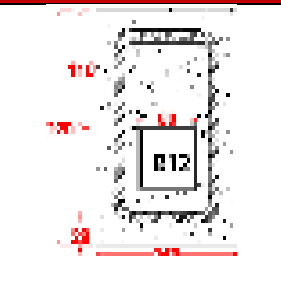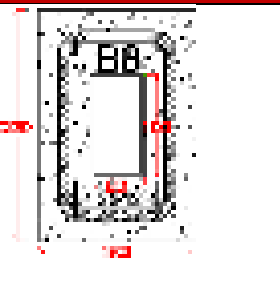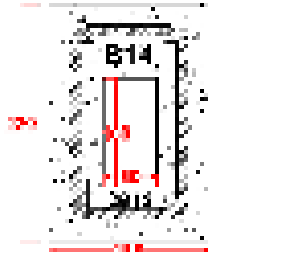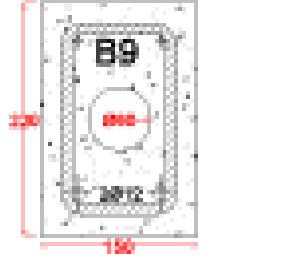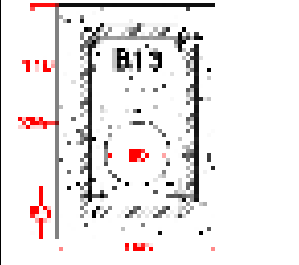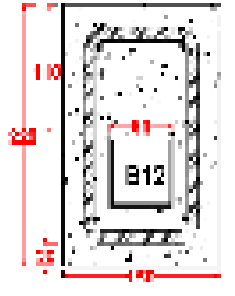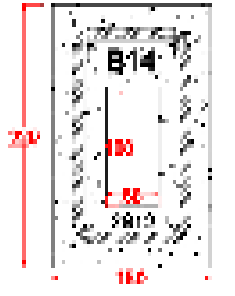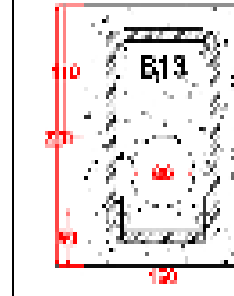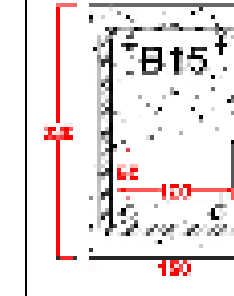
Name of group	Group No.(4): Changing the shape of the steel box		
Cross-section			
Load capacity	230 kN	239 kN	200 kN
Moment capacity	53.6 Kn.m	55.7 kN.m	46.6 kN.m
Name of group	Group No.(5): Changing the arrangement of shear connectors		
Cross-section			
Load capacity	230 kN	220 kN	210 kN
Moment capacity	53.6 Kn.m	51.3	48.9
Name of group	Group No.(6): Changing the locations of steel box		
Cross-section			
Load capacity	230 kN	240 kN	239 kN
Moment capacity	53.6 Kn.m	55.9 kN.m	55.7 kN.m

Table (4.2). Continued.

Cross-section			
Load capacity	245 kN	200 kN	240 kN
Moment capacity	57.1kN.m	46.6 kN.m	55.9 kN.m
Name of group	Group No.(7): Changing the shape of the steel box in the tension zone		
Cross-section			
Load capacity	240 kN	245 kN	240 kN	250 kN
Moment capacity	55.9 kN.m	57.1 kN.m	55.9 kN.m	58.3 kN.m

hollow beams with a high number of shear connectors reach yield stage at load higher than composite hollow beams with lesser number of shear connectors.

For **GR.No.6** it is noticed from Fig. (4.4.6) that the values of yield and ultimate loads increasing when the steel box is lowered towards the tensile zone, therefore the yield and ultimate deflections also increased because it reaches late to yield and ultimate phase.

For **GR.No.7** it is seen that yield, and ultimate loads of composite hollow beams which have rectangular steel hollow box are higher than those with square and circular steel hollow sections.
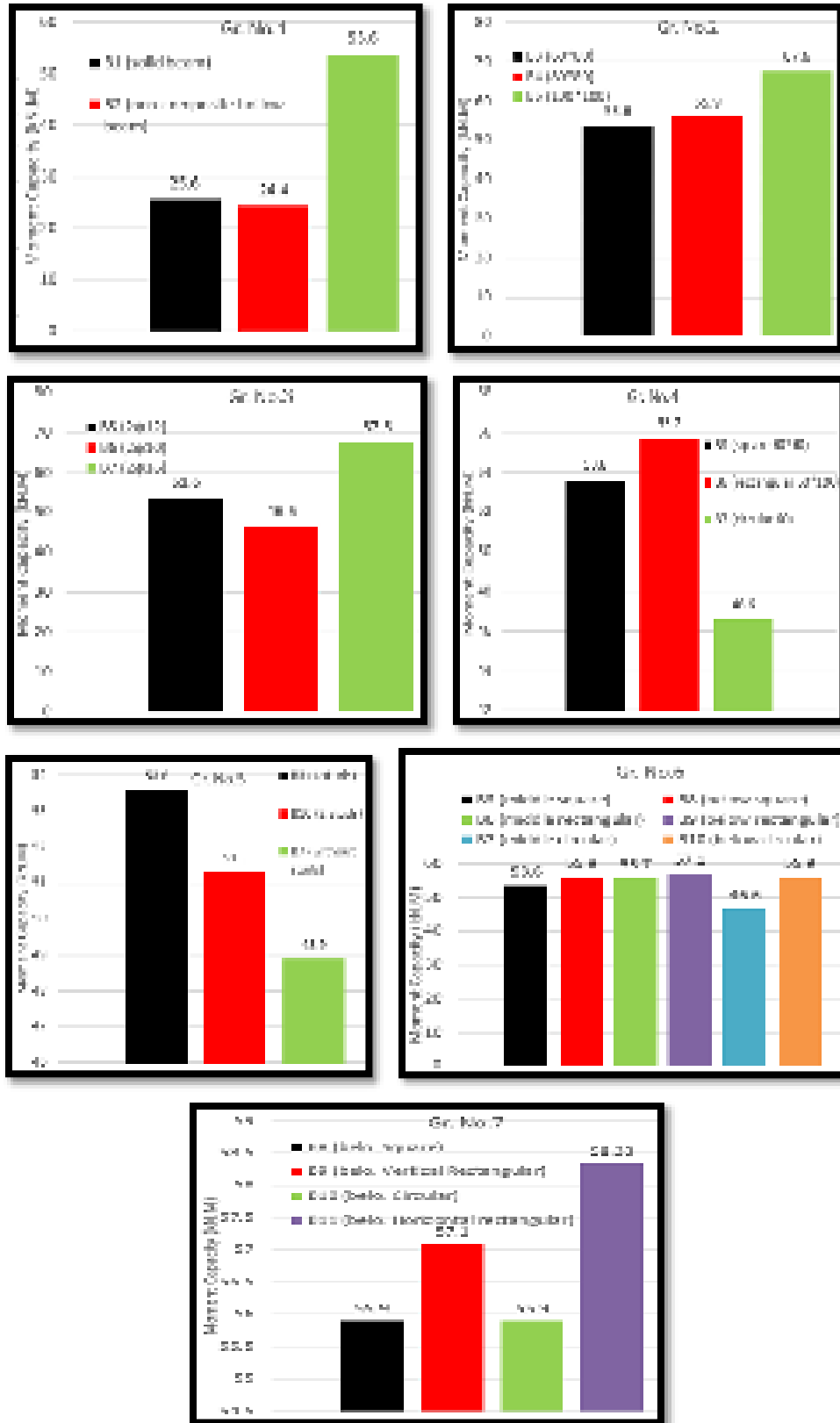
Fig. (4.3) Moment capacity comparisons of the tested beams in seven groups.
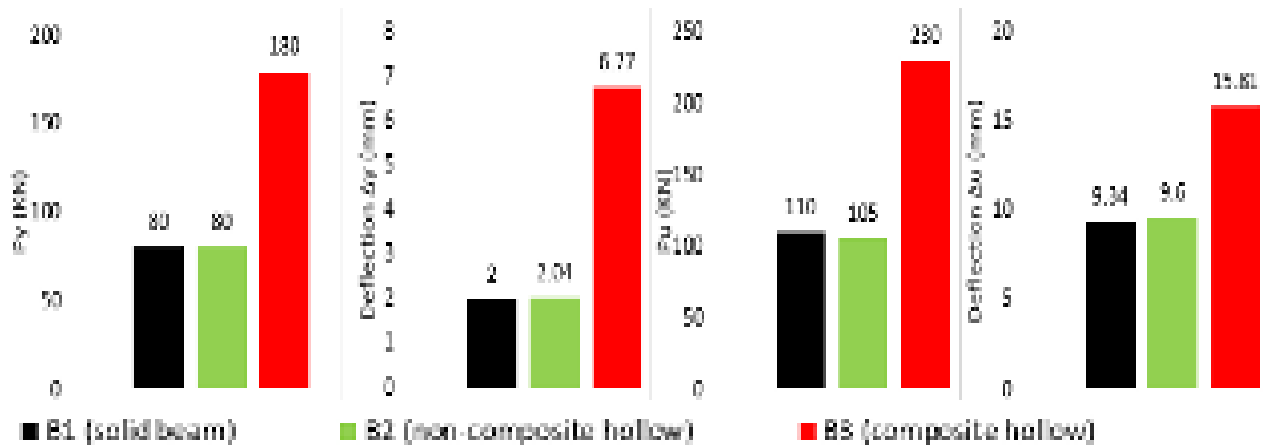
Fig. (4.4.1) Yield, ultimate results for Group No.1 (hollow core material)
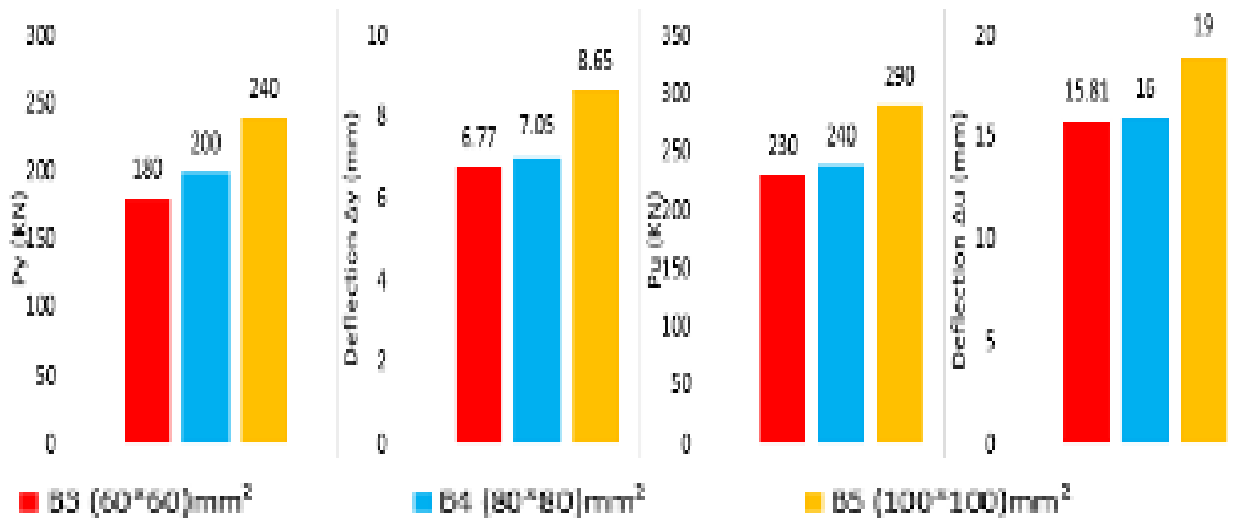
Fig. (4.4.2) Yield, ultimate results for Group No.2 (area of hollow steel section).
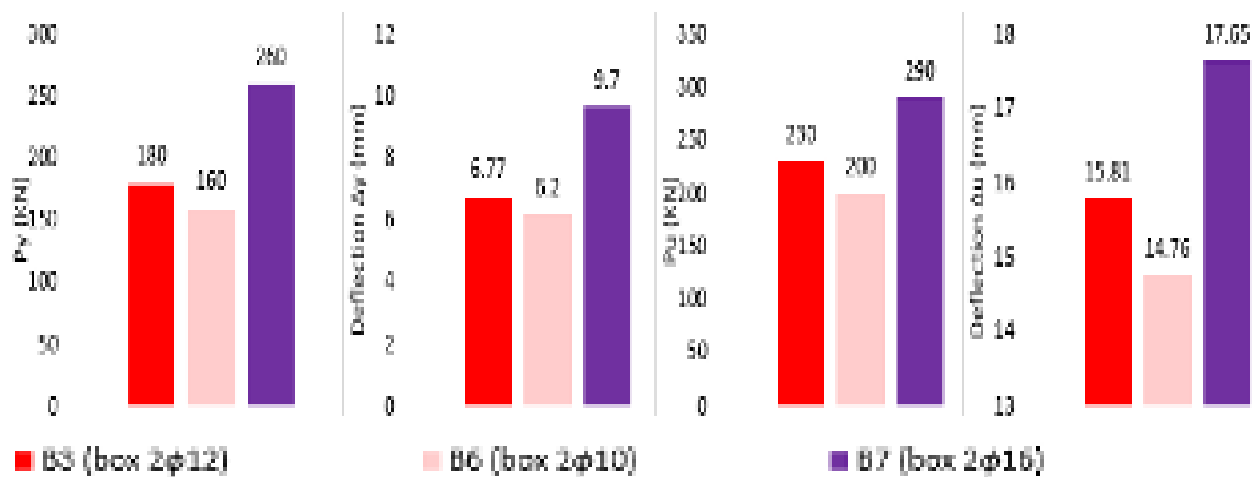
Fig. (4.4.3) Yield, ultimate results for Gr. No.3 (longitudinal reinforcement's ratio)
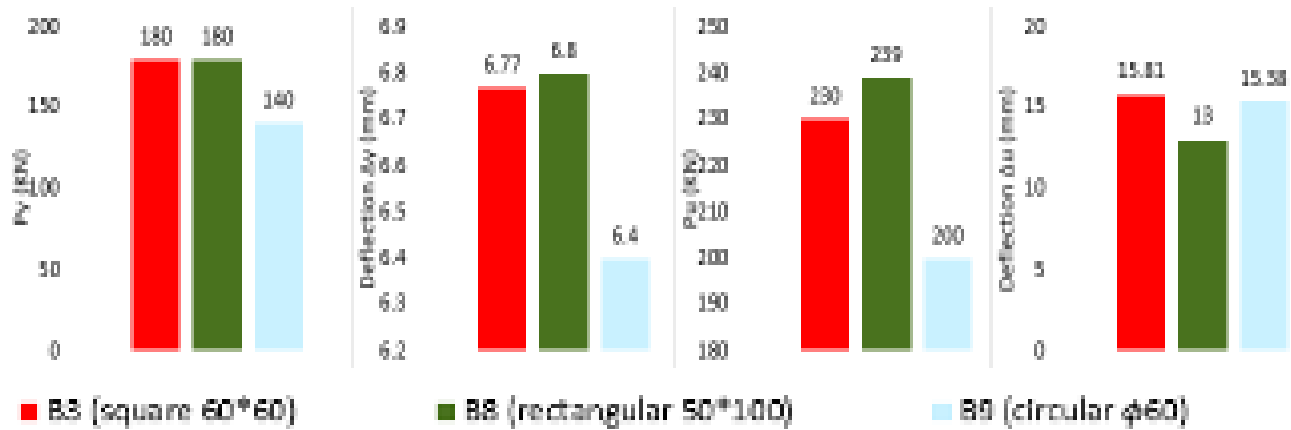
Fig. (4.4.4) Yield, ultimate results for Group No.4 (shape of hollow steel section)
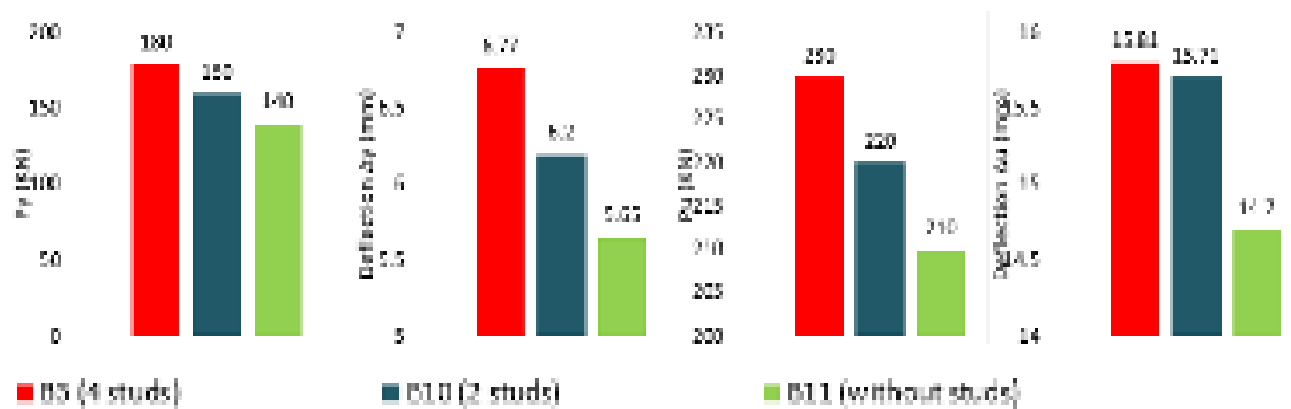
Fig. (4.5.5) Yield, ultimate results for Group No.5 (number of shear connectors)

	B3(mid. square)	B12 (belo.square)	B2 (mid. Rectangular)	B14 (belo. Rectangular)	B9 (mid. Circular)	B13 (belo. Circular)
Py	180	160	180	180	140	160
Δy	6.77	5.45	6.8	6.8	6.4	5.9
Pu	230	240	240	145	200	240
Δu	15.81	12	13	11.24	15.58	13.6
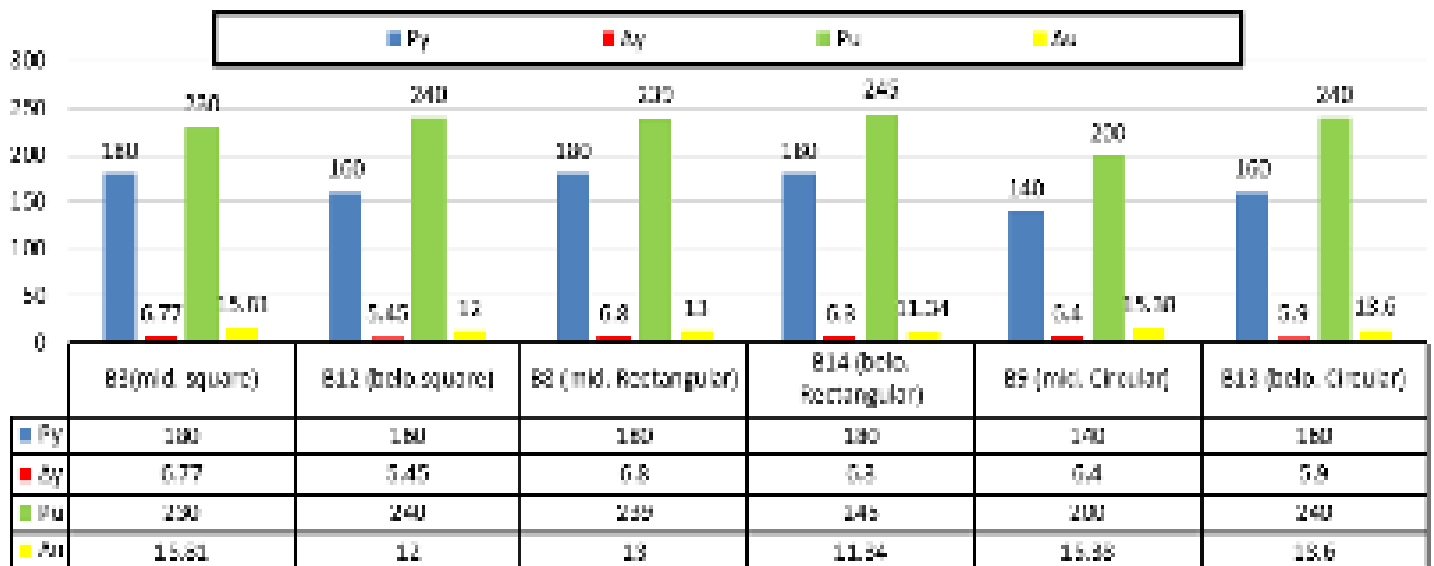
Fig. (4.4.6) Yield, ultimate results for Gr. No.6 (location of hollow steel sections)
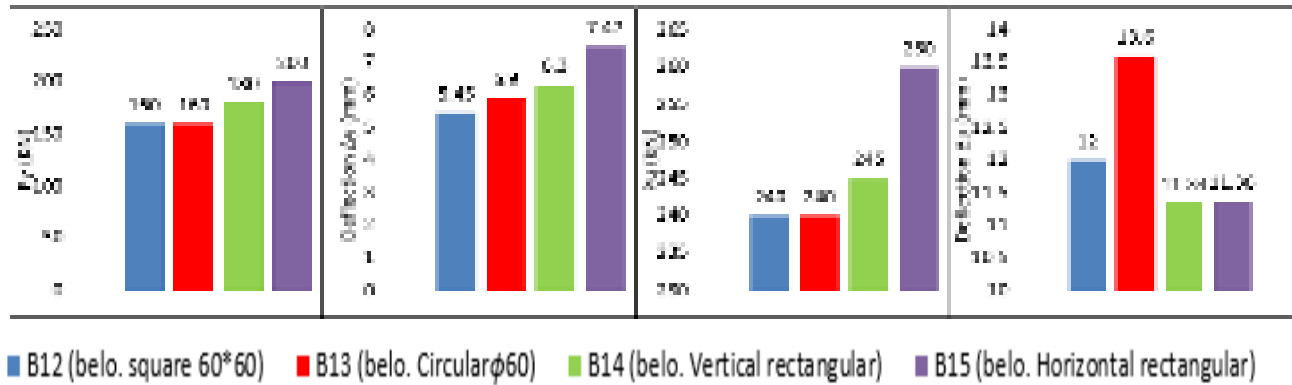
Fig. (4.4.7) Yield, ultimate results for Gr. No.7 (shape of steel box sections in tension zone)

4.7 Loads- Deflections comparisons for tested beams

Load-deflection curves of the tested beams at mid-span at all stages of loading up to failure were constructed and shown in Figs. (4.5.1) To (4.5.7). For comparison of load-deflection, seven groups of curves are established. These are [Gr. No.1 (effect of core material), Gr. No.2 (effect of steel box area), Gr. No.3 (effect of longitudinal reinforcement), No.4 (steel box shape effect), Gr. No.5 (number of shear connectors), Gr. No.6 (location of steel sections) and Gr. No.7 (shape of steel sections in tension zone)]. As shown in Figs. (4.5.1 to 4.5.7) All the tested beams have approximately the same initial load-deflection behavior until reaching the first crack load. Also, the initial change of slope of the load-deflection curves was between (50kN to 75kN) The interpretation of this convergence due to the beams were subjected to same materials properties and same concrete mechanical properties and same manufacturing environments (mixing, placing, compacting and testing). The difference between linear slopes for the curves during convergence can be obtained by P = 60 as minimum cracking load as shown in Fig. (4.4) for all tested beams, so the maximum difference in linear slopes was (20.6) for beams (B1 to B7) and (18.4) for beams (B8 to B15).

For specimens in **GR.No.1** in Fig. (4.5.1) It is noticed that non-composite hollow beam (B2) shows higher deflections compared to the solid beam (B1) due to the decrease in moment of inertia capacity of the section due to the existence of hollow core in the section. However, the behavior of the solid beam (B1) was similar to the hollow beam (B2), but the curve deviated gradually with increasing loads. This indicated a slight decrease in (B2) strength due to the presence of hollow core. When the hollow steel box was encased in the section in a composite hollow beam (B3) lead to decrease the deflections lesser than the deflections of non-composite beams (B1) and (B2) in specific loads. However, for the maximum deflections in Gr. No1 it is noticed, a significant increase in maximum deflection of the composite hollow beam (B3) was observed when comparing with (B1 and B2), this is due to the higher difference in ultimate strength between the beams.

For specimens in **GR.No.2**, in Fig. (4.5.2) It noticed that the composite hollow beam (B5) with higher steel box area (100*100) mm² has the higher ultimate load and higher deflection resistance than (B3) and (B4) with steel box areas (60*60) mm² and (80*80) mm² respectively. It also noticed that the load-deflection curve for the composite beam with highest steel box area and highest hollow core (B5) has a modulus of elasticity higher than composite hollow beams (B3) and (B4). This indicates that the stiffness of the composite beam (B5) was highest. Therefore, this result has a structural and economic benefit at the same time as the hollow steel section with the largest area reduced the amount of concrete and reduced the weight of structural member as the weight of the concrete heavier than the weight of steel and at the same time increased it is stiffness.

For specimens in **GR.No.3** in Fig. (4.5.3) It is noticed clearly that composite hollow beam (B7) has a higher ultimate load than beams (B3 and B6). Also, higher maximum deflection than (B3 and B6) due to the increase in ultimate load. However,

composite hollow beam (B7) has the less deflection along the curve in comparing with (B3 and B6) at specific loads.

For specimens in **GR.No.4** in Fig. (4.5.4) It is noticed that composite hollow beam (B8) which has rectangular steel box show the higher ultimate load and higher deflections resistance compared with composite hollow beams with square and circular steel boxes (B3) and (7) respectively. With this result, it can observe the apparent effect of the increasing moment of inertia of the section and its effect against bending stresses, since the rectangular section has a moment of inertia higher than the other sections when considering all other factors are the same.

For specimens in **GR.No.5** in Fig. (4.5.5) it is clear that the composite hollow beam (B3) which has a higher number of shear connectors (studs) has greater ultimate load and maximum deflection rather than (B7) and (B8), this slight increase in maximum deflection in (B3) is due to the slightly increased in ultimate load, it also noticed that the deflections values along the curve in (B3) were lesser than deflections in (B10) and (B11). It may be inferred here that the number of shear connectors is independent for deflections but is dependent for the section flexural capacity.

For specimens in **GR.No.6**, in Fig. (4.5.6) It noticed that the lowering the hollow steel sections would increase the ultimate loads and increase maximum deflections, but the deflections along the curve were decreased in comparing the specimens at specific loads. This may mean that the flexural contribution given by the hollow steel section is higher than the contribution that (UHPC) gave in the tensile zone of the section.

For specimens in **GR.No.7**, in Fig. (4.5.7) Is important to notice that the composite hollow beams containing horizontal rectangular steel hollow section (B15) give the highest ultimate load and fewer deflections compared to the rest of specimens in

group No.7 at same specific loads. This can be explained by the presence of the horizontal rectangular steel box within the tensile area is provided an additional quantity of reinforced steel for the quantity of longitudinal reinforcement and make the section more efficient in resisting the deflections and resulting cracks.
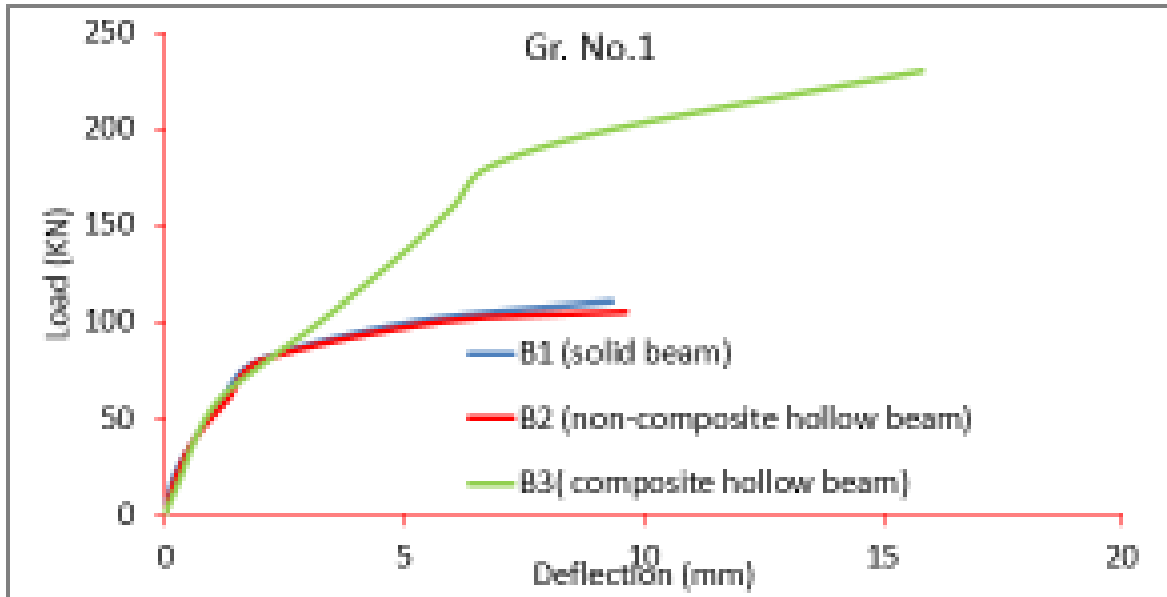
Fig. (4.5.1) load-deflections comparison for Gr. No.1 (effect of core material)
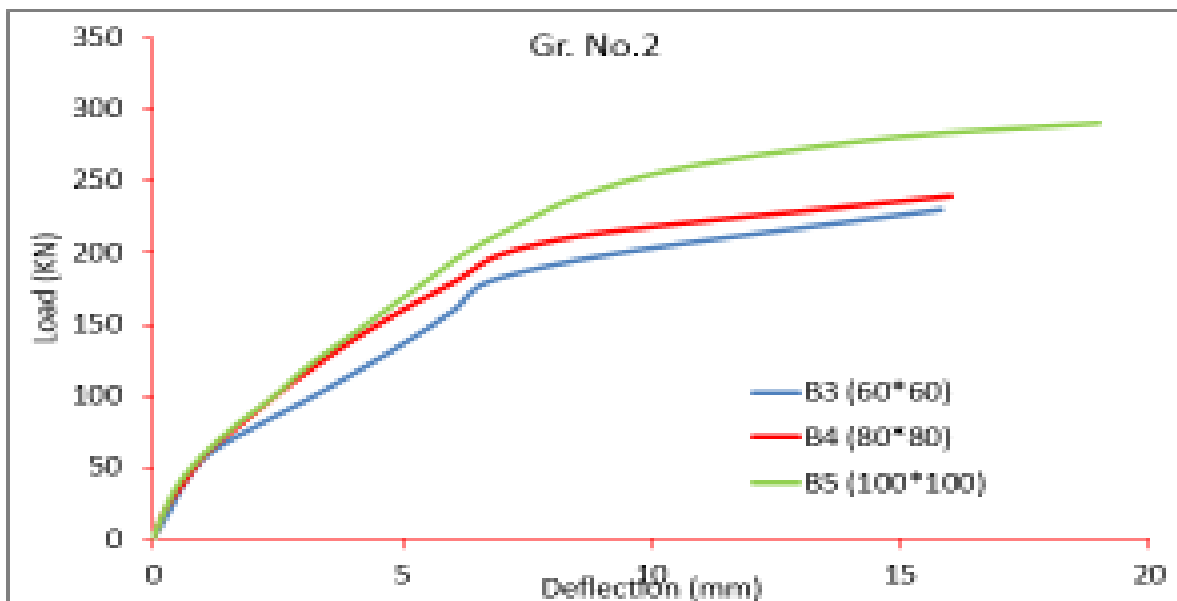
Fig. (4.5.2) load-deflections comparison for Gr. No.2 (effect of steel box area)
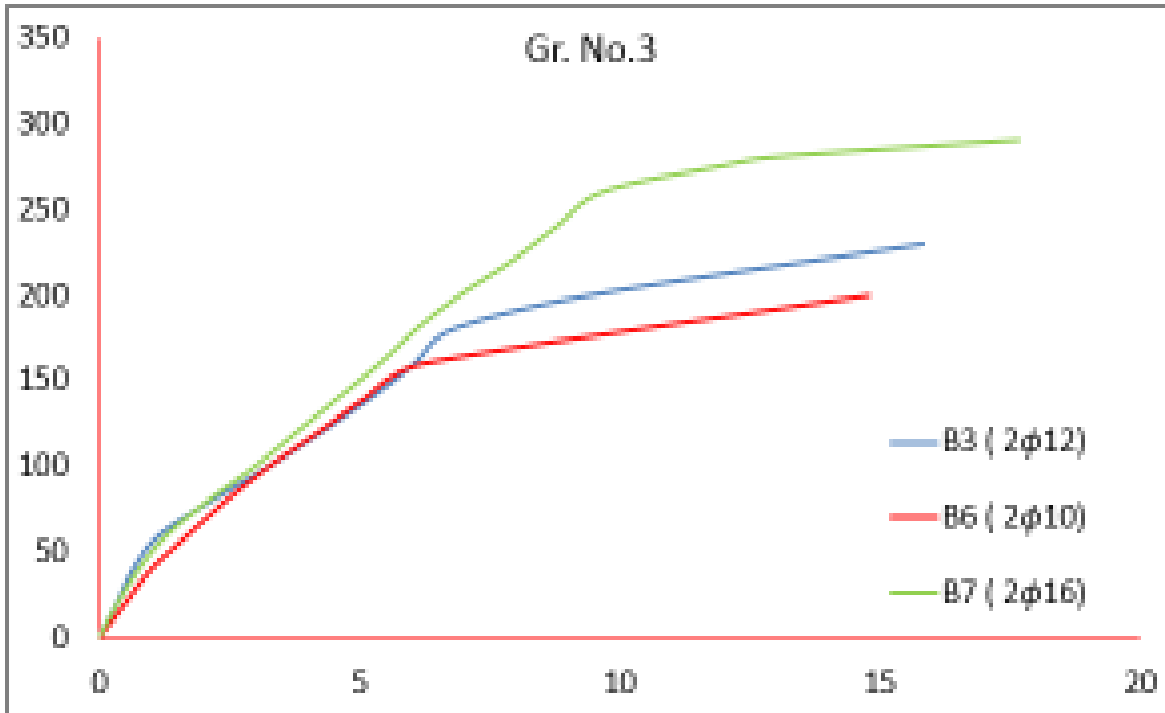
Fig. (4.5.3) load-deflections comparison for Gr. No.3 (effect of longitudinal reinforcement).
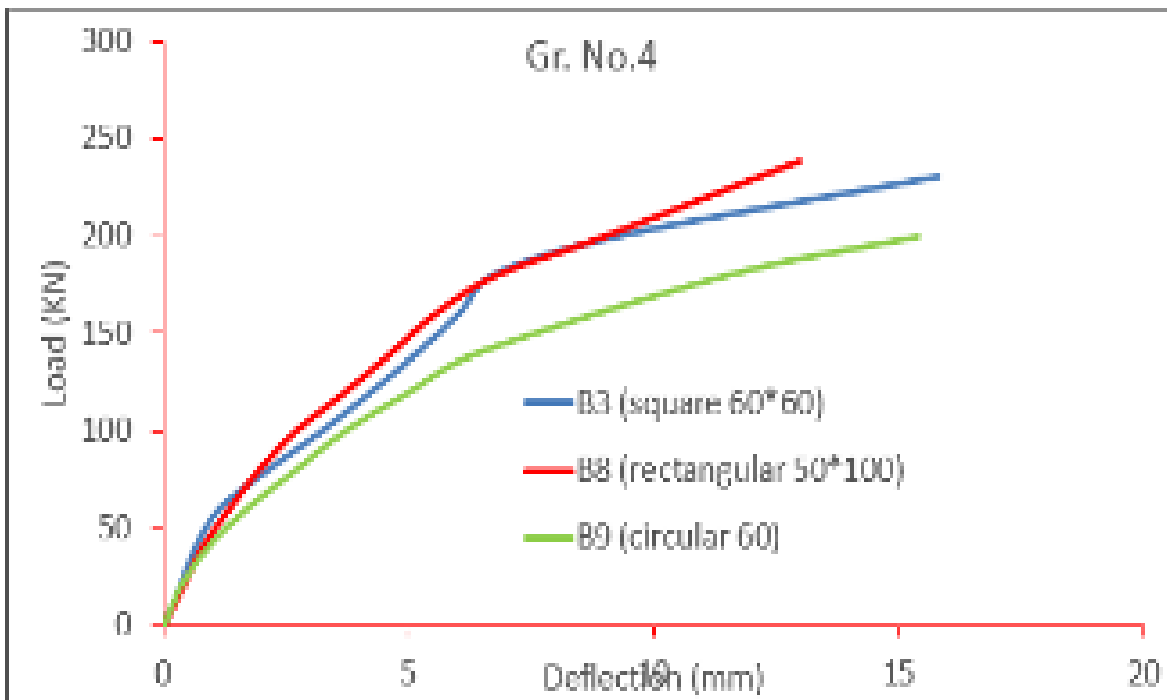
Fig. (4.5.4) load-deflections comparison for Gr. No.4 (steel box shape effect)
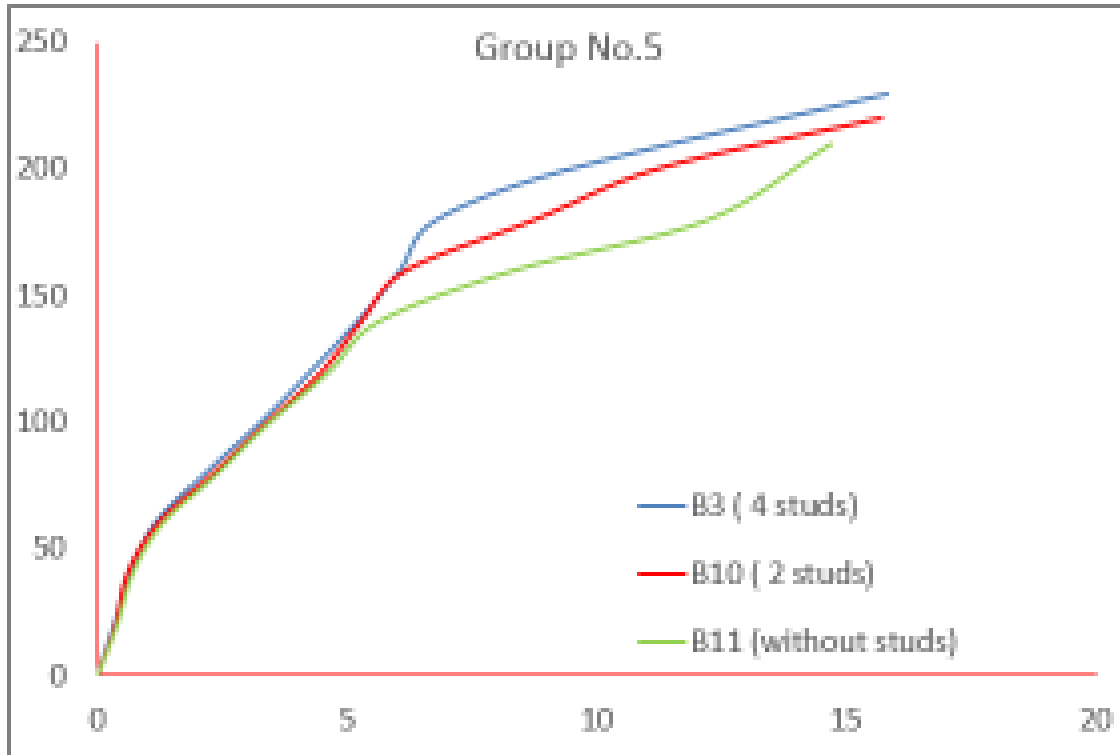
Fig. (4.5.5) load-deflections comparison for Gr. No.5 (number of shear connectors)
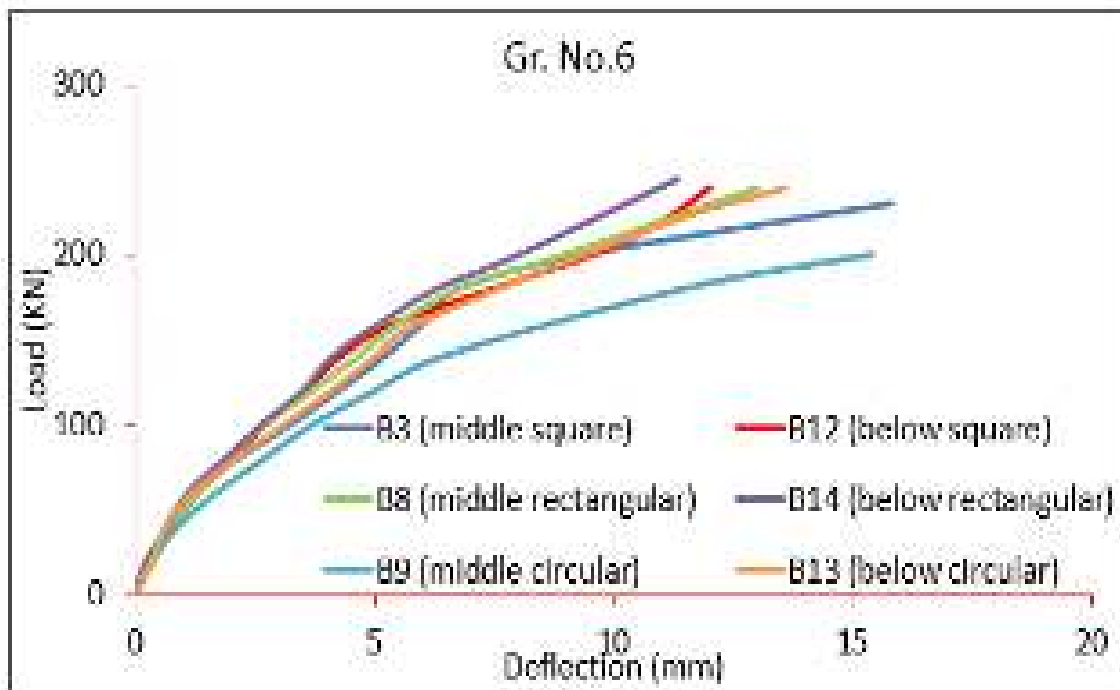
Fig. (4.5.6) load-deflections comparison for Gr. No.6 (location of steel sections)
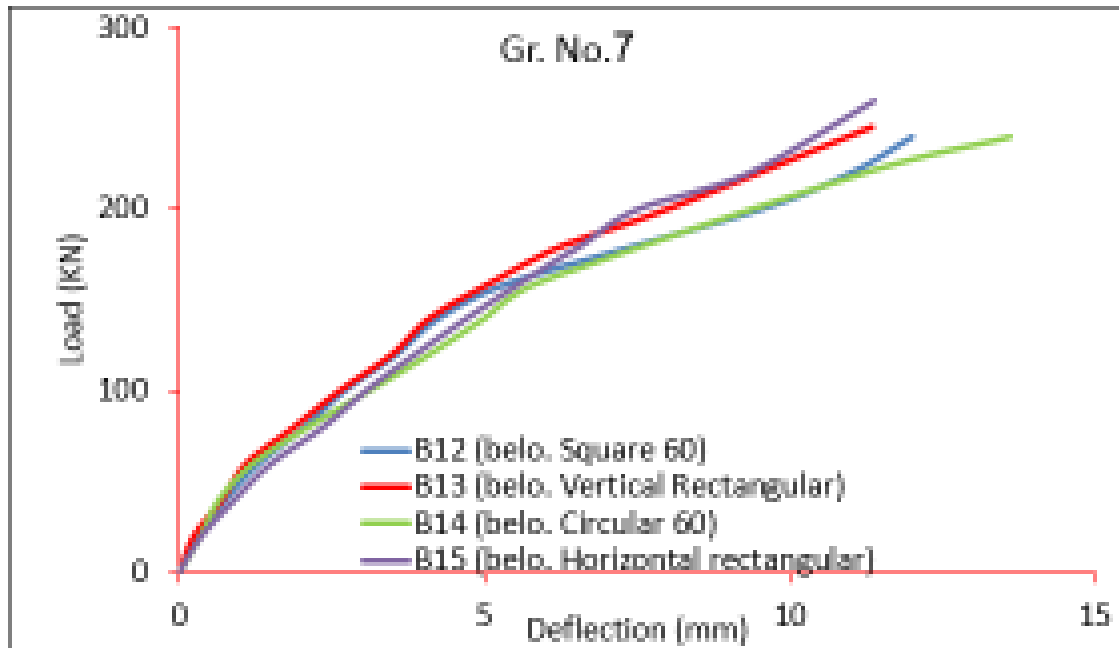
Fig. (4.5.7) load-deflections comparison for Gr. No.7 (shape of steel sections in tension zone)

4.8 Stiffness comparisons for the tested beams

Stiffness can be defined as the required load for causing one-unit of deflection. The value of the stiffness can be calculated by dividing the ultimate load on the maximum deflection in the tested beam[32]. So, in general, the beam that has a higher ultimate load and less deflection will have a higher stiffness value. The stiffness values at ultimate loads of the tested beams are presented in Fig. (4.6).

For **GR.No.1**, it noted that in the first group that the composite hollow beam (B3) has a higher stiffness than non-composite hollow beam (B2) by 33% and higher than solid beam (B1) by 23.5%. It indicates that when steel hollow section encased in concrete will increase the stiffness of the section by increasing the ultimate load of the beam.

In **GR.No.2** in Fig. (4.6.2) it can notice that a composite hollow beam (B5) which has encased steel box section with geometric properties {[A= (100*100)mm²] and the steel section ratio [A box = 4.73% * Ac]} has the higher stiffness than composite hollow beam (B4) which has geometric properties {[A= (80*80)mm²] and the steel section ratio [A box = 3.25% * Ac]}, and higher than (B3) which has geometric properties {[A= (60*60)mm²] and the steel section ratio [A box = 2.17% * Ac]}. So consequently. The composite hollow beams with steel section ratio 4.73% have a stiffness higher than those having steel section ratio of 3.27% and 2.17%. This indicates that stiffness of the composite hollow beams increases as the steel section ratio of encased steel section increases.

In **GR.No3** shown in Fig. (4.6.3) It can notice that the composite hollow beam (B7) that has higher longitudinal reinforcement give the higher stiffness than (B3) and (B6) by 12.9% and 21.2% respectively. This indicates that stiffness of hollow composite beams increases when it is longitudinal reinforcement ratio increases.

In **GR.No4** shown in Fig. (4.6.4) it is noticed that the composite hollow beam (B8), which has encased steel section with following geometric properties [A=(5000)mm², A box = 2.88% * Ac, box shape= rectangular, I box=416.6 cm^4, I box= 3.23%*Ic] has stiffness (26.3%) higher than (B3) which has geometric properties [A=(3600)mm², A box = 2.17% *Ac, box shape= square, I box=108 cm^4, I box= 0.81%*Ic]. And (41.38%) higher than (B9) which has geometric properties [A=(2827.4)mm², A box = 1.66% *Ac, box shape= circular, I box=63.61 cm^4, I box= 0.48%*Ic]. Consequently, the composite hollow beams having encased steel section moment of inertia ratio 3.23% have stiffness higher than those having encased steel section ratios of 0.81% and 0.48%. This indicates that the stiffness of the composite hollow beams increases as the steel ratio of the encased steel section increases.

In **GR.No5** shown in Fig. (4.6.5) It is noticed that composite hollow beam (B3) which has shear connectors connecting the encased steel box with concrete by welded studs on 4 plates (flanges and webs) of the steel box, has the highest stiffness and higher by 3.9% than (B10) which has studs welded only 2 plates (only flanges) of the steel box. Also, the stiffness of (B3) higher by 6.9% than (B11) which has not any shear connectors connecting the steel box with concrete. This indicates that the stiffness of composite hollow beams increases as the number of shear connectors increases.

In **GR.No.6** shown in Fig. (4.6.6) It is noticed that when the square steel box lowered towards the tension zone in the composite hollow beam (B12) will increase its stiffness by 37.4% higher than composite hollow beam (B3). Also, when lowered rectangular steel box in (B14) will increase its stiffness by 18% higher than (B8). Also the lowering of the circular steel box in (B13) increase stiffness by 35% then (B9). This indicates that the stiffness of hollow composite beams increases as the location of the hollow steel section lowered toward the tensile zone of the section.

In **GR.No.7** shown in Fig.(4.6.7), it is noticed that composite hollow beams (B15) which have a horizontal rectangular steel box within the tensile zone has stiffness higher than (B14) which has vertical steel box, This increase may be due to the increase of ultimate load and the decrease in the maximum deflection of (B15) and can be explained that presence of the horizontal rectangle within the tensile area is provided an additional quantity of reinforced steel to the quantity of longitudinal reinforcement and make the section more efficient in resisting the deflections and resulting cracks. From the figure, it is also noticed that composite hollow beam (B14) which has a rectangular steel box has stiffness higher by 22.3% than (B13) which has a circular steel box. Also, higher by 8% than (B12) which has a square steel box.

(1). Gr. No.1 (hollow core material)   (2). Gr. No.2 (effect of steel box area)
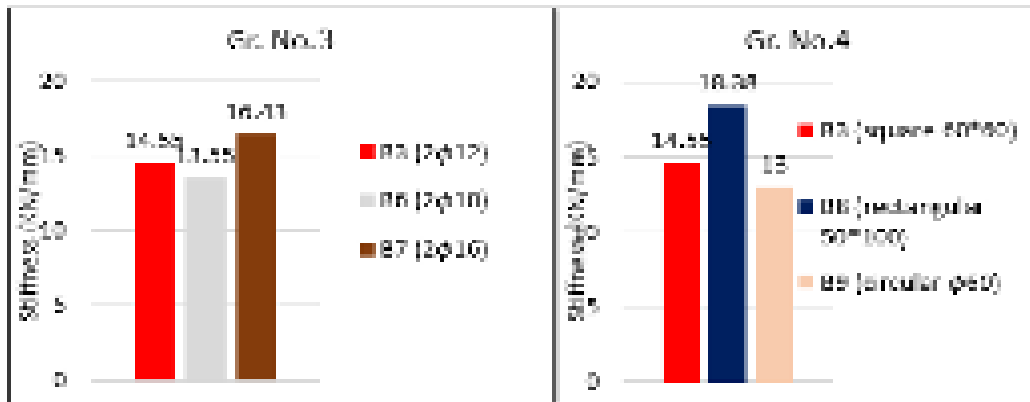
(3). Gr. No.3 (longitudinal reinforcement)   (4). Gr. No.4 (steel box shape effect)
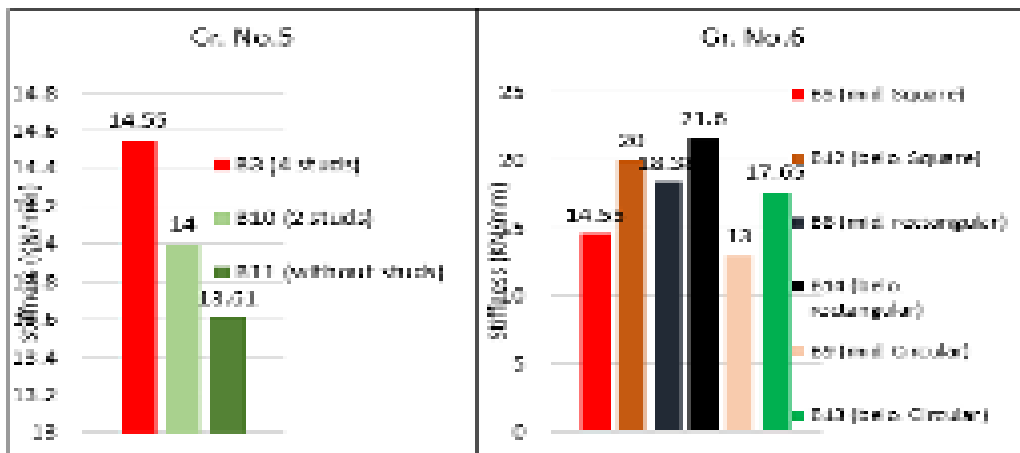
(5). Gr. No.5 (shear connectors)   (6). Gr. No.6 (location of steel sections)
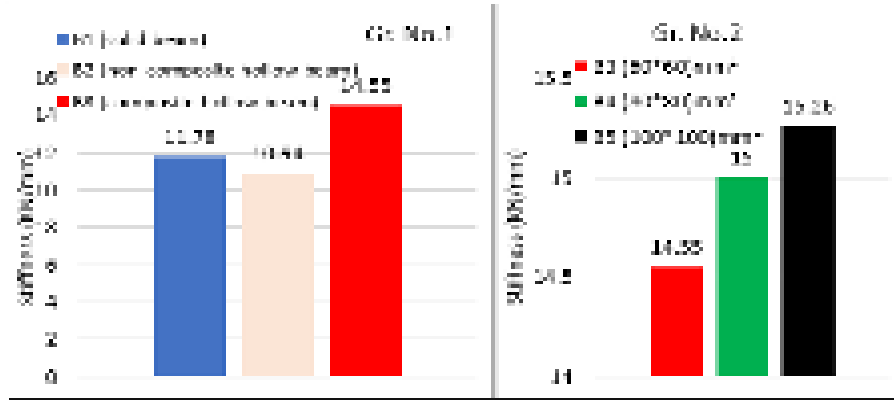
Fig. (4.6) Stiffness values of the tested beams.
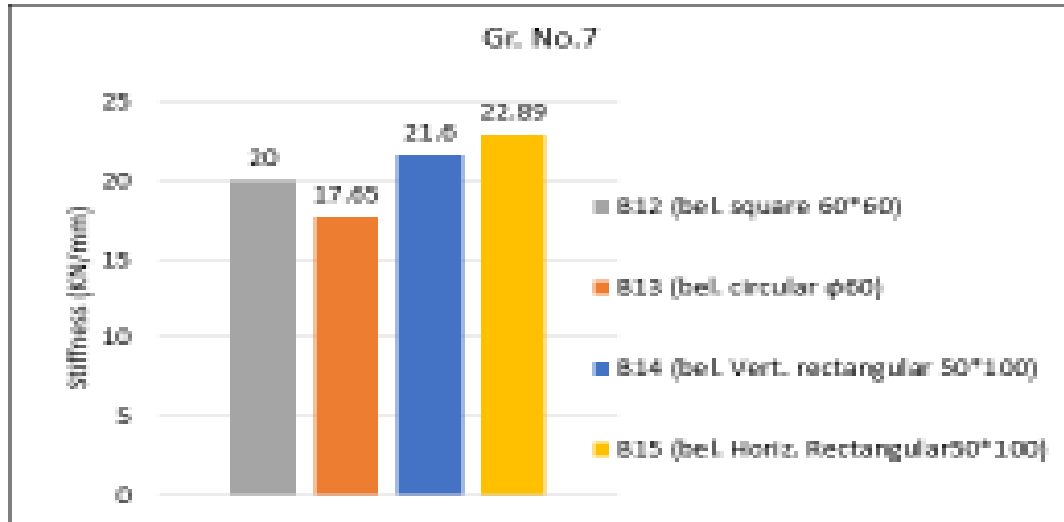
(7). Gr. No.7 (shape of steel sections in tension zone)

Fig. (4.6) Continued.

4.9 Ductility comparisons for the tested beams

Ductility is one of the most important features to be taken into account in the designs of structures exposed to a large number of inelastic deformations resulting from different loading conditions [32]. It can be defined as the structural member's ability to undergo inelastic deformations beyond yield deformation without significant loss in its load-carrying capacity. The ductility in the flexural member can be obtained through its load-deflection curve. It is the ratio between the deflection value when the member fails, to the deflection value at the time of yield stage occur, it is known as ductility factor ($\mu = \Delta u / \Delta y$). It can be calculated by dividing the maximum deflection (Δu) on the yield deflection (Δy). Fig. (4.7) represents the ductility factor values for the tested beams. It shows that ductility is increased by 0.85% when hollow core fabricated in a non-composite hollow beam (B2). This may be due to the concrete usually gives a brittle behavior, so the presence of the hollow core in the concrete in (B2) led to a little reduction in the proportion of brittleness of the

section, and also because the stiffness of (B2) less than (B1) as shown in Fig. (4.6.a). Also, it may be explained that the hollow beam (B2) has a moment of inertia I $=13202$ cm^4 less than a moment of inertia of the solid beam (B1) (I $= 13310$cm^4) so the presence of hollow core lead to decrease the moment of inertia of section by 0.81%. From Fig. (4.7.1) it can notice that the ductility is decreased when hollow core fabricated using hollow steel section in (B3). The reason for this may be because the addition of the steel section led to an increase in the rate of reinforced section to resist the deflections, leading to making the section reach in late to the yielding stage of loading, so the deflection value of (B3) at yield (Δy) was greater and since the value of (Δy) inversely proportional to the ductility factor ($\mu = \Delta$u / Δy), so the ductility factor for (B3) was less than the solid beam (B1). This explained because the difference between yield and maximum deflection in the composite beam is lowest than the difference between yield and maximum deflection in the solid beam. That means the ductility in non-composite hollow beams higher than the solid beams, and also higher than composite hollow beams. From Fig. (4.7.2) it noticed that composite hollow beam (B5) has a reduction in ductility about 6.3% than (B3) and 3.1% than (B4). This reduction may be to the increase in development of ultimate strength with lower ultimate deflection. It also indicates the section shows increasing in stiffness and decreases in ductility. From Fig. (4.7.3) in group No.3 it is noticed that hollow composite beam (B7) containing the highest longitudinal steel reinforcement ratio has less ductility factor by 28.5% than (B3) and 30.7% than (B5). This means that the section that contains more longitudinal reinforcement has a greater ultimate load (Pu=290kN for B7). So, It reaches yield stage lately, where the elastic phase is greater than the plastic phase, which causes an increase in yield deflection value (Δy) lead to decrease the ductility factor ($\mu = \Delta$u / Δy). In the fourth group shown in Fig. (4.7.4) it noticed that composite hollow beam (B8) which has a rectangular steel section shows less in ductility factor by 25.6% in compared with

(B9) and by 22.5% in compared with (B3). This can be explained by returning to the load-deflection in fig. (4.7.4) it noticed clearly that composite hollow beam (B8) shows the less ultimate deflection than (B9) and (B3). From Fig. (4.7.5) in group No.5, it noticed that composite hollow beam (B3) has decreased in ductility of the section by 8% then (B10) and by 11% then (B11). This indicates that the increase in the number of shear connectors increase the stiffness of section and decrease its ductility. From Fig. (4.7.6) in group No.6 it is noted that ductility in composite hollow beam contained steel box below the section (B12) decreased by 5.9% than the composite hollow beam containing steel box in the middle of section (B3). This may be due to the stiffness of (B12) is greater than (B3) and the presence of the hollow core below the section leads to the weakening of the concrete strength against tensile stresses, which leads to increase the emergence of cracks in the early stages of loading, which leads to a decrease in the ductility of section. Therefore, the best location for the hollow core when taking into account the ductility of the section is in the tensile zone of the concrete section. From Fig. (4.7.7) it showed the ductility of (B9) has ductility higher by (5%, 28%, and 51%) than (B12, B13, and B15) respectively. This is very obvious by observing the load-deflection curve of these beams in Fig. (4.7.7), also it is noticed that the ultimate load of (B15) is the highest, but the deflections were the lowest, which leads to this difference between (B9) and (B15) in ductility.

In general, if the uses of this type of steel sections in encased to the beams, will lead to reduced its ductility and increases their stiffness and rigidity. The reason for this reduction in ductility for these steel sections is that the values of its yield tensile stress (fy) of these sections are usually less and less than the usual reinforcing steel, but its ultimate tensile stress (Fu) is higher.
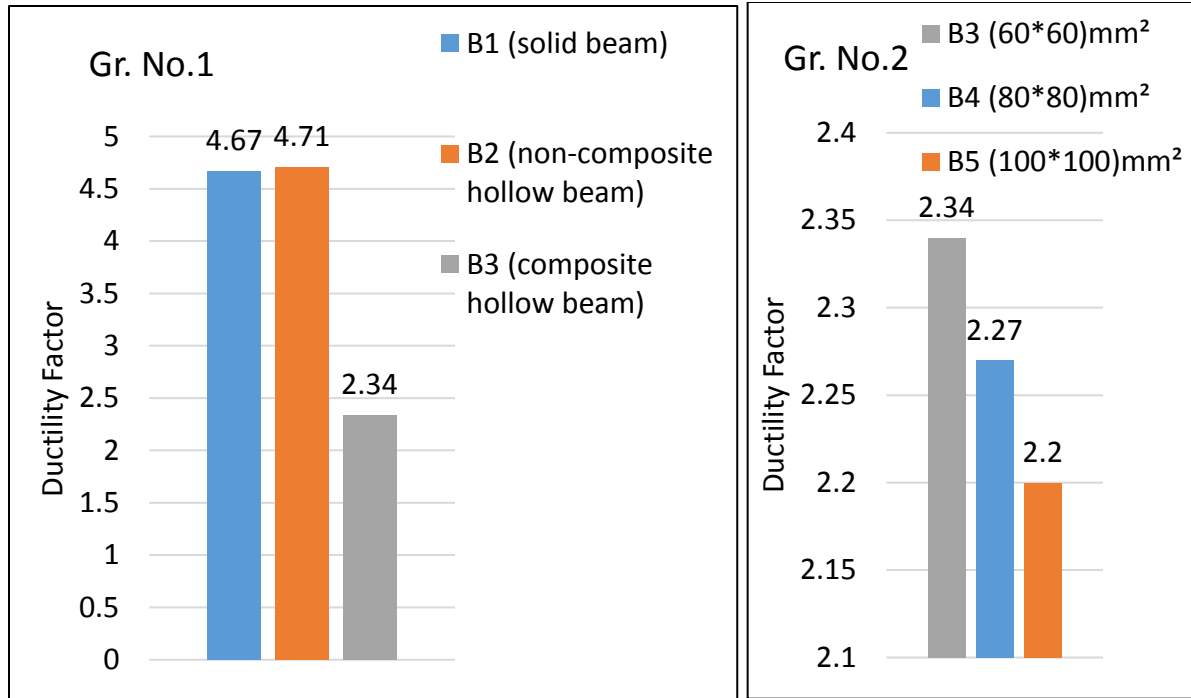
(1). Gr. No.1 (hollow core material)   (2). Gr. No.2 (effect of steel box area)
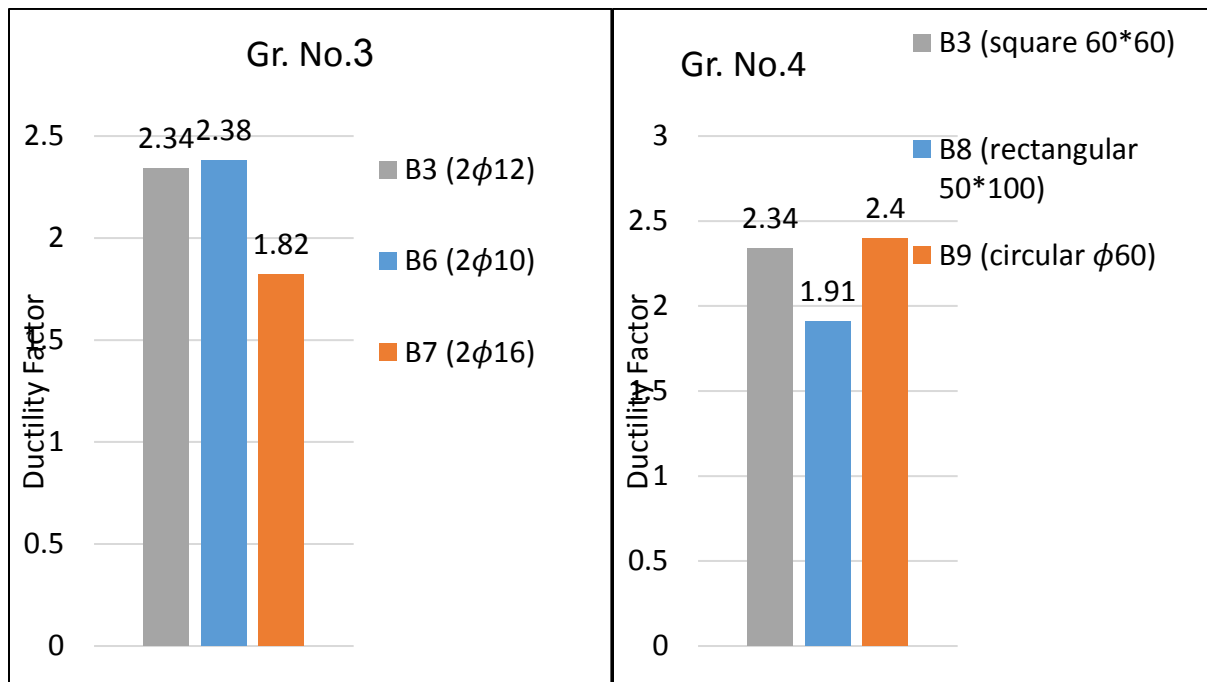
(3). Gr. No.3 (longitudinal reinforcement)   (4). Gr. No.4 (steel box shape effect)

Fig. (4.7) Ductility values of the tested beams.
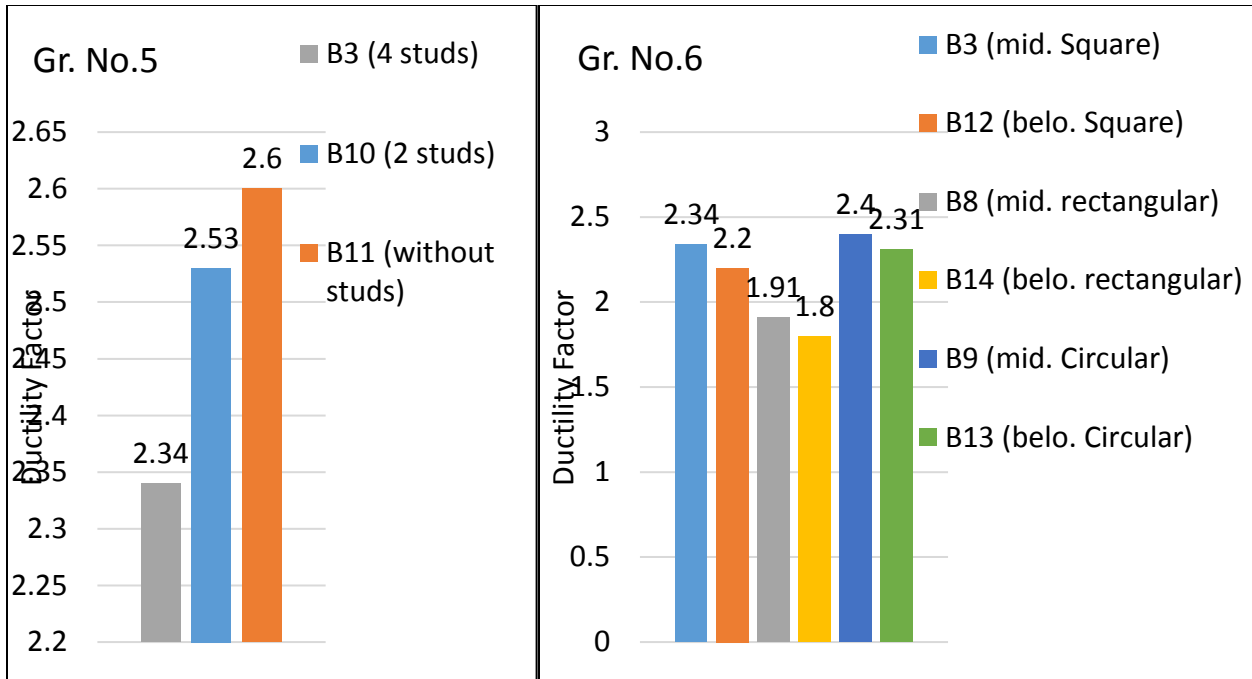
(5). Gr. No.5 (shear connectors)

(6). Gr. No.6 (location of steel sections)
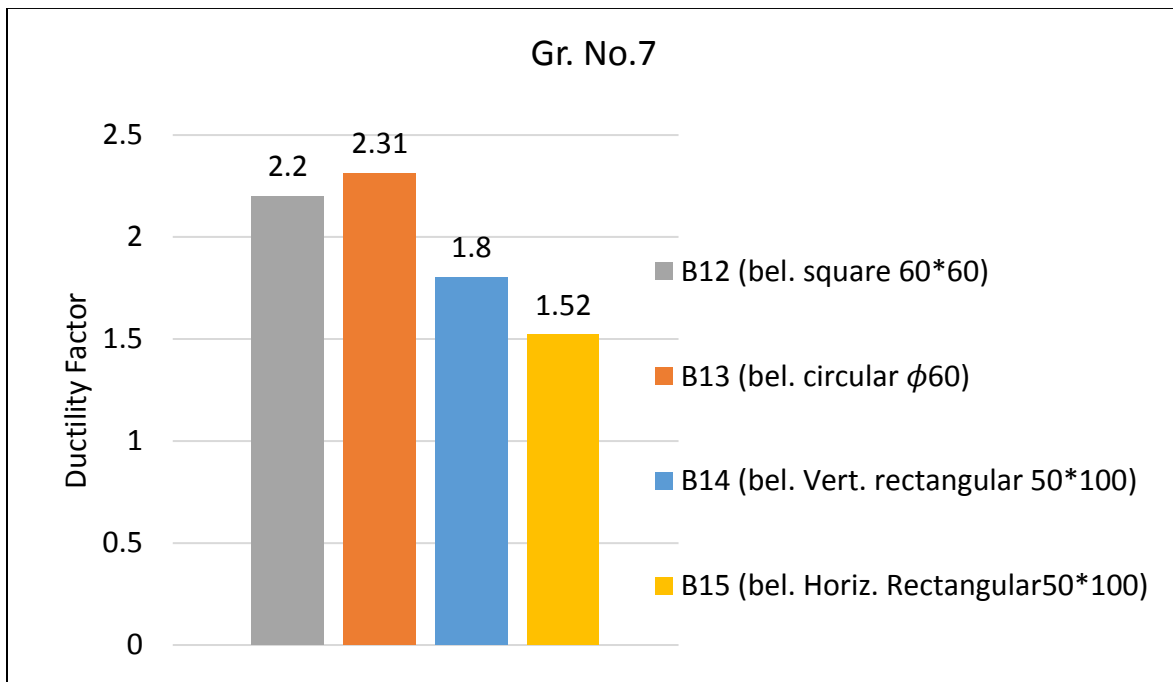
(7). Gr. No.7 (shape of steel sections in tension zone)

Fig. (4.7) Continued.

4.10 Cost analysis and feasibility

One of the prime objectives of this study was to provide a cost-effective analysis. The approximate cost calculation for each beam specimen is shown in Fig. (4.8). The cost analysis was based on $2000 for one meter cube of ultra-high performance concrete, $1136.36 for one ton of steel bars and structural steel tube it is based on the type of steel hollow section it (size and shape), All materials costs for each UHPC beam included in Appendix B. And labor, transport and other expenses (construction costs) were equally distributed to all beams, as well as the cost of shear connectors (studs) and their welding cost also added. The increase in flexural capacity of each beam specimen was compared with its costs as shown in Fig. (4.8). It indicates that composite hollow beams provided capacity higher than solid and non-composite hollow beams[66].
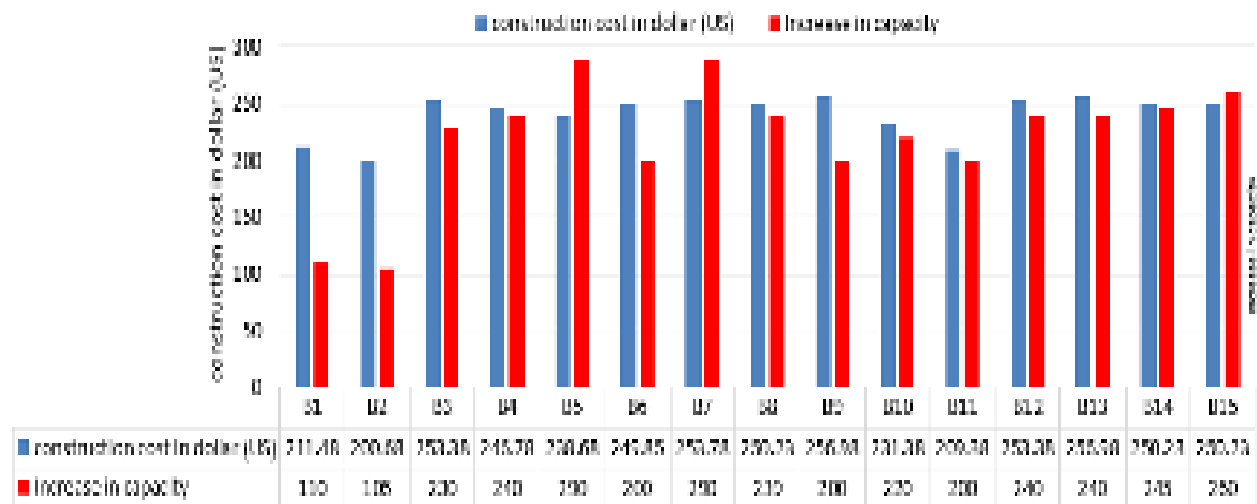
Fig. (4.8) Cost analysis of all specimens.

Feasibility and efficiency as shown in Fig. (4.9) for beam specimens were calculated using an efficiency scale, E, defined by Equation (1).

$$E = \frac{Increase\ in\ Strength}{Construction\ costs\ in\ (U.S)\ dollars} \times 1000 \qquad \text{......... Eq. (4.1).}$$
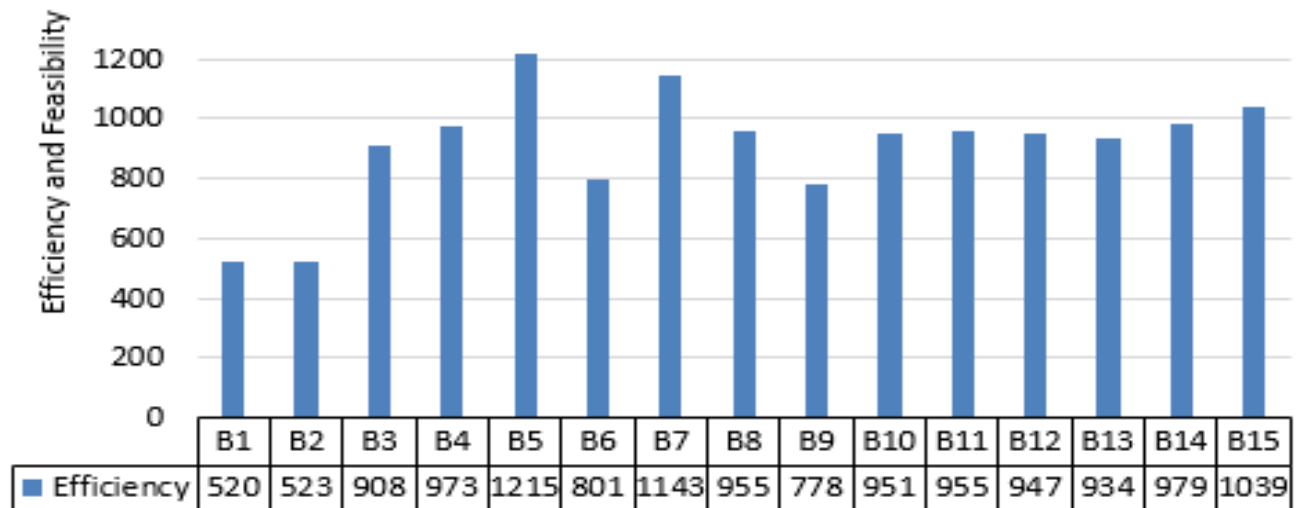
Fig. (4.9) The efficiency of all beam specimens.

The results show that using of encased hollow steel section in the composite hollow beam is an efficient technique in terms of strength improvement and construction cost compared to the solid beam (B1) and non-composite hollow beam (B2) depending on the steel hollow section configurations.

4.11 Concrete strains

Concrete strains were recorded by using electrical strain gauges fixed on faces of concrete and steel hollow section. These strain gauges were distributed at the upper and lower flanges of concrete and steel hollow sections. Attached to the top surface of the concrete, the top surface of steel hollow section (embedded in concrete), and the on the bottom surface of concrete and steel hollow section, at the mid-span of UHPC composite hollow beam.

Fig. (4.10) show the applied load versus the concrete strains recorded by strain gauges during the experimental test for each tested beams (B3, B4, B8, B12, B14, and B15). Very small strains were recorded at the first stage of loading up to the onset of cracks in concrete when a sudden –increase in the strains took place,

thereafter the strains increased almost linearly with increasing the load. The maximum concrete strain in compression was measured at topmost fibers of the concrete surface, while the gauge located on the top and bottom surfaces of steel hollow section and embedded in concrete may record either compression or tension strain, based on the neutral axis movement.
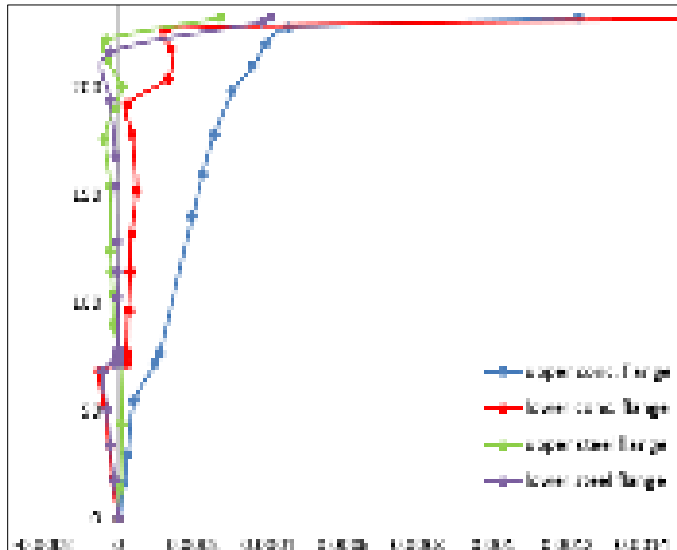
Fig. (4.10.1) load-strains for (B3).
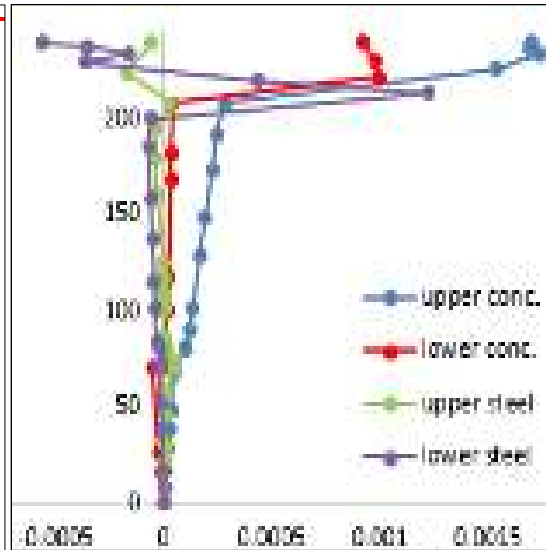
Fig. (4.10.2) load-strains for (B4).
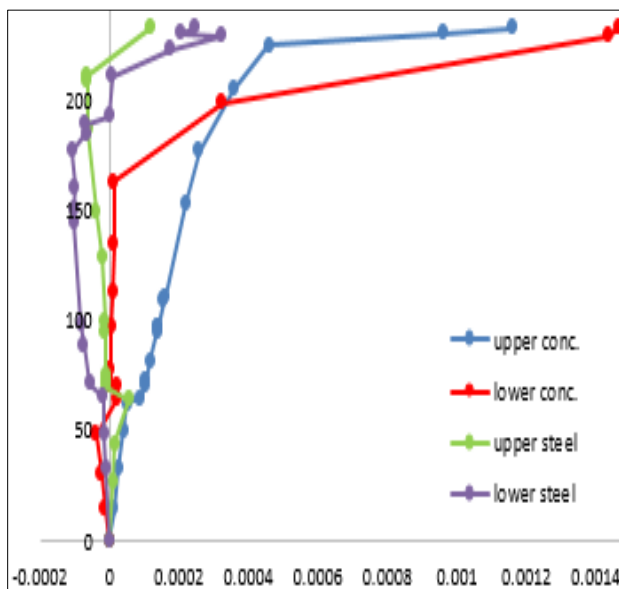
Fig. (4.10.3) load-strains for (B8).
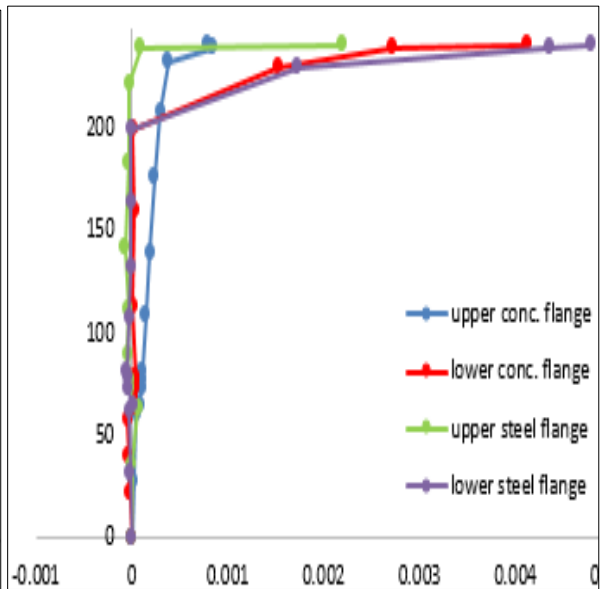
Fig. (4.10.4) load-strains for (B12).
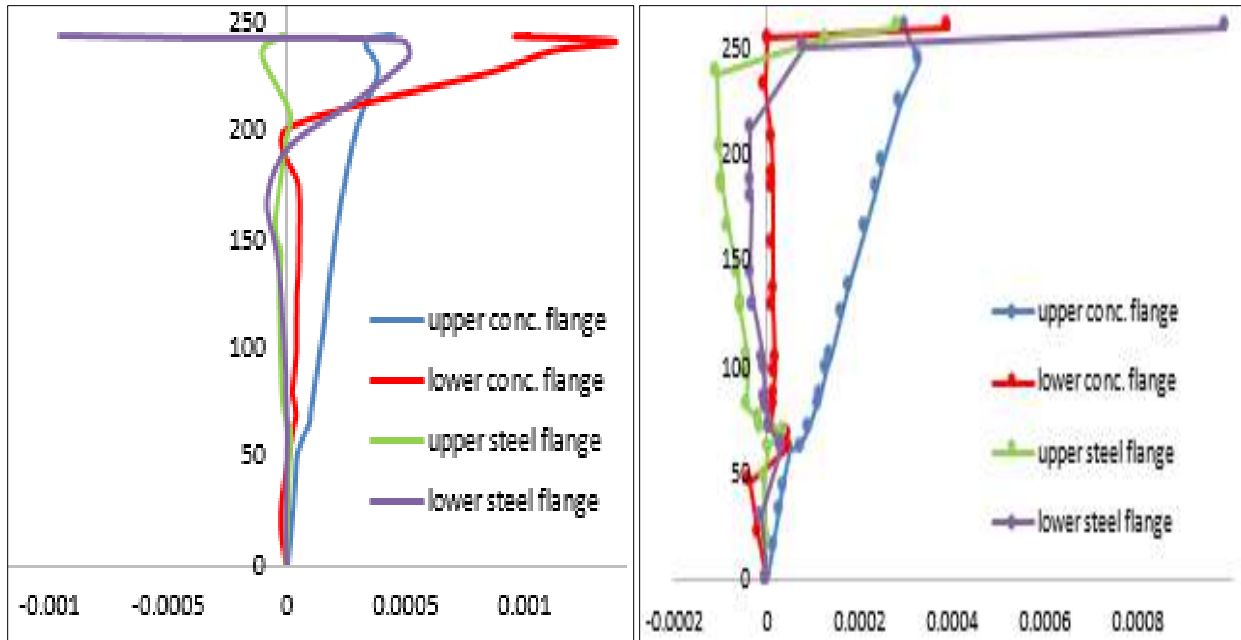
Fig. (4.10.5) load-strains for (B14).   Fig. (4.10.6) load-strains for (B15).

4.12 Flexural strength calculation by plastic theory

To determine the bending strength of the composite section, the following assumptions must be followed in the determination of plastic moment resistance:

1- There is a full degree of connection between structural steel section, steel reinforcement, and concrete.

2- The effective structural steel element area is stressed to its yield strength in tension or compression.

3- Plane – sections of the steel and concrete parts of a composite section each remain plane.

4- The effective area of concrete in compression stressed to $\alpha 1 fc'$ is constant over the whole depth of compression block. $\alpha 1$: is factor related to depth of compression concrete block.

4.12.1 Relationships for UHPC Beam Sections under Bending Stresses

4.12.1.1 Compressive Stress-Strain Relationship of UHPC

Internal compressive force of UHPC above neutral axis can be calculated as the volume of the compressive stress distribution bounded by the stress – strain curve. Moment capacity of UHPC beam using actual compressive stress-strain diagram is difficult to establish and requires large effort and calculation time, therefore an equivalent stress block is proposed in JSCE [4] to simplify such behavior and replace the curved compressive stress distribution by an equivalent rectangular one. Fig (4.11) show a rectangular stress distribution simplifying by dividing the compressive strength (f'c) on design safety factor (γc=1.3). The standard also sets the value of the modulus of elasticity UHPC as (50000 Mpa).
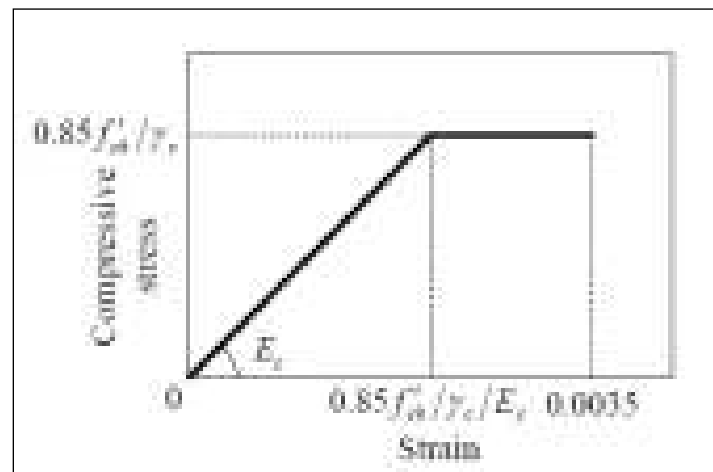
Figure (4.11) Stress-strain relationship -JSCE [3].

4.13.1.2 Tensile Stress-Strain Relationship of UHPC

Internal tensile force of UHPC below neutral axis is considered in estimating the flexural strength of UHPC beams due to post-cracking characteristics of UHPC and its relatively high tensile strength. Presences of steel fibers in concrete improve its post-cracking and increase its fracture energy. The post-cracking behavior of UHPC

is very important because it may dispense with conventional reinforcement in the design of some Ultra High Performance Concrete or UHPC structures. the tensile strength of UHPC in the present work is taken based on the JSCE, (2006) [65] design equation (0.4√ f'c). The steel fiber geometric properties are 13mm length and 0.2mm diameter.

4.12.1.3 Analysis of The Composite UHPC Hollow Beams Sections

The analysis of this type of composite UHPC hollow beams is based on the Eurocode 4 [8] Standard for Composite Sections. The same principle of analysis was followed by firstly finding the neutral axis location using the trial and error and equilibrium equations. As a summary of the following steps:

- Investigate the neutral axis location is above the steel box (in concrete flange) or in the steel box flange or in within the steel box web.

- Compare the compressive force of the concrete above the steel box with all the tensile forces below the steel box to see if the neutral axis at the edge of the box or not.

- If the compressive strength of the concrete above the steel box is greater than all the tensile forces below it, it gives evidence that the neutral axis is located within the concrete flange above the steel box

- To calculate the depth of the neutral axis, should use the principle of equilibrium between the compression forces and tensile forces.

The calculated theoretical flexural strength and flexural loads are reported in Table (4.3) and Appendix A.

Table (4.3) Calculated and Experimental Flexural Capacity for Beams

Beam	Flexural Capacity (MPa)		Flexural Load (kN)	
No.	Calculated	Experimental	Calculated	Experimental
B1	31.39	25.6	134.7	110
B2	30	24.4	128.8	105
B3	50.35	53.6	216.1	230
B4	52.24	55.9	224.22	240
B5	59.35	67.6	254.72	290
B6	43.5	46.6	186.8	200
B7	62.72	67.6	269.1	290
B8	49.44	55.7	212.19	239

4.12.2 Stress-strain distribution in composite hollow beam

After found the depth of neutral axis as in the calculation of Appendix A. for the composite hollow beam (B3) as a control beam for the composite beams, the following stress-strain distribution in the plastic stage of loading was found.
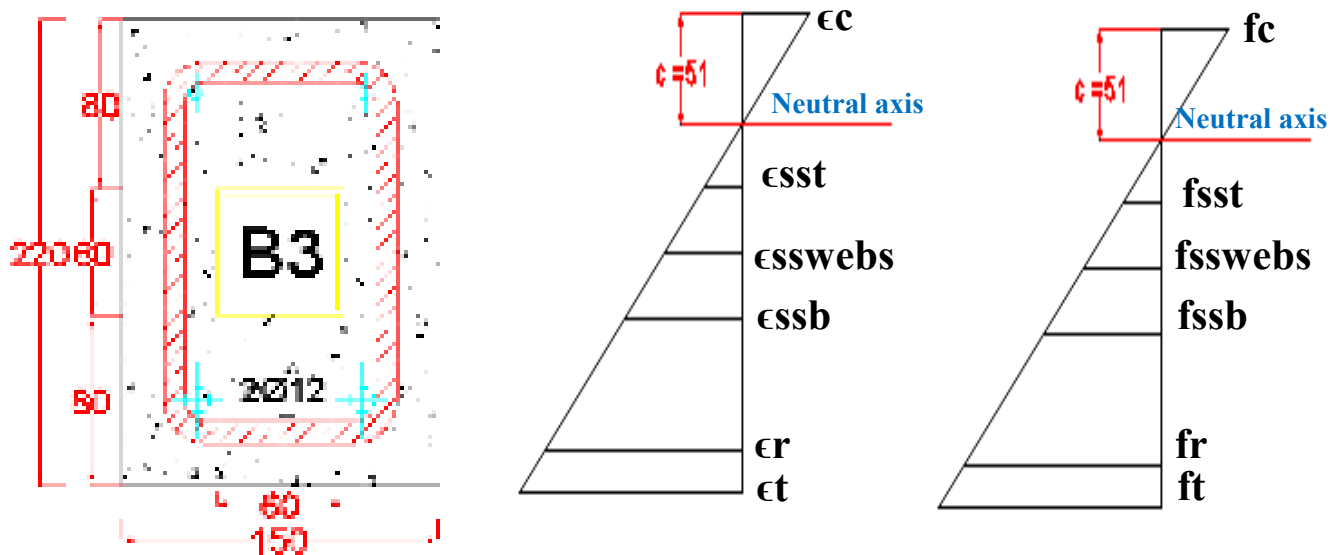
Table (4.4) Stress-strain distribution for control composite hollow beam.
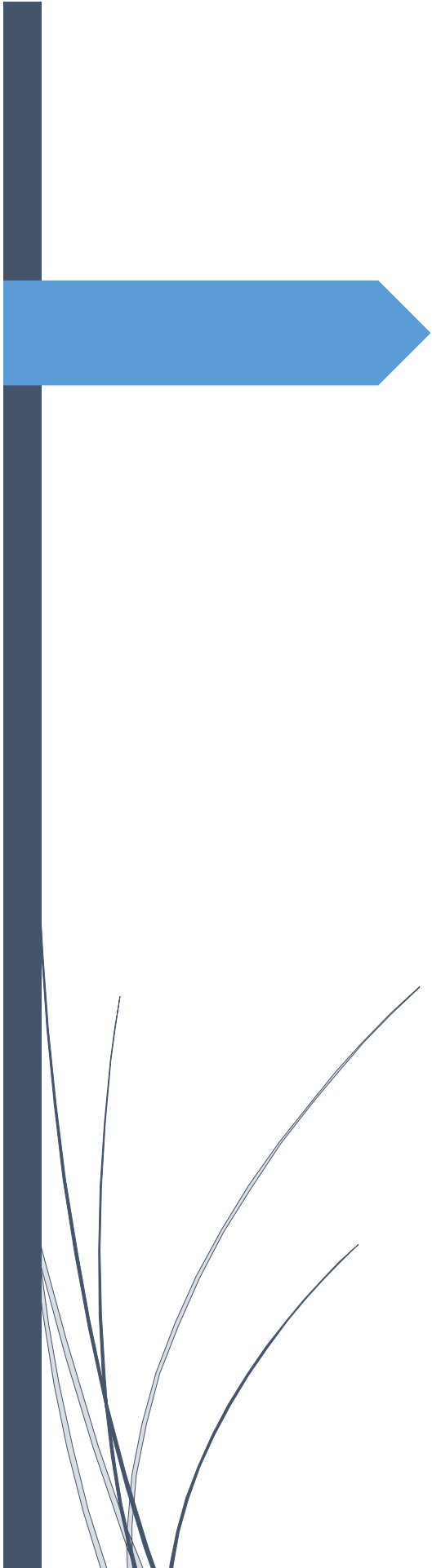
[CHAPTER FIVE]

FINITE ELEMENT MODELING

AND ANALYSIS

CHAPTER 5

FINITE ELEMENT

FINITE ELEMENT FORMULATION AND ANALYSIS

5.1 General

Typically, the reinforced concrete structures are designed and analyzed using empirical equations derived by the global specifications based on the experimental data, but Recently, however, concrete buildings and structural elements have become somewhat complicated, and can not be analyzed or designed directly or are not mentioned in the international construction standards, as a result of the complexity and continuous development in the production of new materials used in the construction and the development of new concrete mixtures that not mentioned yet in the international construction standards. Also, as a result of the development of new structural elements by the researchers that did not derive empirical equations to design and analysis it manually. Therefore, the numerical methods began to use to solve such complex structural elements. Finite element method considered one of the essential methods of these numerical methods. The use of the principle of manual representation of the finite element method, many problems in it, and cause a loss in the time of the user, so many software programs have been developed to model the finite element analysis. As an example of these engineering programs SAP, NASTRAN, ANSYS, etc. Therefore, it is easy to model any engineering structure or solid through these engineering programs through several simple commands, and then analyze it and extract the results of the analysis in the form of data or in the form of computer graphics, which helps to save the effort of the engineer and reduce the wasting time.

In the present research, the principle of finite element analysis carried out by computer program **ANSYS 15**, to model fifteenth Ultra-High-Performance Concrete solid /non-composite hollow beams/composite hollow beams were cast and tested under flexural loads in the laboratory. This chapter focused on the best representation and modeling of the non-composite hollow concrete beam and the composite hollow concrete beam, and analyze and discuss the results after applied two point loads, to study the flexural behavior of these new structural elements. Also, then compare the results of the **ANSYS 15** analysis (numerical results) with the experimental results obtained during the laboratory test. In this study, it was assumed that there is a complete bond, between the steel reinforcement and surrounding concrete. In this research, the concrete mixture used in these structural elements is the Ultra-High-Performance Concrete mix (UHPC) which containing steel fibers in its mixture. Therefore, the focus of this chapter was to find the best representation and modeling of these steel fibers by using the experimental mechanical properties of this mixture, as will be explained later. In the present study, the results of the finite element analysis included the maximum load capacity of the beam, the load chart compared with the resulting deformation and the deformation shape of the specimens.

5.2 Numerical programs

In the last days, many commercial engineering programs in civil engineering were widely spread to analyze the engineering structures by using the finite element principles, and examples of these engineering programs ANSYS, NASTRAN, SAP, etc. All these computer programs were working by generating three-dimensional modeling of the specimens by generating a finite number of elements and a finite number of nodes connecting these elements. In this research, **the ANSYS** program

of version (15.0) was used for several positive reasons, the most important of which are :

- Modeling the concrete material in a good way, which helps us to find the best model for Ultra-High-Performance Concrete (UHPC).

- Modeling of the steel reinforcement efficiently and simulated to the practical reality.

- The ease of introducing the stress-strain curve, whether concrete or steel materials.

- Gives us a simplified sketch of the form of crack and crush in the concrete and how the concrete model will fail.

- The ability to represent the Steel fibers in several models and comparing them.

- The method of the program to display the results and data in a good way and plot it graphically.

5.3 Specimens' geometry and description in finite elements

In general, to simulate the practical reality and get a good approximation of the results among the experimental and numerical results. The models implemented in this study related to experimental beams in terms of geometry and properties of the materials such as concrete, steel reinforcement and steel box obtained from laboratory tests as mentioned in the previous chapter. The dimensions of the ANSYS model in terms of overall depth and length of the span were the same as the dimensions of the experimental specimens. The figures below show the dimensions of the experimental and numerical specimens.

In addition to study the comparison between the experimental and numerical results, this chapter includes two parametric studies to evaluate the using of the

hollow UHPC beams in broad form and then compare the results and analysis it to find maximum specimens capacity and load - deflection curves.

5.4 Finite element models by ANSYS

The use of the finite element principle, which is used by the ANSYS 15 program to represent the Ultra High-Performance UHPC concrete model for composite beams with rectangular sections relative to the tested beams in the laboratory. In order to reduce the wasted time, half the concrete beam was used for the modeling by used two-point loads used the benefit of the symmetry in the geometry, the properties of the materials and the symmetry in the loading method. In the ANSYS program, in order to format the models that simulate the experimental specimens, there are steps should be taken before modeling, to define the materials and the dimensions details, which can be explained as follows:

1. Choosing the element-type for the used material.
2. Defining the real-constants for the elements.
3. Defining the material properties for choosing elements.

5.4.1 Element types

In this research, three elements were used to represent the materials of the model as shown in Table (5.1). These elements are:

5.4.1.1 SOLID 65 element

The finite element, which is used to represent concrete material mixtures of various types, must be capable of representing the cracking and the crushing of concrete and representation of the bond between concrete and reinforcing steel and the bonding between the concrete and the steel fiber to prevent the growth of cracks. In the present study modeling of the concrete was done by used three-dimensional

brick element, and it is a designation in ANSYS15 (solid 65), The geometry shape of this element consists of eight corner nodes and each corner accepts displacements in three directions (u, v and win x, y, and z-direction respectively). As well as solid 65 element contains the option for plastic-deformation (the cracking) in three-orthogonal-directions. Also, It also has the option of crushing. Also, it has three embedded bars with any entity angle. The configuration of the solid 65 elements shown in Fig. (5.1).
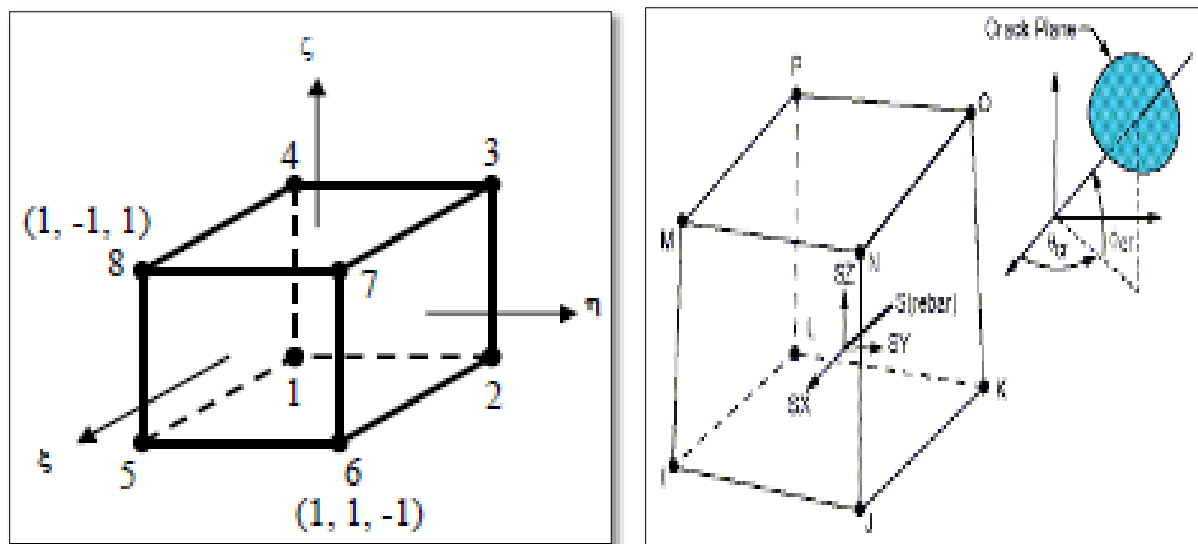
a) Element's Geometry in local coordinate   b) Stress Output
Fig. (5.1) The configuration of SOLID 65 Element.

5.4.1.2 SOLID 185 element

To overcome the concentration of stresses during the modeling when applying the load on the concrete, steel plates are used at the support and the loading area. In this research, these steel plates modeled using (solid185) elements. Also, this type of element was used to model an embedded steel empty box in the UHPC section. This element has eight nodes; each of these nodes has three degrees of freedom in three directions (x, y, and z) and the geometry of this element shown in Fig. (5.2).
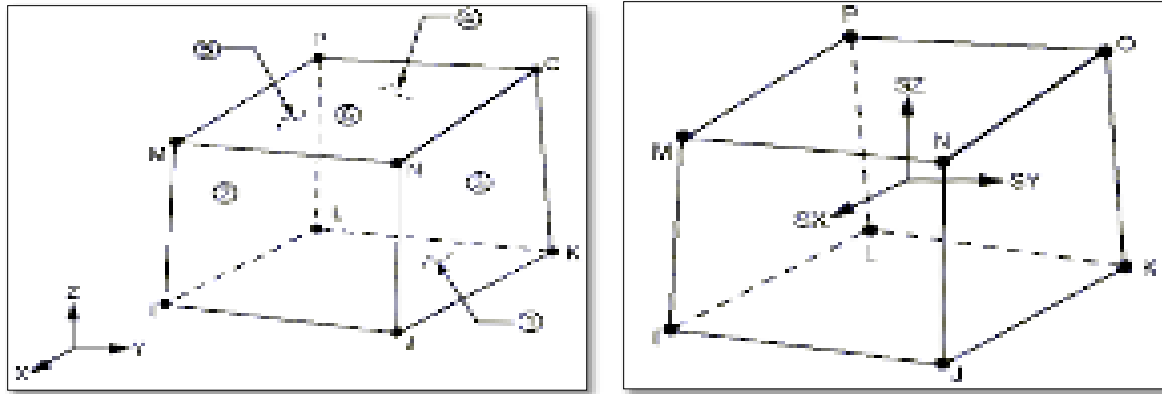
a) Element's Geometry   b) Stress Output

Fig. (5.2) Configuration of SOLID185.

5.4.1.3 LINK 180 element

All steel reinforcement used in this research, whether longitudinal steel (flexural rebars) or horizontal steel (stirrups) were modeled by using 2-node discrete (link180 element). The reinforcement modeling in the ANSYS program assumes that it is capable of transmitting only the axial force. The full bond between reinforcing steel and concrete is assumed. This element has two nodes. Each node has a three-degrees of freedom in orthogonal directions as shown in Fig. (5.3).
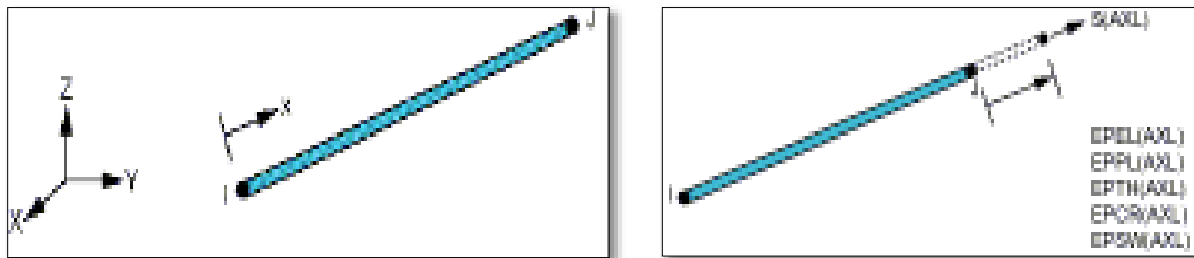
a) Element's Geometry   b) Link180 Stress Output

Fig. (5.3) LINK180 (Steel Rebar).

Table (5.1) Types of Element in the Present Study.

Material Type	ANSYS Element
Concrete	SOLID 65
Steel plates and Supports	SOLID 185
Steel hollow section	SOLID 185
Steel reinforcement	LINK 180

5.4.2 Real constants

To model the structural model should introduce an important entity is the real constants. It is worth mentioning that an individual element can insert real constants. ANSYS neglects any introduction of the real constants using this element. All the real constants used in the modeling in this research are shown in Table (5.2).

Table (5.2) Real constants for ANSYS Models.

Real constant set	Element type	Constants			
1	LINK180	Cross-sectional area (mm^2)- Ø 6 mm	28.27		
2	LINK180	Cross-sectional area (mm^2) - Ø 10 mm	78.54		
3	LINK180	Cross-sectional area (mm^2) - Ø 12 mm	113.1		
4	LINK180	Cross-sectional area (mm^2) - Ø 16 mm	201		
		Properties	Real Constants		
			rebar1	rebar2	rebar3
6	SOLID65	Material number	Under study	Under study	Under study
		Volume ratio	Under study	Under study	Under study
		Orientation angle THETA(horizontal angle)	Under study	Under study	Under study
		Orientation angle PHI (Vertical angle)	Under study	Under study	Under study

So far there is no problem in the definition and introduction of the real constants of any material using the ANSYS except the steel fibers where the distribution of steel fibers inside the concrete mix has a direct effect on the results. Therefore, the researchers used two methods to introduce the effect of the steel fiber distribution within the concrete mix. A few of the researchers are introducing the effect of the steel fiber distribution by using the stress and strain curve of the concrete because the steel fiber distribution will result in a change in the stress and strain characteristics of the concrete. However, other researchers, have been introduced the effect of the steel fibers distribution in the concrete mix by using models showing

the orientation angles of steel fiber in the concrete mixture. In the previous table, paragraph number 7 shows the real constants of the used concrete element solid65 and includes several functions that need clarification which are :

- The element is supposed to be smeared to represent the main tensile reinforcement, and these fields are usually filled with zero values, and the same fields will be filled with default values for the steel fibers in the concrete mixture.

- The volume ratio indicates the ratio between the existing reinforcement to the size of the element.

- The angle of orientation, whether horizontal or vertical, indicates the angle of orientation of the reinforcement.

- The number of reinforced smeared rebars is three.

The rest of the sets of the table above show the real constants used to define the steel rebar in the concrete beam where the values of these constants represent the area of the cross-section of the rebar used.

5.4.3 Material properties

To complete the representation of the materials used in this research, ANSYS needs to introduce another important entity is the introduction of the parameters that belong to the materials to be modeled. The properties of the material needed by ANSYS element for each material are:

 1. **Material Properties for element Solid 65**

The element used to model the concrete material is solid 65 element needs to introduce some of the properties of the concrete that used to represent the failure of the concrete. **Solid 65** element required **Linear Isotropic – Multilinear Isotropic - Concrete** properties:

1- **Linear Isotropic properties:**

- **EX:** the modulus of elasticity of concrete (Ec) which we obtain from the practical test or through the equations of a global standard or empirical equations by researchers.

- **PROXY:** is the Poisson's ratio (v), which is assumed with a value of 0.2 for ultra high-performance concrete

2- **Isotropic Multilinear properties:**

- **stress-strain curve:** ANSYS program also requires the introduction of the stress-strain curve of the concrete used, in the current research, the stress-strain curve of ultra high-performance **UHPC** concrete can be obtained either through laboratory testing or through empirical equations by former researchers or through international specifications such as the Japanese specification JSCE for ultra-high-performance concrete.
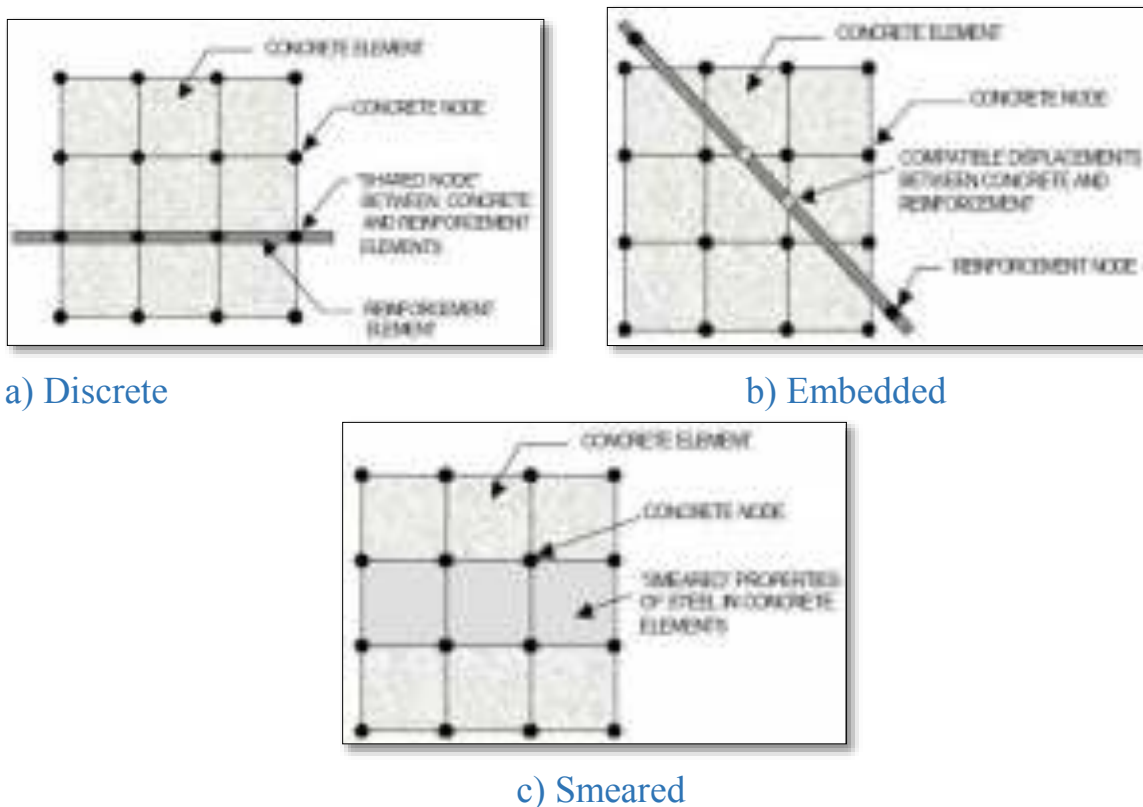
a) Discrete   b) Embedded

c) Smeared

Fig. (5.4) Models for Reinforcement in Reinforced Concrete.

3- Concrete properties

- **Constants of concrete:** ANSYS program has a group of a constant that should be known. These constants are shown in Fig. (5.5) Below.
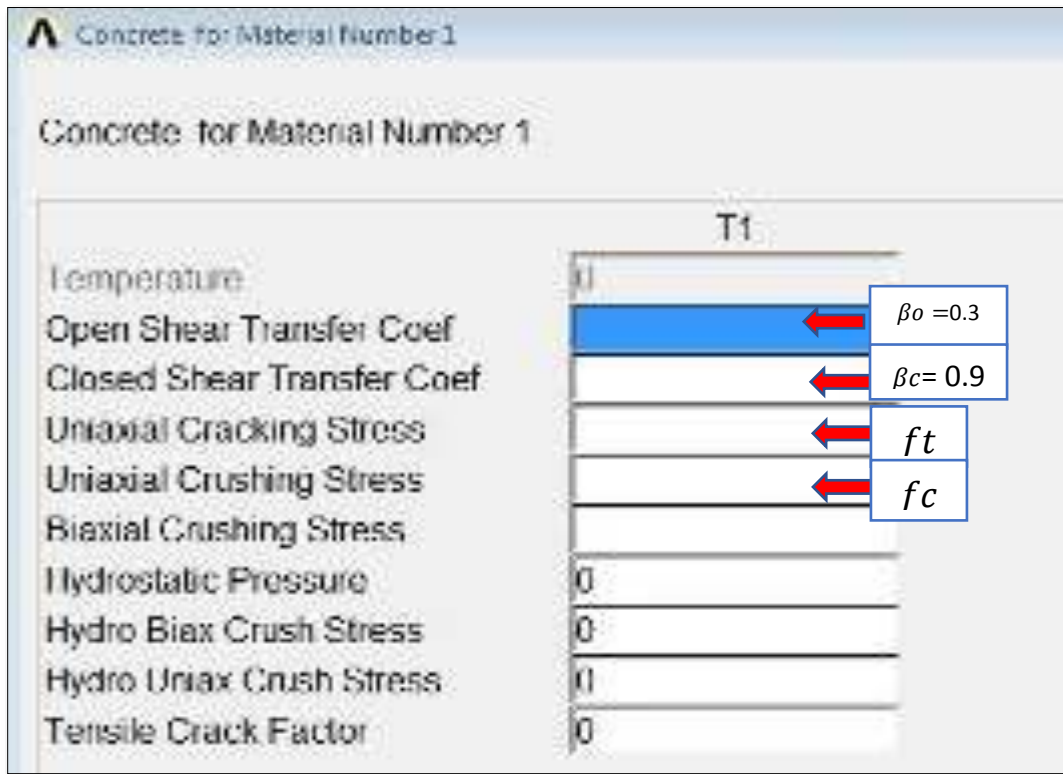
Fig. (5.5) The concrete constants for ANSYS 15.

The values of a typical shear-transfer coefficients (0 to 1), where the value of (0) means that the crack is soft and at the beginning of its phase (a complete loss in the shear transfer) and that the value of (1) means that the crack has become rough (there is no loss of shear transfer). Depending on the experience and on the previous researchers, the value of the open crack shear transfer is (0.65), while the value of the closed crack shear transfer is (0.9). ANSYS program requires the entity of tensile strength for concrete. In the current research, the tensile strength for Ultra-High-Performance Concrete (UHPC) either taken from an experimental tensile test (11.43 MPa) or depending on the international specifications, including the Japanese specification, which states that the tensile strength for Ultra-High-Performance

Concrete equals to $(0.4.\sqrt{fc'})$. The blank data leads to remove the capability of cracking and crushing.

2.**Material Properties for element LINK185**

LINK185 element represents the model of steel reinforcement material. It required **Linear Isotropic – Bilinear Isotropic** properties :

1-Linear Isotropic properties

- **EX:** the modulus of the elasticity of the steel 200Gpa.

- **PROXY:** the Poisson's ratio of concrete (0.3)

2- Bilinear Isotropic properties

- **Yield Stress:** the yield stress (fy) which is taken in the present work 500MPa.

- **Tang Mod:** the hardening stress which is taken as 2000 MPa. To avoid the convergence problem during iteration. As shown in Fig. (5.6).
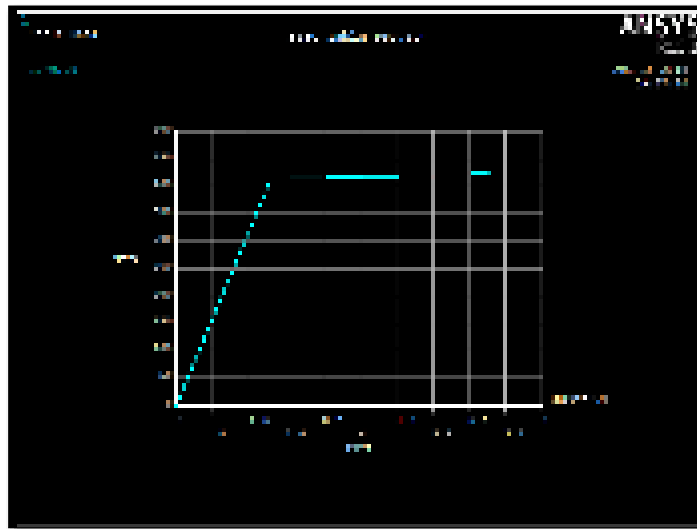

Fig. (5.6) Bilinear model for steel reinforcement.

5.5 Building and meshing the model

To build and mesh the model three essential steps should be taken, as follows:

1- **Mesh or divide the model into small sizes of elements :**

This step is a significant step in the modeling process because the principle of the finite element depending on this step because after complete the model

and apply the loads these small elements will be deforming and the stresses and strains appear on the integrations points (nodes) between elements. For good results, the model must be divided into square or rectangular elements.

2- **Generate the nodes :**

In this step, several nodes will be generated in the "Cartesian working plane" by generating nodes in (x y) plane to model the section of the beam (width and overall depth of beam) and then copy these nodes to the other plane to model the long span of the beam.

3- **Generate the elements :**

After modeling the specimens by nodes, now the elements should be generated between these nodes, by selecting the element type for each material and generate the element. Then the copy system will be applied to this element to generate the whole cross-section by elements in (x y) plane And then the coping all these elements to the other plane to complete modeling the full beam by small elements.

In the figure (6.6), half of the entire model was modeled, containing one steel plate in the support and one steel plate in the load location, the dimensions of these steel plate (150,30,25) mm. The steel plate located below the beam was restrained by using roller support and constrained in the y-direction in order to prevent cracks from appearing in that direction. In the axis of symmetry, the nodes were constrained in both x and z directions respectively.

Since our focus in the present research is the study of the flexural behavior, so the two points were loaded in the middle span so that the span is divided into two shear spans, and one pure moment span in the middle of the beam. The shear reinforcement is modeled along the beam except for the pure moment span that lies between the axis of symmetry and the left part of the loading point. Fig. (5.7) Shows

the model that was modeled in ANSYS15 and the element types used for each material of the model. Table (5.3) shows the numbering of element types.

Table (5.3) The numbering of element types.

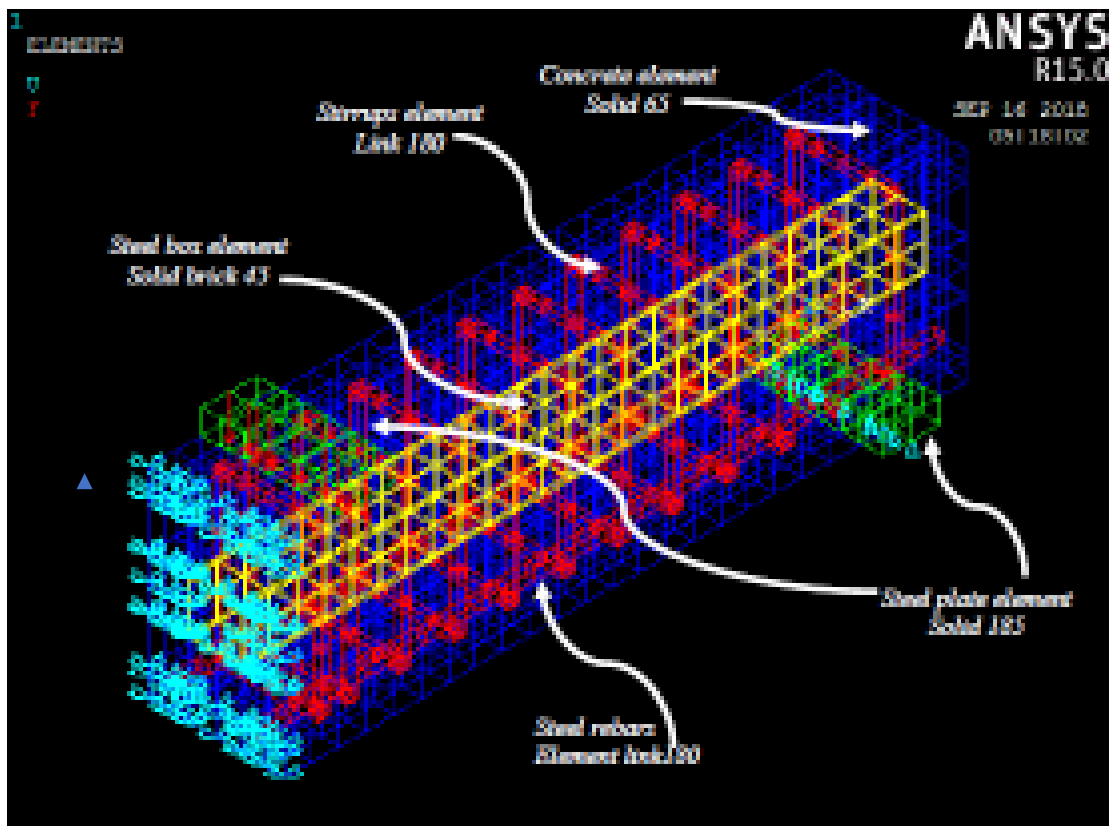| Model Parts	Element Type	Material Number	Real Constant Set
Steel Ø6*mmmm*Rebar	LINK180	2	2
Steel Ø10*mmmm*Rebar	LINK180	3	3
Steel Ø12*mmmm*Rebar	LINK180	4	4
Steel Ø16*mmmm*Rebar	LINK180	5	5
Beam - Concrete	Concrete 65	1	1
Steel Plate-Load	SOLID185	7	N/A
Steel Plate-Support	SOLID185	7	N/A
Steel Plate-Box	SOLID185	6	N/A

Fig. (5.7) Typical details of FE mesh used for the analysis of concrete beam.

5.6 Loading and boundary conditions

To get a complete and precise solution, the model must be restricted and made in a manner that simulates the actual reality of the laboratory test device. In this

research, the boundary conditions were applied, and the model was restricted by ANSYS 15, by applying zero-value displacements to prevent the model from rotating or moving. To apply boundary conditions to the model, the axis of symmetry and the supports must be restricted to the following directions:

- constrain all nodes in the vertical plane of the axis of symmetry in the direction of x and z, and allow the vertical displacement.

- Constrain the roller support in the y-direction at nodes lie in mid-line of steel plate and allow all the rotational movement.

After representing the definition of all materials, modeling the model and completing the application of the boundary conditions, Now the flexural load is applied by placing the forces on the steel plate but the loading process should simulate the experimental test so the forces in ANSYS15 model should be applied as nodal forces on the steel plate, as shown in Fig. (5.8).
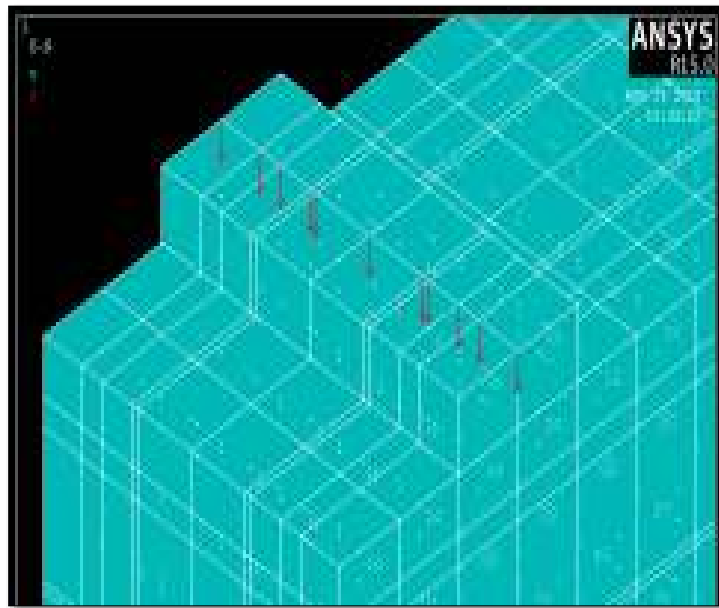

Fig. (5.8) Applied lumped forces.

5.7 Analysis types

In this study, all models were analyzed by the static analysis, as the analysis was taken as small displacements with linear static performance and the displacements

resulting from large deformations were ignored. The loads were placed in the form of time steps, where the total steps represent the sum of the forces captured, and the time at the last loading step refers to the end of the loading, and the time step refers to the time increment with maximum and minimum size.

5.8 ANSYS flexural failure loads

After completing apply loads and the end of the solution process of the program, we now should extract the results and see the output failure modes, where failure loads were calculated depending on the characteristics of the materials extracted from laboratory tests. The experimental and numerical results of all the studied models in terms of the ultimate flexural load are shown in Table (5.4).

Table (5.4) Analytical and experimental comparison at the ultimate stage.

Sample	Ultimate load Pu (Kn)		
	Analytical	**Experimental**	**%Pex./Pansy.**
B1	114	110	103.6%
B2	115.6	105	110%
B3	233.7	230	101.6%
B4	260.7	240	108%
B5	272.8	290	106%
B6	218.4	200	109.2%
B7	316.5	290	109.1%
B8	232.3	232	100.%
B9	153.6	200	130%
B12	251	240	104.5%
B13	200	240	120%
B14	244.94	245	100%
B15	272.1	260	95.5%

5.9 Load-Deflection relationship

In the stage of showing the results of the solution, a comparison and a diagram are drawn between the load and the resulting vertical displacements (deflections). Also, to verify the numerical results with the experimental results so the load-deflection curve should be measured at the same position of the experimentally tested beam. In the ANSYS program, the deflections are measured at the middle lower point of the model's span below the edge of the symmetry axis in the y-direction. Then the deflection results are read and converted to an Excel sheet to plot the curve of load versus deflection and make the comparison with the experimental deflection readings. Figure (5.9) below shows the form of failure and deformities occurring in the mode after completion of the solution.

5.10 Parametric study (1): replacing pattern of steel reinforcement in tabular steel-UHPC composite hollow beams

In this part, the possibility of replacement of the usual longitudinal reinforcing steel with a hollow steel section was studied and encased in the same place of reinforcing steel rebars to take advantage of its steel properties as a structural benefit and from the existing hollow core as an economic benefit by reducing the amount of UHPC and dead-weight of the structural element. The beam models have the same dimensions of the experimentally tested beams which have a length (400mm), height (220mm) and width (150mm). Also the same type of concrete used in experimental work and its properties. These steel sections are further lowered below the section and leaving 30 mm as concrete cover. The parametric study presented below consists of analyzing ninth beams that have been modeled using ANSYS (Version-15) software. The considered parameters in this numerical study include, GR.1 encasing square (60*60)mm² Steel box with and without steel reinforcement, GR.2 encasing

vertical rectangular (50*100)mm² Steel box with and without reinforcement and the final group GR.3 encasing horizontal rectangular (50*100)mm² steel box in different number with and without steel reinforcement. Beam specimen (B8) contains two horizontal encased steel box. Beam specimen (B9) contains one horizontal steel box and one hollow core using cork in the middle of the section.

5.10.1 Flexural capacity of numerical case study (1)

The numerical results of the ultimate load capacity are reported and given in Table (5.6). It is noticed clearly that composite hollow beams capacities were higher than non-composite solid beam (B1). In GR.1 when encasing square steel box (60*60)mm², composite hollow rein. Beam (B2) with reinforcement shows capacities higher by 120% than solid beam (B1), and the composite hollow non-rein. Beam (B3) without reinforcement was higher by 52.8% than a solid beam (B1). In GR.2 when rectangular steel box used the capacities of composite hollow rein. Beam (B4) was higher by 114% than solid beam (B1), and composite hollow non-rein. Beam (B5) was higher by 63.3% than (B1). In GR.3 when a horizontal rectangular box was used. It is noticed that composite hollow rein. Beam (B6) shows capacities higher by 138.5% than (B1), and composite hollow rein. Beam (B7) was higher by 81.5% than (B1). The composite hollow non-rein. Beam (B8) shows the higher capacities than all of the tested beams, and higher by 154.3% than solid beam (B1). Also, this is because of the encasing of the two-steel box inside the concrete.
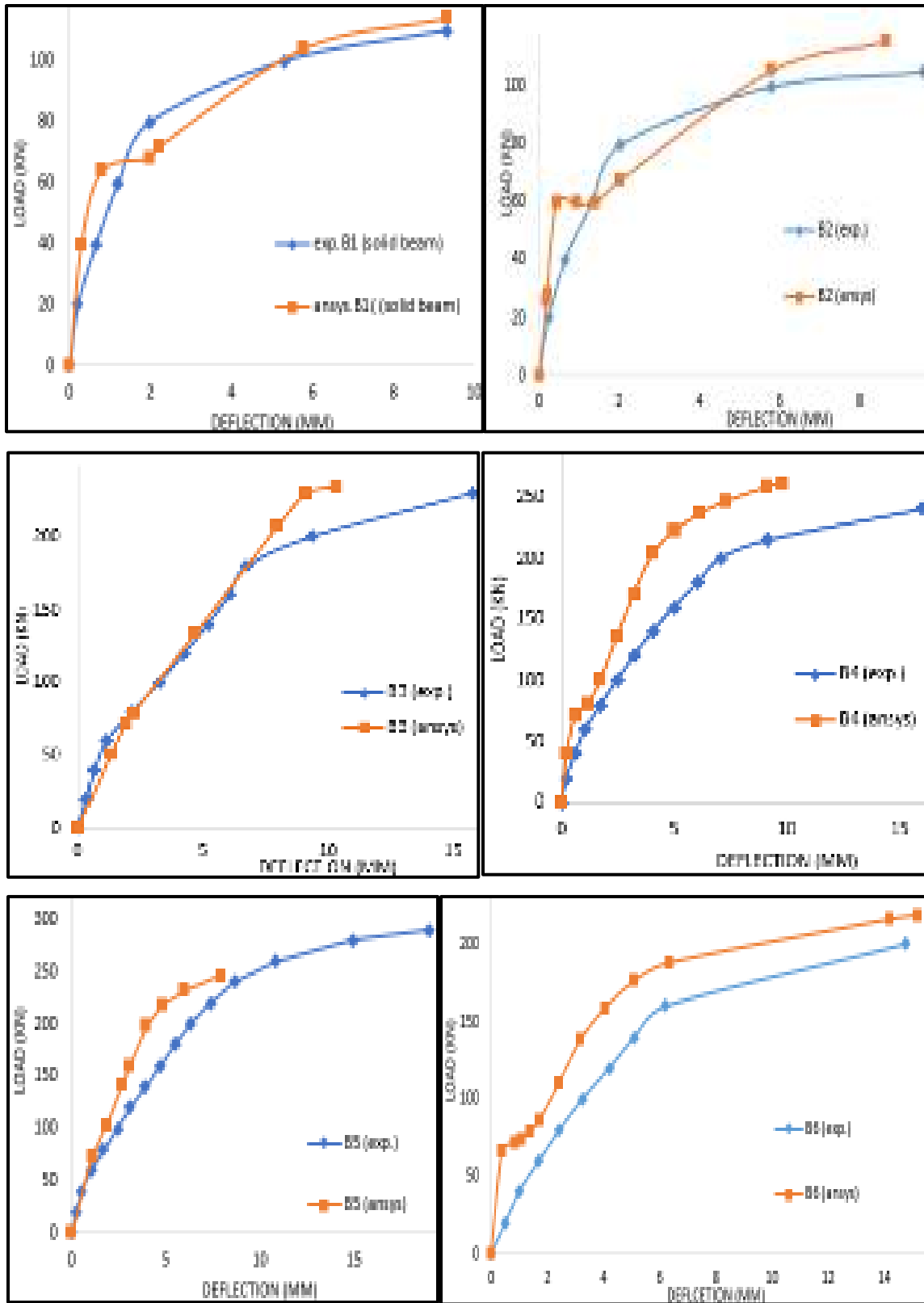
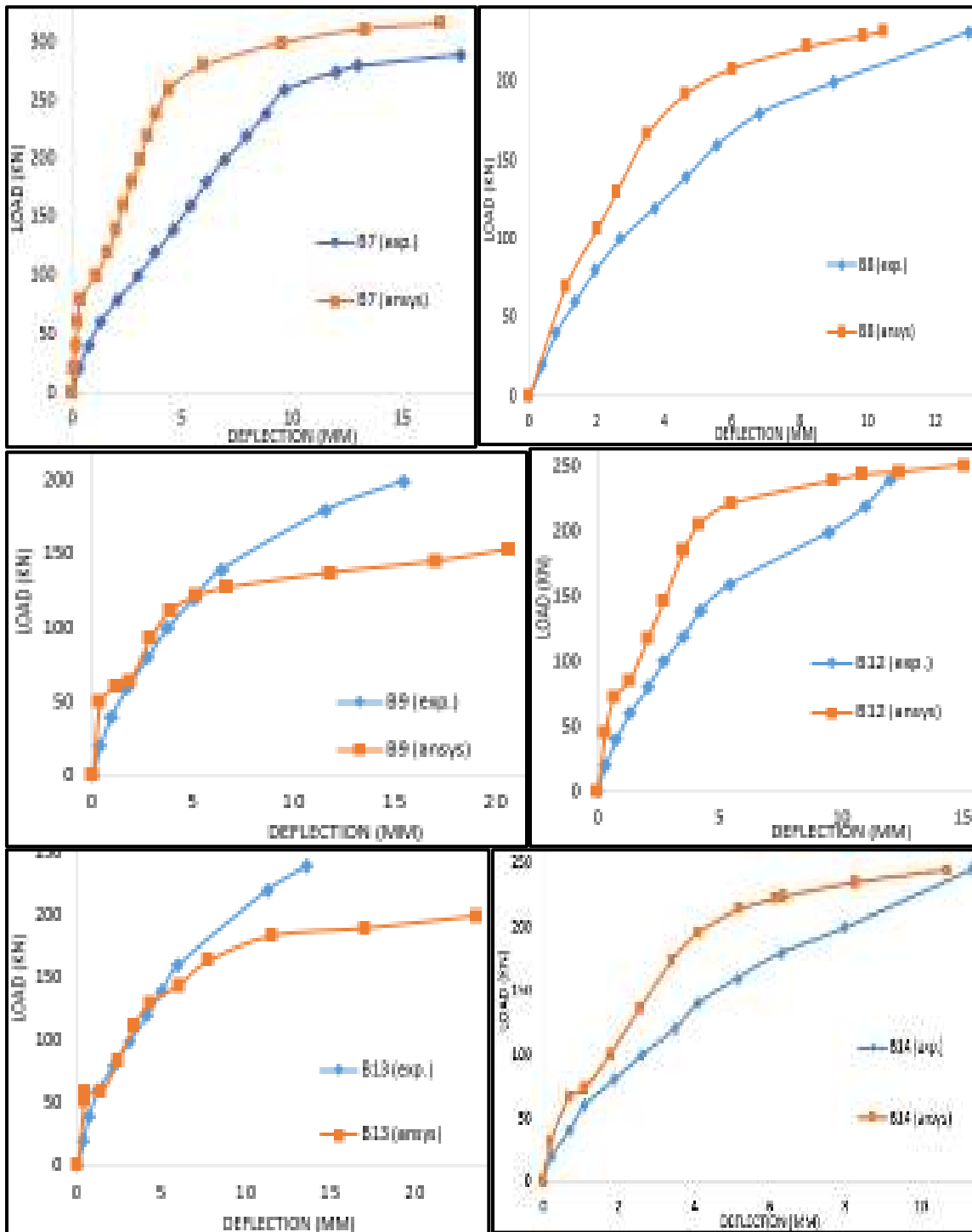Fig. (5.9) Experimental and Analytical Load-Deflection Curves.
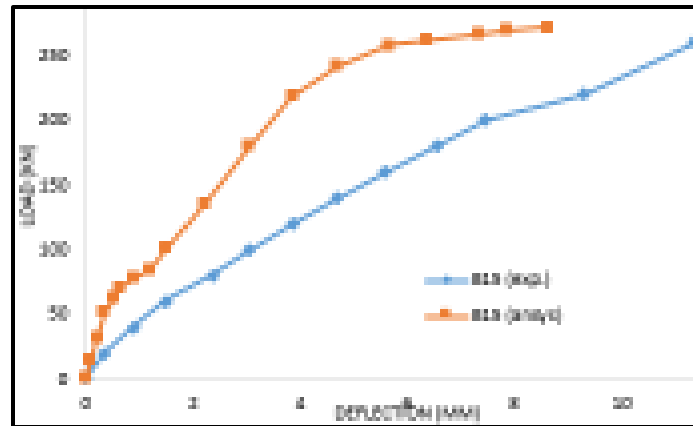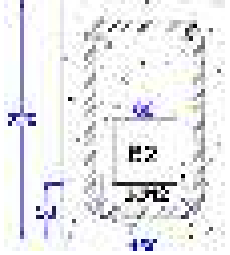
Fig. (5.9) Continued.
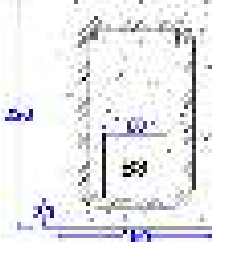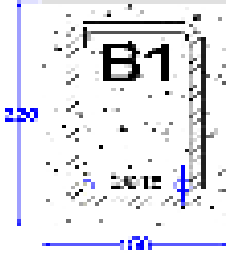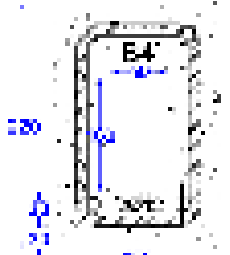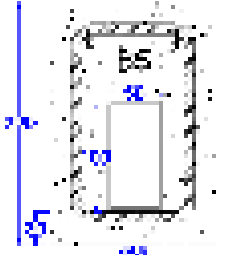
Fig. (5.9) Continued.
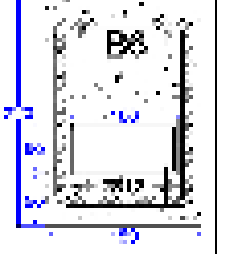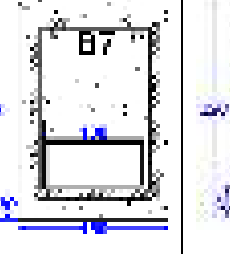
Table (5.5) Geometry details of the numerical case study (1)

Type of beam	Solid beam (control)	Composite hollow beam with the rein.	Composite hollow beam without rein.		
GR.1 Using Square (60*60)mm² Steel box					
GR.2 Using Vertical rectangular (50*100)mm² Steel box					

Type of beam	Solid beam (control)	Composite hollow beam with the rein.	Composite hollow beam without rein.	Composite hollow beam with 2-steel box	Composite hollow beam with steel and cork box
GR.3 Using Horizontal rectangular (50*100)mm² Steel box					

Table (5.6) Ultimate load and Moment capacity of a case study (1)

Type of beam	Solid beam (control)	Composite hollow beam with the rein.	Composite hollow beam without rein.
GR.1 Using Square (60*60)mm² Steel box			
Load capacity	114 kN	251 kN	174.3 kN
Moment capacity	25.6 Kn.m	24.4 Kn.m	53.6 Kn.m
GR.2 Using Vertical rectangular (50*100)mm² Steel box			
Load capacity	114 kN	244.9 kN	186.2 kN
Moment capacity	25.6 Kn.m	55.9 kN.m	67.6 kN.m

Type of beam	Solid beam (control)	Composite hollow beam with therein.	Composite hollow beam without rein.	Composite hollow beam with 2-steel box	Composite hollow beam with steel and cork box
GR.3 Using Horizontal rectangular (50*100)mm² Steel box					
Load capacity	114 kN	272 kN	207 kN	290 kN	214.4 kN
Moment capacity	53.6 Kn.m	55.9 kN.m	55.7 kN.m	57.1kN.m	46.6 kN.m

5.10.2 Load – Deflection curves for numerical case study (1)

The deflection measurements may give logical reasons for the model carrying capacity. The load-deflection curves of all numerical models were divided into three groups as shown in Fig. (5.10) Below. It is noted that the non-composite solid model (control beam) in all comparisons gave a behavior far from other models in terms of maximum load and deflections were high compared with deflections of composite hollow models at specific loads. In GR.1, it observed clearly that (B2) model, which contains reinforced with longitudinal rebars, gave maximum load and fewer deflections compared to the rest models. However, the model (B3) which has non-reinforced and removed longitudinal rebars from it and replaced it entirely by lowering steel box location by 20 mm more than (B3), it gave less load and more deflection than (B2) but remained better than the non-composite solid reinforced model (B1). In GR.2, the composite reinforced model (B4) shows maximum capacity and fewer deflections compared to the non-reinforced composite model (B5), but the non-reinforced composite model still better in all respects than the standard reinforced solid model (B1). In GR.3, several details noticed, such that the non-reinforced model but contains two encased steel boxes (B8) gave higher capacity than others. The capacity of the reinforced composite model contains one steel box (B6) higher than the non-reinforced composite model (B7). However, the non-reinforced model, which was has a steel box below, and hollow core in the middle of the section (B9) shows us good properties compared to the solid reference model (B1). The structural property is by increasing capacity and economic property by decrease the amount of used UHPC expensive mix. This (B9) model shows a massive increase in the maximum-deflection compared to the rest of the models due to the presence of the large hollow core which fabricated by the cork in the center of the section, which led to a reduction in the Moment of inertia of the section.
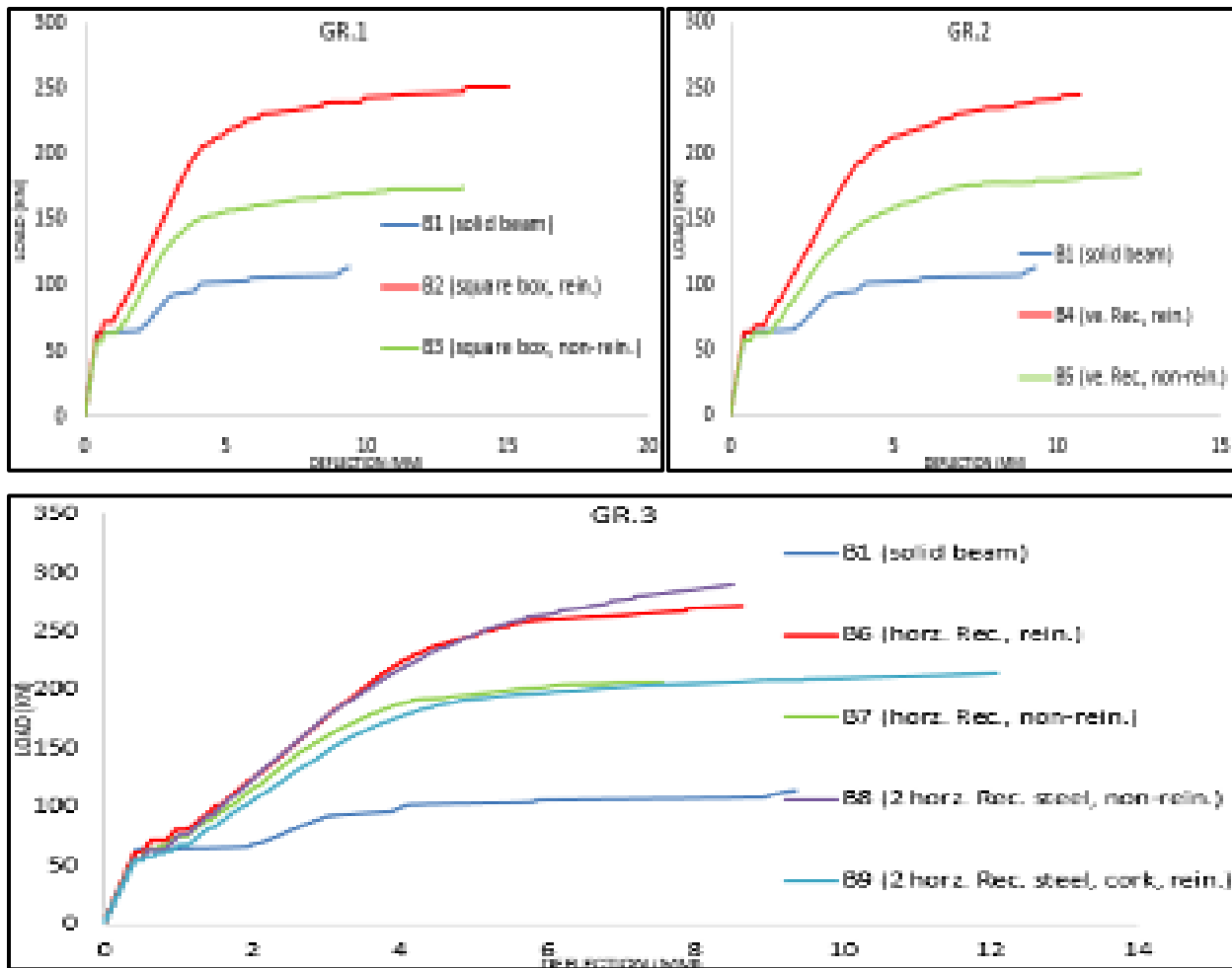
Fig. (5.10) Load-deflection relationships of the numerical case study (1).

5.11 Parametric study (2): numerical study for effects of longitudinal opening on the flexural strength of UHPC beams

This part includes a numerical study of the flexural capacity of UHPC beams with different longitudinal openings, as these openings have the economic benefit of reducing the used concrete materials and structural benefit by reducing the dead-weight of the structural element. The models in this study have the same dimensions and characteristics of the materials used in the previously mentioned experimental part, but without using a hollow steel section as shown in Table 5.7. The adopted variables in this study are the size, shape, and location of hollow core and effect of

changing longitudinal reinforcement of these non-composite hollow UHPC beams. Details of the variables represented in this study are shown in Table 5.4. The study included the modeling of twelve models of ultra-high performance concrete beam using (Ansys 15). The models were divided into six groups. GR.1 contains a comparison between the solid beam and a hollow beam using a square opening (60*60)mm². GR.2 study effect of hollow core size using three sizes of longitudinal; opening (60*60)&(80*80) And (100*100)mm². GR.3 study effect of changing the longitudinal reinforcement ratio of these beams (2Ø10, 2Ø12 & 2Ø16). GR.4 study the effect of hollow core shape in the middle zone of the section using square (60*60)& Rectangular(50*100) &circular(Ø60) core. GR.5 study the effect of core location comparison between the middle & below zones of the section. GR.6 study the effect of changing the hollow core shape within the tensile zone of the section.

5.11.1 Ultimate load and flexural strength results of case study (2)

As mentioned previously, the main purpose of the current research paper is to know the flexural strength of the Ultra-High-Performance Concrete UHPC beams with or without longitudinal openings in their sections. The flexural strength and the variation in the load capacity are reported and presented in Table (5.6) and Fig. (5.11).

For **GR.1** the ultimate load for the experimental solid beam (ex.B1) was (110kN), and the mode of failure was a flexural failure as shown in Fig.8, the load level was reduced by (4.76%) in the experimental hollow beam (exp.B2) compared with the solid beam (B1).

For **GR.2** the ultimate load of beam specimen B3(80*80) was (114.89kN) which is lesser than B2(60*60) by (0.09%) and ultimate load in B4(100*100) decreased by (0.69%) than B2(60*60), This small decrease in capacity when

increasing the hollow core area from (60*60 to 100*100)mm, can be explained by that the increasing hollow core size does not affect much as long as hollow core is far from compressive zone of the concrete. In structural engineering, when the compression strength (f'c) of the concrete mix is increased, the depth of the compression zone will be reduced in order to balance the compressive force of the concrete with the tensile force provided by the reinforcing steel used. Therefore, due to the high compressive strength of UHPC, so the depth of the compression zone is usually minimal, so increasing the size of the hollow core in the center of the section will not significantly effect on the section capacity.

For **GR.3** it is clear that the increase in the longitudinal reinforcement (from 2Ø10 in B5 to 2Ø12 in B2) increased the capacity by (17.8%), while increased reinforcement from (2Ø12 to 2Ø16) led to (74%) increase in load capacity.

For **GR.4** It is well noted that the hollow beam, which has a circular hole in the middle of the section in B8(mid.circ.60), has greater bearing capacity than the rest of the hollow beam with rectangular and square holes. This is due to the fact that the decrease in section's moment of inertia by (0.48%) when fabricating a circular opening was less than the hollow beam B2(mid.squ60*60) with a square hole, which reduced the section's inertia by (0.81%) and less than the hollow beam B7(mid.rec50*100) with a rectangular hole that reduced the section's inertia by (3.23%).

For **GR.5** Hollow beams noticed to have a longitudinal hole below the section gave higher capacity than the hollow beams that have a hole in the center of the section and this is sufficient evidence that the fabricating of the longitudinal hole far as from the compression zone of section will not reduce the capacity of the section regardless of the shape of the longitudinal hole.

For **GR.6** The hollow beam B10(bel. Circ.6) noticed to contains a circular longitudinal hole below the section gave higher capacity than the rest of the hollow beams, and this gives an impressive enough that the circular opening is better than other shapes of opening because it does not contain sharp edges where the applied stresses are concentrated at it. Also, the circular opening does not reduce the moment of inertia of the beam section much as with square and rectangular openings.

Table (5.7) Ultimate Load for the experimental and numerical tested beams.
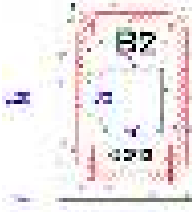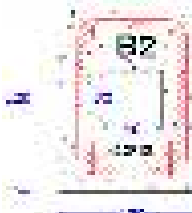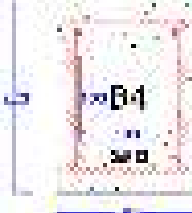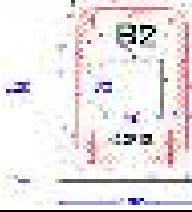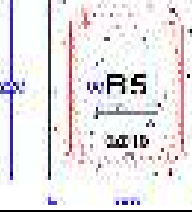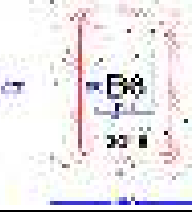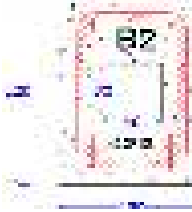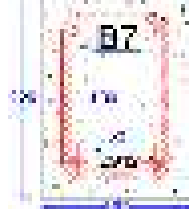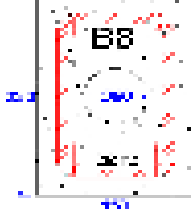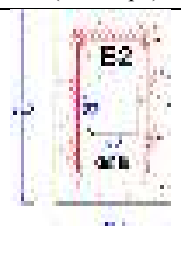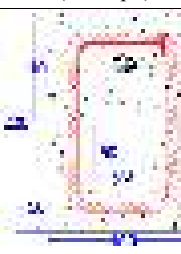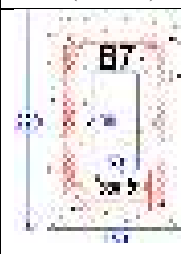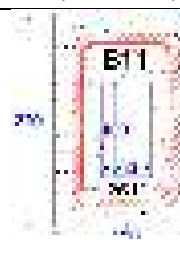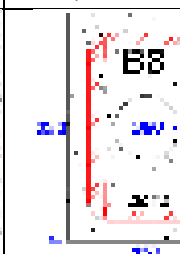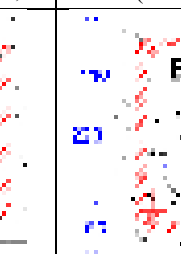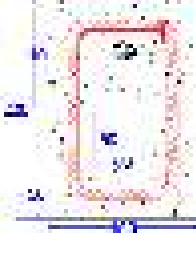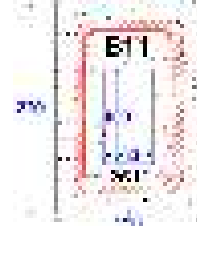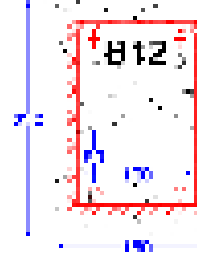
Beam Encoding	Solid beam (ex.B1 & B1)		Hollow beam (ex.B2& ans.B2)
GR.1 between the solid beam and hollow beam using Square opening (60*60)mm²			
Load capacity	ansy.=114kn		ansy.=115kn
Beam Encoding	B2 (60*60)mm²	B3 (80*80)mm²	B4 (100*100)mm²
GR.2 study effect of hollow core size Using (60*60)&(80*80) And (100*100)mm²			
Load capacity	115kn	114.89 kn	114.21 kn
Beam Encoding	B2 (2Ø12)	B5 (2Ø10)	B6 (2Ø16)
GR.3 study effect of changing longitudinal ratio (2Ø10, 2Ø12 & 2Ø16)			
Load capacity	115kn	97.6 kn	201 kn
Beam Encoding	B2 (mid. Squ.60*60)	B7 (mid.rec.50*100)	B8 (mid.circ. Ø60)
GR.4 study hollow core shape in the middle zone using a square (60*60)& Rectangular(50*100) &circular(Ø60) core.			
Load capacity	115kn	112.2 kn	128 kn

Table (5.6) Continued.

Beam Encoding	B2 (mid. Squ.)	B9(bel.Squ.)	B7 (mid.rec)	B11(bel.ver.rec.)	B8 (mid.circ. Ø60)	B10(bel.circ.60)
GR.5 study core location comparison between middle& below section						
Load capacity	115kn	119.25	112.2 kn	119.49	128 kn	119.69

Beam Encoding	B9(bel.squ.60)	B10(bel.circ.60)	B11(bel.ver.rec.)	B12(bel.horz.rec.)
GR.6 Changing core shape within the tensile zone				
Load capacity	119.25	119.69	119.49	117.66
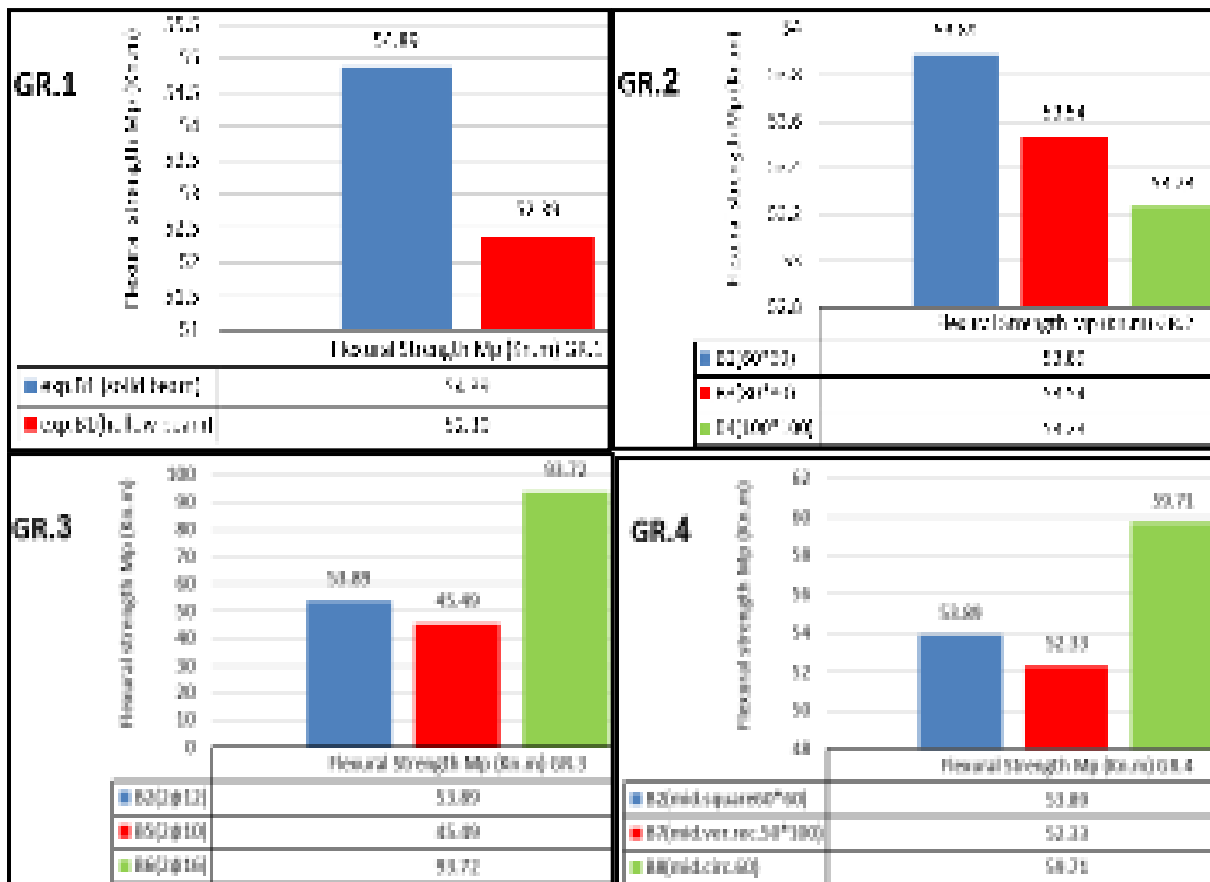
Fig. (5.11) Flexural strength vs. section type of UHPC beam.
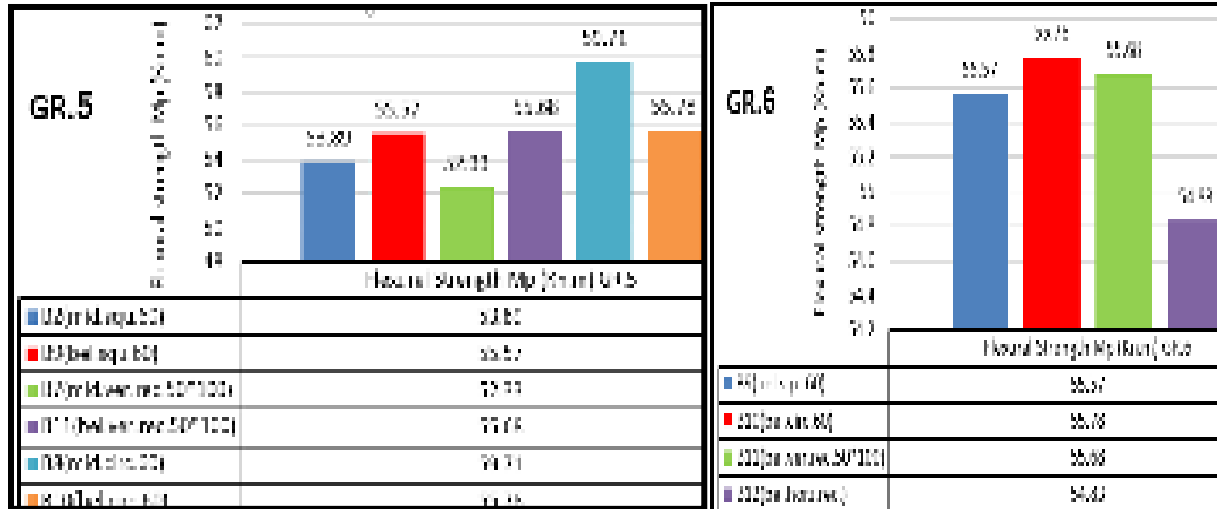
Fig. (5.10) Continued.

[CHAPTER SIX]

Conclusions and Recommendations

CHAPTER SIX

Conclusions and Recommendations

6.1   Conclusions

Since the efficient structures are those structures, have large stiffness to weight ratio, and that was achieved by either using high strength materials such as or rearranging a section with a specific geometry in which produces high stiffness to cross-sectional area. Thus, the current experimental research includes a study that investigates the flexural behavior to a new type of composite beams, where it is composed of a hollow steel section that is fully encased in the concrete with several variables, the most important of which are the location of steel section, the longitudinal reinforcement ratio, area of the hollow steel section, shape of the hollow steel section and the arrangement of the shear connectors between them. The main conclusions obtained in this study are:

1) Fully encased steel hollow section in the concrete beam is a useful technique for enhancing its flexural capacity. The load capacity of a composite hollow beam (B3) increases by 109% than the solid beam (B1) and 119% than the non-composite hollow beam (B2).

2) The flexural moment capacity decreased by (1%) when longitudinal opening made in the concrete section using cork material. However, the flexural moment capacity increases significantly by (109%) when the hollow core was fabricating using hollow steel section material. The composite hollow beams have greater moment capacity than the non-composite hollow beams.

3) The ultimate load and moment capacity of the hollow composite beam increase when the cross-section area of the hollow steel section increased. Also, at the same time, this result has a structural and economic benefit at the same time as

the hollow steel section with the largest area reduced the amount of used of concrete ((in the present research type of concrete is the UHPC whose materials are relatively expensive)) and reduced the weight of structural member as the weight of the concrete heavier than the weight of steel and at the same time increased it is stiffness.

4) In this new type of structural elements, moment of inertia of steel hollow section playing an important role and has a direct indicator to the moment capacity of the section. In the present research, when used rectangular steel hollow section (50x100)mm² has (I = 416,6666 mm4), the result load capacity was higher than when used square hollow section (60x60)mm² has (I = 108,0000 mm4), and higher than the circular steel hollow sections (Ø60mm) diameter has (I = 63,6172 mm4).

5) The ultimate load and moment capacity of composite hollow sections increased when the location of steel hollow section lowered to the tension zone of the beam cross-section. However, the negative problem maybe occurs the rapid emergence of initial cracks in tension zone as a result of weakness the tensile capacity of concrete below the section due to the presence of the hollow core. Therefore, in this research, it was confirmed that the hollow center or longitudinal openings should be located within the middle zone of the concrete section.

6) Stiffness values of the composite hollow beam (B3) are higher than the solid beam (B1) and non-composite hollow beam (B2) by 23.5% and 32.9% respectively. The stiffness values increases as the longitudinal steel reinforcement increases. Where the composite hollow beam (B7) with $2\phi16$ has a higher stiffness than composite hollow beams (B6) and (B3) which have less longitudinal steel reinforcement.

7) The finite element model has proved to be effective in terms of evaluating the ultimate load capacity and load-deflection behavior. It was found good

correlations between what was modeled and the actual experimental results have been achieved.

6.2   Recommendations and further researches

Some points were suggested to involve the recommended future work for

composite and non-composite hollow beams as follows:

1. The analysis presented in this thesis aims to develop a new structural element (composite hollow beams) with a structural and service benefit. Where studied its flexural behavior experimentally and numerically but did not investigate its sheer capacity behavior. Therefore, many tests required in this field to explore the shear behavior of this new type of elements.

2. In this thesis, the test was performed using two point-loadings but is proposed in future studies to test the behavior using different load conditions such as distributed loads, cyclic loads, etc.

3. In this thesis, the work includes only the investigation of the longitudinal opening (hollow core) fabricated using hollow steel section, so future experimental tests should be done to investigate the behavior of composite hollow beam using steel sections with web opening or sinusoidal openings in the encased steel section.

4. Investigating the chemical bond between ultra-high performance concrete UHPC and hollow steel section instead of a mechanical bond as a shear connector to study the composite action.

5. A dedicated study is recommended to investigate the sufficient type, number, and distances of shear connectors in this new type of structural

6. This work can be further extended by using another different hollow steel section since there are many shapes of hollow steel sections.

7. The same adopted experimental program can be used to examine the effect of torsion or axial forces on the behavior of composite hollow beams.

REFERENCES

[1] Ali ihsan salah aldin., " behavior of steel beams embedded in concrete", Ph.D. Thesis, University of Technology, Baghdad, Iraq, 2008.

[2] Johnson, R.P.,«Composite Structure of Steel and Concrete», Vol.1, Crosby Lockwood Staples, Londen, 1975.

[3] Shariati, A., RamliSulong, N. H., & Shariati, M. (2012). Various types of shear connectors in composite structures: A review. International Journal of Physical Sciences, 7(22), 2876-2890.

[4] BS 18, "Method for tensile testing of metals (including aerospace materials). (Cited by reference 11).

[5] Eurocode 3: Design of steel structures, part 1-1: General rules and rules for buildings, (2005).

[6] EN 13918, International standard ISO 13918, "Welding –studs and ceramic ferrules for arc stud welding", 2nd edition, (2008).

[7] British standards institution (BSI), BS 5950: Structural use of steel work in building, part 3: Design in composite construction, section 3.1 code of practice for design of simple and continuous composite beams, (1990).

[8] Eurocode 4, "Design of composite steel and concrete structures-part 1-1: General rules and rules for building", (2004).

[9] American Institute of Steel Construction (AISC), Manual of Steel Construction, 13th Ed, Chicago, (2005).

[10] AASHTO, AASHTO LRFD Bridge Design Specifications, 3rd Edition, American Association of state High way and Transportation Officials, Washington, DC, (2004).

[11] Supplement to CHBDC S6-00, Bridge Standards and Procedures Manual (2006).

[12] GB50017-2003, Code for design of steel structures, Ministry of Construction of China, Beijing: China planning press.

[13]   Korea Building Code (KBC 2009), Design codes for building structures, Korean.

[14]   British standards institution (BSI), BS 5950: Structural use of steel work in building, part 3: Design in composite construction, section 3.1 code of practice for design of simple and continuous composite beams, (1990).

[15]   Johnson R.P., "Composite structure of steel and concrete", (volume 1), Blackwell Scientific publication (second edition), U.K, (1994).

[16]   Japan Road Association, specification for highway bridges and commentary, II steel highway bridges volume, JRA (2002).

[17]   AASHTO, AASHTO LRFD Bridge Design Specifications, 3rd Edition, American Association of state High way and Transportation Officials, Washington, DC, (2004).

[18]   Slutter R., and Driscoll G., "Flexural strength of steel and concrete composite beams" Journal of the structural division, ASCE, Vol. 91, No. ST2, pp71-99, (1965).

[19]   American Institute of Steel Construction (AISC), Manual of Steel Construction, 13th Ed, Chicago, (2005).

[20]   AASHTO, AASHTO LRFD Bridge Design Specifications, 3rd Edition, American Association of state High way and Transportation Officials, Washington, DC, (2004).

[21]   American Institute of Steel Construction (AISC), Manual of Steel Construction, 13th Ed, Chicago, (2005).

[22]   American Institute of Steel Construction (AISC), Manual of Steel Construction, 13th Ed, Chicago, (2005).

[23]   British standards institution (BSI), BS 5950: Structural use of steel work in building, part 3: Design in composite construction, section 3.1 code of practice for design of simple and continuous composite beams, (1990).

[24]   BS 5400: part 5, "Design of composite bridges", British Standards Institution, London, (1979).

[25]   Eurocode 4, "Design of composite steel and concrete structures-part 1-1: General rules and rules for building", (2004).

[26]   Standards Australia, composite structures part 1: simply supported beams. AS2327.1, Sudney (Australia), (2004).

[27]   IS: 11384-1985, Code of practice for composite construction in structural steel and concrete.

[28]   JSCE, "Standard specification for steel and composite structures", Japan Society of Civil Engineers, (2009).

[29]   Supplement to CHBDC S6-00, Bridge Standards and Procedures Manual (2006).

[30]   Neelima Khare, V.S. Shingade, Flexural and shear response of concrete encased steel beams, IJIRSET J. 5 (7) (2016) 13482–13491.

[31]   Neelima Khare, V.S. Shingade, Experimental study on performance of composite beams with and without shear reinforcement, Int. J. Eng. Res. Develop. 12 (7) (2016) 10–16.

[32]   Ahmed Youssef Kamal, Encased beam with variable upper steel flange position, Int. J. Appl. Innov. Eng. Manage. (IJAIEM) 4 (4) (2015) 60–66.

[33]   Shallal., "Flexural Behavior of Concrete-Filled Steel Tubular Beam" 978-1-5386-3540-7/18/31.00$©2018 IEEE.

[34]   V. Kvocˇaˊ ka, L. Draba, Partially-encased composite thin-walled steel beams, Procedia Eng. 40 (2012) (2012) 91–95.

[35]   Hegger J. and Goralski C., "Structural behavior of partially concrete encased composite sections with high strength concrete", Composite Construction in Steel and Concrete, ASCE, 2006. pp. 346-355.

[36]   Outlines of JSCE "Recommendations for Design and Construction of Ultra High Strength Fiber Reinforced Concrete Stru.

[37]   Richard, P., Cheyrezy, M. H., " Reactive Powder Concretes with High Ductility and 200-800 N/mm2 Compressive Strength", SP 144-24, 1994, pp. 507-518.

[38]   Prabha, S. L., Dattatreya, J. K., Neelamegam, M., & Seshagirirao, M. V. (2010). Study on stress-strain properties of reactive powder concrete under uniaxial compression. International Journal of Engineering Science and Technology, 2(11), 6408-6416.

[39]   Silvia C., Troli, R., Monosi, S., and Orlando, G., "The influence of the fiber type on the performance of RPC", Industrial Italian Cement, Vol. 786, 2003, pp. 334-341.

[40]   Gowripalan N, Ian R Gilbert (2000), "Design Guidelines for Ductal Prestressed Concrete Beams", REFERENCE ARTICLE, VSL (Aust) Pty Ltd, Australia .

[41]   Simao P.F. Santos , Joaquim A.O. Barros and Lúcio A.P.Lourenço (2008), " Steel Fibres For The Shear Resistance of High Strength Concrete Beams ", 7PthP RILEM International Symposium on Fiber Reinforced Concrete , RILEM Proceedings Pro 60 ,PP.429 ,Chennai, India.

[42]   Federal Highway Administration (FHWA) (2006)," Material Property Characterization of Ultra-High Performance concrete", PUBLICATION NO. FHWA-HRT-06-115, USA.

[43]   Haider M. Hekmet (2014)," Analysis and Behavior of RPC T-Beams in Flexure" , MSc. Thesis, Building and Construction Engineering Department, University of Technology.

[44]   Samir P.Y. Hannawayya (2010)," Behavior of Reactive Powder Concrete Beams in Bending" , Ph.D. Thesis, Building and Construction Engineering Department, University of Technology .

[45]   Murugesan, A., and Narayanan, A. (2017). "Influence of a longitudinal circular hole on flexural strength of reinforced concrete

beams." Pract. Period. Struct. Des. Constr., 10.1061/(ASCE)SC.1943-5576.0000307, 04016021.

[46]   Hadi N. Ghadhban (2013). "Experimental Behavior of Hollow Non-Prismatic Reinforced Concrete Beams" Journal of Engineering and Development, Vol. 17, No.5, November 2013, ISSN 1813- 7822.

[47]   Iraqi specification No. 5, "Portland Cement," Baghdad, 1984.

[48]   National Ready Mixed Concrete Association, "What, Why and How

[49]   ASTM C1240-04, "Standard Specification for the Use of Silica Fume as a Mineral Admixture in Hydraulic Cement Concrete, Mortar and Grout", Vol. 4.2, 2004, 6p.

[50]   B.S. 882; "Specification for Aggregates From Natural Sources for Concrete ", British Standards Institute, 1992.

[51]   ASTM C 494/C 494M – 1999a, "Standard Specification for Chemical Admixtures for Concrete", Vol. 04.02, 1999, pp.1-9.

[52]   ACI Committee, & International Organization for Standardization. (2008). Building code requirements for structural concrete (ACI 318-08) and commentary. American Concrete Institute.

[53]   Scott, R. H., Feltham, I., & Whittle, R. T. (1994). Reinforced concrete beam-column connections and BS 8110. Structural engineer, 72(4).

[54]   AISC, "Load and Resistance Factor Design Specification for Structural Steel Buildings", American Institute of Steel Construction, Chicago, Illinois, 1999.

[55]   ASTM A 370-05, "Standard Test Method and Definition for Mechanical Testing of Steel Products," 2005 Annual Book of ASTM Standards, Vol.01.01, ASTM, Philadelphia, PA., 2005.

[56]   B.S. 4449, "Carbon Steel Bars for the Reinforcement of Concrete" No.4449/1997.

[57]   Mahdi, B.S., "Properties of Self Compacted Reactive Powder Concrete Exposed to Saline Solution", Ph.D. Thesis, Building and Construction Engineering Department, University of Technology,Baghdad,February 2009, 223p.

[58]   Strain gauges, TML catalog, Tokyo Sokki Kenkyujo Co., Ltd. www.tml.jp/e.

[59]   ASTM C39-86, "Standard Test Method for Compressive Strength of Cylindrical Test Specimens", Annual Book of Standard American Society for Testing and Materials, Vol.04.02, 2003.

[60]   ACI 318M-08, "Building Code Requirements for Structural Concrete (ACI318M.08) and Commentary", American Concrete Institute, Farmington Hills, Michigan, USA, 473 pp., 2008.

[61]   ASTM C496/C496M-04, "Standard Test Method for Splitting TensileStrength of Cylindrical Concrete Specimens", Vol. 04.02, 2004, 5p.

[62]   ASTM C78-84, "Standard Test Method for Flexural Strength of Concrete (Using Simple Beam with Two Points Loading", Annual Book of ASTM Standard, Vol. 04.02, 2003.

[63]   Habel, K., Viviani, M., Denarié, E., and Brühwiler, E., (2006), "Development of the mechanical properties of an Ultra-High Performance Fiber Reinforced Concrete (UHPFRC)," Cement and Concrete Research, Vol.36, pp 1362–1370.

[64]   Tareq K. (2018). Efficiency of hollow reinforced concrete encased steel tube composite beams. International journal of civil engineering and Technology 0976-6316

[65]   Institute for steel development & growth INSDAG, chapter 21"Composite beams-I", 22 "Design of composite beams-II", 28 "Composite beam, Steel beams with web openings", Teaching materials, www.steel-insdag,org.

[66]   Bunni, Z. J., "Shear Strength in High-Strength Fiber Reinforced Concrete Beams", M. Sc. Thesis, University of Technology, Baghdad, 1998, 105 PP.

[67]   Jungwirth, J., "Under-spanned bridge structure in reactive powder concrete (RPC)", Swiss, 2002, pp. 1-6.

[68]   Graybeal B. and Marshall D. (2008), " Cylinder or Cubes: Strength testing of 80 to 200 MPa (11.6 to 29 ksi) Ultra-High-Performance Fiber-Reinforced Concrete" , ACI Materials Journal, Technical Paper, No. 105-M68 .

APPENDICES

Appendix-A
Design Example of The Composite hollow Beam

Number of Stud Shear Connectors :

To calculate the number of studs shear connectors required to weld in the composite hollow beam (B3) so that it can getting a full interaction between the steel hollow section and the surrounding concrete, the method of the upper shear connectors should be used.

1- Shear resistance (Q_n) of a stud is lesser of :

- Resistance of Concrete; $Q_n = 0.5\ A_{sc}\ \sqrt{f_c' E_c} = 96.1\ kN$
- Resistance of Stud; $Q_n = A_{sc} F_u = 78.53\ kN$

Where A_{sc}= cross sectional area of stud
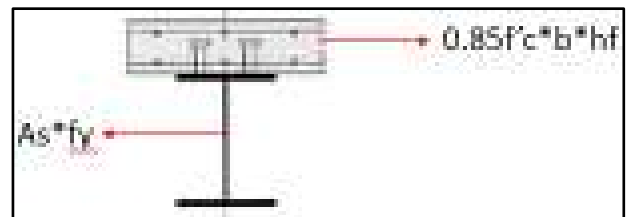F_u= ultimate tensile strength of stud.
In the present study the diameter of the stud is $(10\ mm)$ and the ultimate tensile strength is assumed $(1000\ MPa)$, average =120 Mpa and $E_c = 50000$ thus $Q_n = 51\ kN$.

Calculating upper required number of shear connectors (full interaction) :

➤ In traditional composite sections :

Vh=0.85 f$_{c'}$ * b * hf

Vh=As * fy

0.85f'c*b*hf

As*fy

Longitudinal shear force V'=min(0.85f'c * b * hf, As * fy)

No. studs=2* $(\dfrac{V'}{Q_n})$.

➤ But in this new section, case is different:

Longitudinal shear force V' is the min. of :

Vh= (0.85/γb) * f$_c$ * b * hfc – 936

Vh= Asb * fy + 0.4 √f$_c$ * Ac (in tension zone) + Asr * fy – 397.4

∴ No. of Studs = 2 × $\dfrac{V'}{Q_n}$ ≅ 11
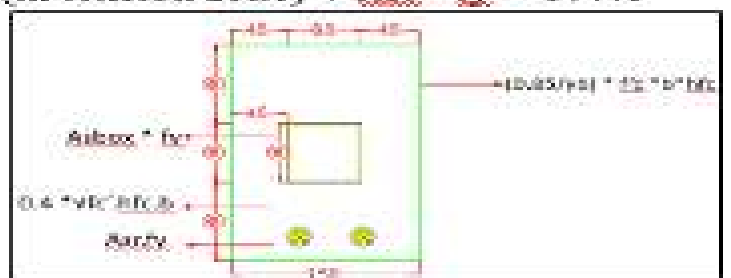
الخلاصة

تعتبر مسارات الخدمة جزءا اساسيا لأي بناية. لذلك فأن استخدام العناصر الانشائية الحاوية على فتحات طولية مختلفة حل فعال لتغطية الحاجة لهذه المسارات مع فوائد اقتصادية. الفوائد الاقتصادية لمواد البناء تتعلق بتقليل كمية المواد المستخدمة وتقليل الوزن الميت للعنصر الانشائي مع المحافظة على مقاومة العنصر الانشائي. لذلك فأن الخصائص الانشائية والاقتصادية للجسور المجوفة هي اثنان. الاولى تعتبر ايجابية لتقليلها الوزن الميت للجسر. والثانية ليست ايجابية لتقليلها مقاومة العنصر وحمل الفشل الاقصى للجسر. لذلك البحث الحالي يحاول تغطية هذه الجزئية بتقليل كمية الخرسانة المستخدمة مع المحافظة وزيادة مقاومة المقطع قدر الامكان عن طريق استخدام مبدأ العناصر المركبة في عنصر انشائي جديد. عناصر المقاطع المركبة مؤخرا تم استخدامها في بناء المنشاءات المتوسطة والعالية الارتفاع. العمل الحالي يتضمن دراسة تحاول تطوير نوع جديد من المقاطع الانشائية المركبة هو المقطع المركب المجوف الذي يحتوي على مقطع حديدي مجوف مغروس بصوره كلية في الكونكريت بوساطة تحري تصرف انشائه عمليا ونظريا. اشكال مواقع مختلفة للمقطع الحديدي المجوف تم استخدامها كمتغيرات للبحث. هذا المقطع الحديدي المجوف غرس كليا في الكونكريت للاستفادة من خصائص الحديد له كوظيفة انشائية والتجويف الموجود فيه كممر خدمي واقتصادي بتقليله الوزن الميت لمواد الكونكريت المستخدم. لذلك فأن استخدام خلطة خرسانية مكلفة مثل خلطة الخرسانة عالية الاداء في هذا النوع من العناصر نوعا ما غرضا خدميا. الخرسانة عالية الاداء هي طفره نوعية في تكنلوجيا الخرسانة لانها تظهر خصائص سوبرية كمقاومة الانضغاط والشد والديمومة والمطيلية لكن لحد الان هي باهظة الثمن نوعا ما.

الجزء الاول من البحث هو تحري عملي يتضمن صب وفحص خمسة عشر جسرخرساني عالي الاداء مركب وغير مركب تحت نقطتي تحميل لحد الفشل. الجسور قسمت الى سبعة مجاميع. المجموعة الاولى تتضمن نوعين من الجسور الخرسانية عالية الاداء المجوفة (مركبة وغير مركبة) بالاضافة بالاضافة الى جسر غير مجوف مرجعي. المجموعة الثانية تتضمن ثلاثة جسور مركبة مجوفة بوجود مقاطع حديديه مغروسة مختلفة المساحات. المجموعة الثالثة تتضمن ثلاثة جسور مركبة مجوفة بثلاثة نسب للتسليح الطولي. المجموعة الرابعة تتضمن ثلاثة جسور مركبة مجوفة بثلاثة اشكال للمقاطع الحديدية المجوفة المغروسة (المربعة60*60, المستطيلة50*100 و الدائرية بقطر 60)ملم. المجموعة الخامسة تتضمن ثلاثة عناصر مركبة مجوفة, احدها يحتوي على روابط قص (براغي) ملحومة على اربع جهات للصندوق الحديدي المجوف, والاخر يحتوي على براغي ملحومة فقط على جهتين من المقطع الحديدي المجوف (الشفتان) والاخر بدون اي روابط قصية. الهدف من هذه المجموعة لمعرفة تأثير عدد وترتيب روابط القص في التي تربط الصندوق الحديدي مع الكونكريت المحيط به. المجموعة السادسة تهدف الى ايجاد افضل موقع للصندوق الحديدي من ناحية قابلية التحميل, التشققات وتهشم الكونكريت. وتتضمن دراسة للجسر المركب المغروس بصندوق حديدي في منطقتي الوسط والشد للمقطع المركب. اخيرا, المجموعة السابقة تدرس تأثير تغيير شكل المقطع الحديدي ضمن المقطع. ان جميع الاعتاب متشابهه من حيث الابعاد والتسليح ونوع الخرسانة. الدراسة الحالية تهدف الى تحري امكانية غرس مقطع حديدي مجوف في الخرسانة عالية الاداء لزيادة مقاومة الانثناء ونوع الفشل للجسور الخرسانية عالية الاداء. ولهذا الغرض فأن الدراسة قدر اجريت من خلال الجانب العملي والجانب النظري والتحليل العددي لدراسة سبعة متغيرات التي تتضمن افضل مادة لعمل تجويف المقطع (خرسانة او فلين او صندوق حديدي مجوف), حجم المقطع الحديدي المجوف المغروس, التسليح الطولي في هذه المقاطع, شكل المقطع الحديد في المنطقة الوسطى ومنطقة شد المقطع وتأثير موقع المقطع الحديدي المجوف.

النتائج العملية تضمن تحديد الحمل الاقصى وقابلية تحمل الانثناء والانفعالات ومخطط الحمل والتشوه والجسائة والمرونة والصلادة واشكال التشققات.

الجزء الثاني هو تحليل عددي بأستعمال مبدأ العناصر المحددة لتحري سلوك الاعتباب الخرسانية عالية الاداء المركبة والغير مركبة. نماذج الدراسة تم تمثيلها بأستخدام برنامج (الانسس 15). حيث احتوت نتائج طريقة العناصر المحددة شكل التشوه والاحمال القصوى ومخططات الحمل والتشوه. حيث أظهرت النتائج أنها كانت في حالة متقاربة مع نتائج الفحوصات العملية.

اخيرا, كانت الاعتاب المركبة ذات مقاومة تحمل اعلى بنسبة تصل الى حوالي 109% من الاعتاب الغير مركبة سواء كانت مجوفة او غيرمجوفة, بينما عملية غرس الصندوق الحديدي المجوف في الخرسانة عالية الاداء حسن من الحمولة القصوى ومقاومة انثناء المقطع والجسائة والصلادة للاعتباب الخرسانية عالية الاداء.

مقاومة الانثناء للأعتاب المركبة من صندوق حديدي والخرسانة عالية الاداء

اطروحة
مقدمة إلى قسم الهندسة المدنية في جامعة ميسان كجزء من متطلبات نيل
شهادة الماجستير في علوم الهندسة المدنية/انشاءات

من قبل

مصطفى رعد عزيز
(بكالوريوس هندسة مدنية 2016)

باشراف

د.ناصر حكيم طعمة

Cont.

Plate (3.16): Results of the modulus of rupture for prism.